Turkish Journal of Chemistry

Volume 47 | Number 5 Article 26

10-31-2023

Benzimidazol-2-ylidene ruthenium complexes for C-N bond formation through alcohol dehydrogenation

ZAHID NAWAZ

NEVİN GÜRBÜZ

MUHAMMED NAVEED ZAFAR

NAMIK ÖZDEMİR

BEKİR ÇETİNKAYA

See next page for additional authors

Follow this and additional works at: https://journals.tubitak.gov.tr/chem

 Part of the Chemistry Commons

Recommended Citation

NAWAZ, ZAHID; GÜRBÜZ, NEVİN; ZAFAR, MUHAMMED NAVEED; ÖZDEMİR, NAMIK; ÇETİNKAYA, BEKİR; and ÖZDEMİR, İSMAİL (2023) "Benzimidazol-2-ylidene ruthenium complexes for C-N bond formation through alcohol dehydrogenation," *Turkish Journal of Chemistry*: Vol. 47: No. 5, Article 26. https://doi.org/10.55730/1300-0527.3606

Available at: https://journals.tubitak.gov.tr/chem/vol47/iss5/26

This Article is brought to you for free and open access by TÜBİTAK Academic Journals. It has been accepted for inclusion in Turkish Journal of Chemistry by an authorized editor of TÜBİTAK Academic Journals. For more information, please contact academic.publications@tubitak.gov.tr.

Benzimidazol-2-ylidene ruthenium complexes for C-N bond formation through alcohol dehydrogenation

Authors
ZAHID NAWAZ, NEVİN GÜRBÜZ, MUHAMMED NAVEED ZAFAR, NAMIK ÖZDEMİR, BEKİR ÇETİNKAYA, and İSMAİL ÖZDEMİR

This article is available in Turkish Journal of Chemistry: https://journals.tubitak.gov.tr/chem/vol47/iss5/26

Turkish Journal of Chemistry

http://journals.tubitak.gov.tr/chem/

Research Article

Turk J Chem
(2023) 47: 1209-1223
© TÜBİTAK
doi:10.55730/1300-0527.3606

Benzimidazol-2-ylidene ruthenium complexes for C–N bond formation through alcohol dehydrogenation

Zahid NAWAZ[1,2], Nevin GÜRBÜZ[2,3,4], Muhammad Naveed ZAFAR[1], Namık ÖZDEMIR[5], Bekir ÇETİNKAYA[6], İsmail ÖZDEMİR[2,3,4,*]

[1]Department of Chemistry, Quaid-i-Azam University, Islamabad, Pakistan
[2]Catalysis Research and Application Center, İnönü University, Malatya, Turkiye
[3]Department of Chemistry, Faculty of Science and Arts, İnönü University, Malatya, Turkiye
[4]Drug Application and Research Center, İnönü University, Malatya, Turkiye
[5]Department of Mathematics and Science Education, Faculty of Education, Ondokuz Mayıs University, Samsun, Turkiye
[6]Department of Chemistry, Faculty of Science, Ege University, İzmir, Turkiye

Received: 31.03.2023 • **Accepted/Published Online:** 30.09.2023 • **Final Version:** 31.10.2023

Abstract: A low temperature hydrogen borrowing approach to generate secondary amines using benzimidazole-based *N*-heterocyclic carbene (BNHC) ruthenium complexes is reported. A series of the piano-stool complexes of the type [(η^6-*p*-cymene)(BNHC)$RuCl_2$] (**1a**–**g**) were synthesized via one-pot reaction of the NHC salt precursor, Ag_2O, and $[RuCl_2(p\text{-cymene})]_2$ and characterized using conventional spectroscopic techniques. The geometry of two precursors, [(η^6-*p*-cymene)($^{Me4Bn}Me_2BNHC^{CH2OxMe}$)$RuCl_2$] (**1f**) and [($\eta^6$-*p*-cymene)($^{Me5Bn}Me_2BNHC^{CH2OxMe}$)$RuCl_2$] (**1g**), was studied by single crystal X-ray diffraction. These catalysts were found to dehydrogenate alcohols efficiently at temperatures as low as 50 °C to allow Schiff-base condensation and subsequent imine hydrogenation to afford secondary amines. Notably, this ruthenium-based procedure enables the *N*-alkylation of aromatic and heteroaromatic primary amines with a wide range of primary alcohols in excellent yields of up to 98%. The present methodology is green and water is liberated as the sole byproduct.

Key words: Benzimidazol-2-ylidenes, ruthenium complexes, amine alkylation, C–N bond formation, mild conditions

1. Introduction

Amines, organic derivatives of ammonia, are extensively found in bioactive molecules and medicines [1]. Amines are the key precursor in the manufacture of a number of relevant therapeutics medicines [2-4]. Conventionally, the most common methods for producing alkylated amines involve alkyl halides [5] or stoichiometric reducing agents, which are used for reduction of imines formed between carbonyls and amines [6,7]. The toxicity of the alkylating and reducing reagents and the generation of huge volumes of undesired byproducts are all significant disadvantages of these reactions. To address these difficulties, catalytic techniques have been devised including Buchwald–Hartwig amination [8], hydroamination [9,10], and hydroaminomethylation [11] as well as hydrogen borrowing or hydrogen autotransfer (HB/HA) methodologies [12].

In the HB/HA procedure, first dehydrogenation of the alcohol produces the equivalent aldehyde, which then undergoes reductive amination to produce the required amine. Because the alcohol functions as the hydrogen donor, an additional hydrogen source is not required in this approach. Furthermore, because a variety of alcohol derivatives are easily available from renewable feedstocks, this technology is particularly well suited for the valorization of biomass or biomass-derived building blocks. The HB/HA technique is the most attractive methodology for their synthesis [13-15]. These reactions are notable for being not only ecologically friendly, but also atom efficient, with only water as a byproduct. Grigg [16] and Watanabe [17] independently described the first examples of amine alkylation with alcohols via hydrogen borrowing while employing the homogeneous ruthenium catalysts $[(PPh_3)_4RhH]$ and $[(PPh_3)_3RuCl_2]$. Since that time, several noble metal-based Ru [18-21], Pd [22-24], Ir [25-27], and Pt [28] complexes and nonnoble metal-based Mn [29] Co [30] Ni [31], and Fe [32] complexes have been used. Heterogeneous catalysts [33], biocatalysts [34,35], and chiral catalysts [36,37] have also been used. Importantly, many of the catalysts that have previously been described for this reaction require relatively high temperatures of 100 °C or greater and high catalytic loading [38-43], but some other complexes have comparative working conditions for this reaction [18,44].

* Correspondence: ismail.ozdemir@inonu.edu.tr

This work is licensed under a Creative Commons Attribution 4.0 International License.

N-Heterocyclic carbene (NHC) ligands have become a common alternative to phosphine ligands in homogeneous catalysis over the last 30 years [45-48], especially in combination with ruthenium salts [44,49-52]. We recently described the synthesis of benzimidazolium salts (the precursors to benzimidazole-based NHC (BNHC) ligands) and their silver(I) complexes, which were determined to be active catalysts for carboxylation of epoxides to generate carbonates [53] and aldehyde–amine–alkyne coupling. The preparation and identification of new ruthenium(II) complexes having the general formula [(η^6-*p*-cymene)(BNHC)$RuCl_2$] (**1a-g**) are described in the present paper (Scheme 1). The hydrogen borrowing approach was used to test these complexes as catalysts for the *N*-alkylation of anilines and amine-substituted heterocycles with a variety of alcohols.

2. Experimental section

2.1. Materials and methods

All metal complex preparation methods and catalytic reactions were performed using normal Schlenk procedures. Reagents were bought from commercial sources and were not purified prior to use. The melting point of the produced compounds was determined using open capillary tubes in an Electrothermal 9200 melting point device. A PerkinElmer Spectrum 100 spectrometer with a range of 4000–400 cm^{-1} was utilized for FT-IR analysis. NMR spectra were obtained using a Bruker Ascend 400 Avance III HD, which operated at 400 MHz (^{1}H) and 100 MHz (^{13}C) using tetramethyl silane as an internal reference. NMR experiments were conducted in high-quality 5-mm Young NMR tubes. Chemical shifts (δ) and coupling constants (J) are expressed in parts per million (ppm) and hertz (Hz). ^{13}C chemical shifts are given relative to deuterated solvents (=77.16 ppm for $CDCl_3$). ^{1}H NMR spectra are referenced to residual protonated solvents (=7.26 ppm for $CDCl_3$).

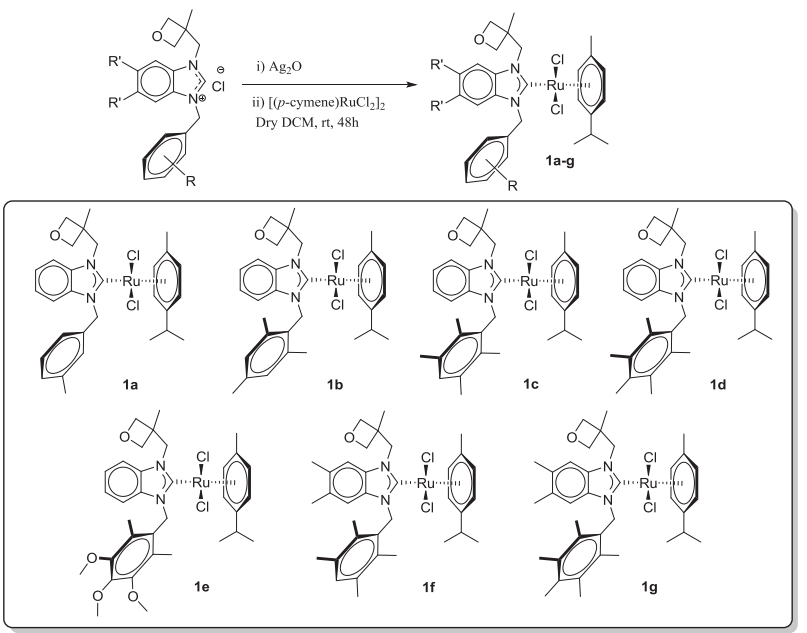
2.2. General synthetic methodologies used for the synthesis of benzimidazol-2-ylidene ruthenium complexes, 1a-g

Complexes [(η^6-*p*-cymene)(BNHC)$RuCl_2$] were synthesized in a one-step process through transmetalation. Dimeric complex of ruthenium $[RuCl_2(p\text{-cymene})]_2$ (0.19 mmol) was added to Ag(I)–BNHC complexes (0.383 mmol) in situ without isolation and the mixture was stirred at 25 °C in dichloromethane (DCM) for 48 h. Orange–brown complexes **1a**, **1b**, **1c**, **1d**, **1e**, **1f**, and **1g** of ruthenium carbene were isolated in good yields of 42.5%–80%. Data regarding the ^{1}H and ^{13}C NMR spectra are given in Tables 1 and 2.

1a. Yield: 63%; orange–brown solid: mp 172–174 °C.

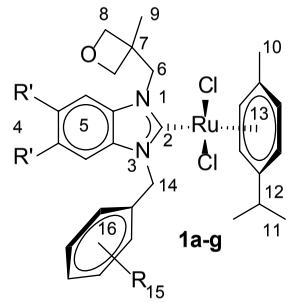
1b. Yield: 55%; orange–brown solid: mp 172–174 °C.

1c. Yield: 67%; orange–brown solid: mp 180–182 °C.



Scheme 1. Synthesis of ruthenium *p*-cymene BNHC complexes.

Table 1. Selected ^{1}H NMR data for **1**.



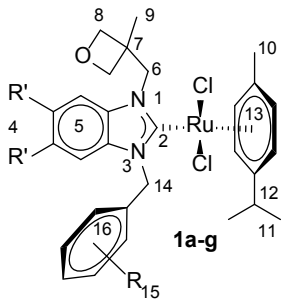
Comp.	4	5	6	8	9	10	11	12	13	14	15	16
1a	-	7.09 (t) 7.18 (td), 7.24–7.40 (m)	4.50 (s)	4.74–5.05 (m)	1.98 (s)	1.15 (s)	1.25 (d)	2.93 (hept)	5.86–5.72 (m)	5.41 and 5.27 (s)	2.21 (s)	6.98 (d), 6.80 (d) 6.39(d)
1b	-	7.19 (dd), 7.04 (d) 7.01–6.93 (m)	5.13 (s)	4.73 and 4.39 (d)	1.88 (s)	1.22 (s)	1.32 (d)	3.03 (hept)	6.68 (s), 6.57 (d), 5.72 (d), 5.43–5.31 (m)	5.52 (d)	2.49(s), 2.25(s) 1.80 and 1.71 (s)	6.57 (s) 6.68 (s)
1c	-	7.16 (t) 7.02 (d) 6.97 (s) 6.91 (t)	5.17 (d)	4.75 and 4.39 (d)	1.79 (s)	1.21 (s)	1.32 (d)	3.02 (hept)	6.36 and 5.53 (d) 5.71 (s)	5.44 and 5.53 (s)	2.34, 2.06, and 1.71 (s)	7.22 (s)
1d		7.21–7.07 (m) 6.99 (d), 6.94–6.83 (m)	5.18 (d)	4.76 and 4.40 (d)	1.95 (s)	1.19 (s)	1.32 (d)	3.02 (hept)	6.35 (d), 5.70 (s) 5.44 (s), 4.44 (s)	5.53 (d)	2.47–1.77 (m)	–
1e		7.32–7.23 (m), 7.22–7.15 (m), 7.06 (d)	5.03 (d)	4.79 and 4.44 (d)	1.91 (s)	1.15 (s)	1.28 (d)	3.02 (hept)	6.26 (d), 5.78 (m), 4.54 (d)	5.43 (d)	3.80 and 3.70 (s)	6.43 (s)
1f	2.28 and 2.02 (s)	7.16 and 6.98 (s)	5.13 (d)	4.74 and 4.37 (d)	1.90 (s)	1.21 (s)	1.31 (d)	3.02 (hept)	6.05, 5.63 (s), 5.36 (d)	5.51 (d)	2.45–2.21 (m), 1.16–1.81(m)	6.77 (s)
1g	2.27 and 2.28 (s)	7.22–6.92 (m), 6.74 (s)	5.14 (d)	4.75 and 4.38 (d)	2.00 (s)	1.19 (s)	1.31 (d)	3.01 (hept)	6.01, 5.63 (s), 5.46–5.31 (m)	5.51 (d)	2.44–2.29 (m) 2.16–2.01 (m) 1.92 (s)	–

1d. Yield: 78%; orange–brown solid: mp 180–182 °C.
1e. Yield: 48%; orange–brown solid: mp 298.5–298.7 °C.
1f. Yield: 80%; light brown solid: mp 145–148 °C.
1g. Yield: 42.5%; dark brown solid: mp 242–243 °C.

2.2.1. X-ray crystallography

X-ray measurements were performed with a STOE IPDS II diffractometer at room temperature using graphite-monochromated MoK**α** radiation by applying the *w*-scan method. Data collection and cell refinement were carried out using X-AREA, while data reduction was applied using X-RED32. The structure was solved by direct methods with SIR2019 [54] and refined by means of the full-matrix least-squares calculations on F^2 using SHELXL-2018 [55]. All H atoms were located in difference maps and then treated as riding atoms, fixing the bond lengths at 0.98, 0.93, 0.97, and 0.96 Å for methine CH, aromatic CH, CH_2, and CH_3 atoms, respectively. The displacement parameters of the H atoms were fixed at $U_{iso}(H) = 1.2\ U_{eq}$ (1.5 U_{eq} for CH_3). Crystal data, data collection, and structure refinement details are given in Table 3. The molecular graphic was generated using OLEX2 [56].

Table 2. Selected ^{13}C NMR data for **1**.



Comp.	2	4	5,13,16	6	7	8	9	10	11	12	14	15
1a	190.3	-	138.7, 137.2, 135.6, 135.5, 128.8, 128.3, 126.7, 122.9, 112.0, 109.3	52.7	40.3	98.9	21.5	18.5	21.7	30.7	55.5	20.6
1b	187.7	-	137.4, 135.9, 135.4, 128.5, 111.5, 109.9, 109.6	50.0	40.8	98.6	21.3	18.5	21.6	30.7	54.2	20.9
1c	187.5	-	135.9, 135.4, 131.9, 131.5, 122.9, 122.8, 111.8, 109.7, 109.5	50.8	40.8	98.5	21.2	18.6	23.2	30.7	54.2	20.9, 20.5, 16.2
1d	187.5	-	135.9, 135.5, 135.2, 128.9, 122.9, 122.6, 112.0, 109.6, 109.5	51.4	40.8	98.5	21.1	18.6	21.1	30.8	54.4	17.2
1e	189.7	-	153.4, 137.3, 135.7, 135.4, 132.4, 123.4, 112.0, 110.4, 109.9, 104.0	53.3	40.7	98.6	20.7	18.6	21.3	30.7	54.6	60.9, 56.1
1f	184.9	20.4, 20.3	134.6, 134.1, 131.8, 131.7, 109.8, 109.6, 98.6	50.6	40.9	98.6	21.3	18.5	21.2	30.6	53.9	20.4, 20.3
1g	184.9	20.4, 20.3	135.1, 134.6, 134.2, 131.6, 131.6, 129.0, 112.5, 109.8, 109.5	51.1	40.8	98.6	21.2	18.5	21.3	30.7	54.1	20.4, 20.3, 17.2

2.3. A general approach: *N*-alkylation of amines with alcohols

At room temperature, compound **1e** (1 mol %), KO^{t}Bu (75 mol %), alcohols (1 mmol), and amine (1 mmol) were added to a 15-mL reaction tube in a glove box. The tube was then closed and taken out of the glove box. The reaction mixture was then heated at 120 °C for 12 h with degassed toluene (3 mL). After cooling to room temperature, the reaction mixture was diluted with ethyl acetate, filtered, and vacuum dried. The product was purified using a suitable mixture of petroleum ether and ethyl acetate in column chromatography over silica gel (300–400 mesh) (80:1).

2.4. A general approach: aniline *N*-methylation with methanol

In a glove box, amine (1 mmol), MeOH (2 mL), **1e** (1 mol %), and KO^{t}Bu were introduced into a 15-mL sealing tube (75 mol %). The tube was then removed from the glove box and sealed with a screw cap. At 110 °C, the reaction mixture was agitated for 12 h. The liquid was diluted with ethyl acetate and filtered through a short pad of silica after cooling to room temperature (2 cm in a Pasteur pipette). Ethyl acetate was used to wash the silica. The crude residue was refined by column chromatography (SiO_2, petroleum ether:ethyl acetate = 80:1) after the filtrate had evaporated.

Table 3. Crystal data and structure refinement parameters for **1f** and **1g**.

Parameters	**1f**	**1g**
CCDC depository	2085163	2173756
Color/shape	Dark red/prism	Light brown/prism
Chemical formula	$[RuCl_2(C_{10}H_{14})(C_{25}H_{32}N_2O)]$	$[RuCl_2(C_{10}H_{14})(C_{26}H_{34}N_2O)]$
Formula weight	682.71	696.73
Temperature (K)	296(2)	296(2)
Wavelength (Å)	0.71073 Mo Kα	0.71073 Mo Kα
Crystal system	Triclinic	Orthorhombic
Space group	*P*–1 (No. 2)	*Pbca* (No. 61)
Unit cell parameters		
a, b, c (Å)	7.1553(5), 15.4318(12), 15.5762(12)	7.2829(2), 21.3438(5), 43.0193(13)
α, β, γ (°)	86.525(6), 85.527(6), 77.055(6)	90, 90, 90
Volume (Å^3)	1669.4(2)	6687.1(3)
Z	2	8
$D_{calc.}$ (g/cm^3)	1.358	1.384
μ (mm^{-1})	0.659	0.659
Absorption correction	Integration	Integration
$T_{min.}$, $T_{max.}$	0.7919, 0.9579	0.8533, 0.9667
F_{000}	712	2912
Crystal size (mm^3)	0.48 × 0.23 × 0.09	0.40 × 0.09 × 0.05
Diffractometer/measurement method	STOE IPDS II/ω scan	STOE IPDS II/ω scan
Index ranges	$-9 \le h \le 9, -20 \le k \le 20, -20 \le l \le 20$	$-8 \le h \le 8, -25 \le k \le 25, -52 \le l \le 52$
θ range for data collection (°)	$1.928 \le \theta \le 27.676$	$1.894 \le \theta \le 25.646$
Reflections collected	26,948	48,873
Independent/observed reflections	7728/6314	6304/3620
$R_{int.}$	0.0768	0.0927
Refinement method	Full-matrix least-squares on F^2	Full-matrix least-squares on F^2
Data/restraints/parameters	7728/0/380	6304/0/385
Goodness-of-fit on F^2	0.999	0.906
Final R indices [$I > 2\sigma(I)$]	$R_1 = 0.0362$, $wR_2 = 0.0727$	$R_1 = 0.0417$, $wR_2 = 0.0708$
R indices (all data)	$R_1 = 0.0519$, $wR_2 = 0.0768$	$R_1 = 0.1006$, $wR_2 = 0.0833$
$\Delta\rho_{max.}$, $\Delta\rho_{min.}$ (e/Å^3)	0.56, −0.34	0.37, −0.40

3. Results and discussion

3.1. Preparation of ruthenium(II) complexes

Starting with previously described benzimidazolium salts [53,57], the addition of Ag_2O followed by $[(p\text{-cymene})RuCl_2]_2$ in dry dichloromethane resulted in the formation of the corresponding $[(\eta^6\text{-}p\text{-cymene})(^{R}BNHC^{CH2OxMe})RuCl_2]$ (**1a**–**g**) compounds after 48 h at ambient temperature (Scheme 1). A large band was observed in the FT-IR spectra of the free ligands in the 1572–1556 cm^{-1} range, which corresponds to the vibration of the C=N bonds in ligands. In the ruthenium complex, these bands shifted to the 1461–1486 cm^{-1} range, which clearly indicated the shifting of double bond (C=N) character to single bond character $\upsilon_{(NCN)}$. The ^1H NMR spectra of these complexes revealed that the characteristic downfield NC*H*N signal of the salts had disappeared. The methine proton of the *p*-cymene group was located as a septet between 2.97 and 3.02 ppm for the respective complexes, while the methyl protons of the *p*-cymene appeared at 1.15–1.21 ppm. In the ^{13}C NMR spectra of complexes **1a**–**g**, the carbene carbon attached to ruthenium gave characteristic signals in the range of 184.9–190.3 ppm (see Tables 1 and 2 and Sup Inf).

3.2. Structural analysis

The molecular structures of **1f** and **1g** with complete atom numbering are displayed in the Figure, while important bond distances and angles are listed in Tables 3 and 4. Both structures consist of a BNHC ligand coordinated to a ruthenium center, which also features a *p*-cymene and two chloride ligands in the coordination sphere. Compound **1f** crystallizes in triclinic space group *P*–1 with two molecules in the unit cell, while **1g** crystallizes in orthorhombic space group *Pbca* with eight molecules in the unit cell.

In the structures, the BNHC ligand is coordinated to Ru(II) in a monodentate manner via a neutral carbenic carbon, while the arene ring of *p*-cymene is coordinated to the metal ion in an η^6-fashion. The complexes can be identified as characteristic three-legged piano stool complexes with a pseudooctahedral geometry that is common for ruthenium half-sandwich arene complexes. Furthermore, the geometry around the metal atoms may be regarded as a tetrahedron with considerable trigonal distortion, if bonding to the p-cymene centroid is considered.

Defining Cg as the centroid of the arene ring, the Ru–Cg distance is 1.7098(11) Å in **1f** and 1.7058(17) Å in **1g**, while the Cl1–Ru1–Cg, Cl2–Ru1–Cg and C1–Ru1–Cg angles are 124.38(4), 127.60(4), and 123.23(7)° in **1f**, and 122.90(7), 126.94(7), and 124.93(12)° in **1g**, respectively. The Cl1–Ru1–Cl2, Cl1–Ru1–C1 and Cl2–Ru1–C1 angles are smaller than the ideal tetrahedral angle (109.47°), which is compensated for by extension of the Cg–Ru–*L* (L is Cl1, Cl2, or C1) angles. The ruthenium atom is bound to the arene ring with a mean Ru–C bond distance of 2.21 Å in both complexes. The Ru1–C1

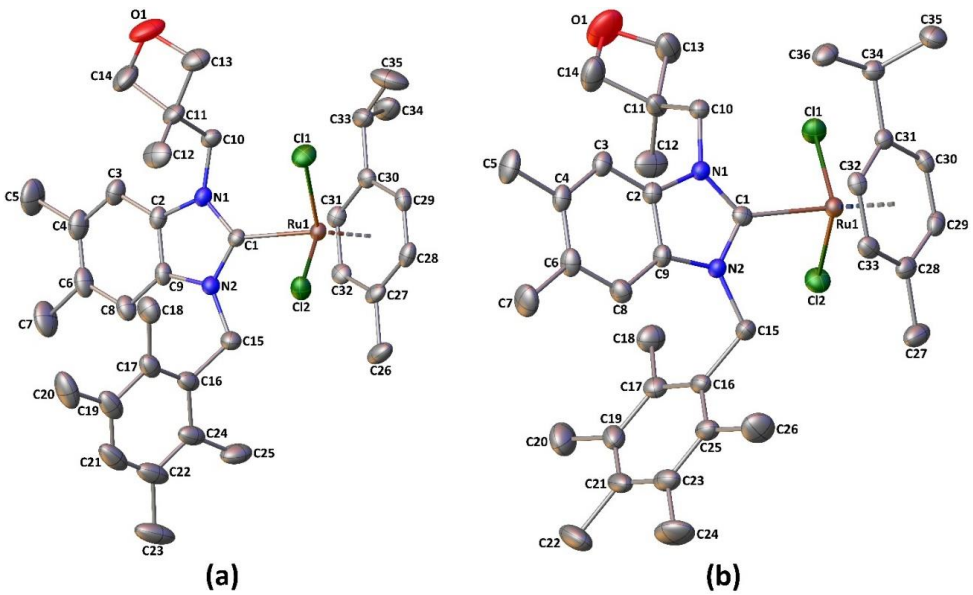


Figure. Molecular structures of **1f** (a) and **1g** (b) drawn at the 30% probability level. H atoms have been omitted for clarity.

bond distance is 2.074(2) **Å** in **1f** and 2.096(4) **Å** in **1g**, while the Ru–Cl bonds range from 2.4122(7) to 2.4307(11) Å. The structural data of the complexes are consistent with those of previously reported NHC-Ru(II)(*p*-cymene)Cl_2 complexes [51,58–63].

3.3. Optimization of amine alkylation with alcohols

The ability of synthesized (BNHC)Ru complexes that might promote amine alkylation was then evaluated, as shown in Table 5. In the presence of potassium tert-butoxide, 1.0 mol % of ruthenium complex **1e**, which features meta and para methoxy substitution, was fully benzylated 4-methoxy aniline (>99% conversion, entry) after 12 h at 120 °C to generate secondary amine product **A**. KO^{t}Bu was an efficient base for obtaining high yields. However, conversion was not possible when substituting weaker bases for KO^{t}Bu, such as K_2CO_3 and Na_2CO_3. KO^{t}Bu was required at 75 mol % to achieve satisfactory conversion. Surprisingly, the reaction still reached 98% conversion at a lower temperature of 70 °C (Table 5, entry 2). However, this trial did lead to the observation of imine product **B** (92:8 **A:B** ratio).

Lowering the temperature even further to 50 °C still allowed 96% conversion with lower selectivity for product **A** (88:12, Table 5, entry 3). A more pronounced loss of selectivity was observed when the catalyst loading was lowered to 0.5 mol % (65:35, Table 5, entry 4). Similarly, stopping a 70 °C reaction after 5 h revealed 98% conversion, but incomplete imine hydrogenation. Compounds **1f** and **1g**, featuring significant methyl substitution, were slightly less effective for this reaction (Table 5, entries 6 and 7). When the reaction was carried out in an open-air environment or in water, conversion was significantly reduced (Table 5, entries 8 and 9).

3.4. *N*-Alkylation on aniline with substituted primary alcohols

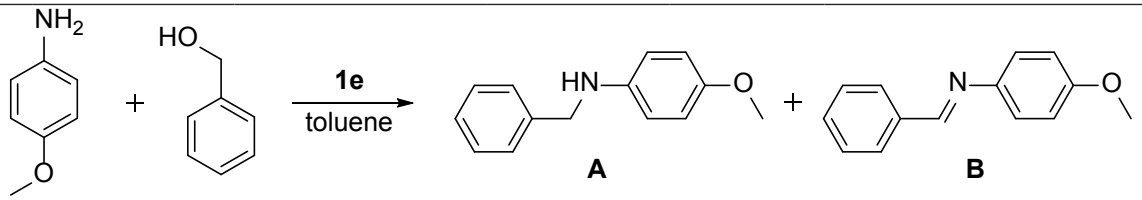
Encouraged by these findings, the scope of aniline *N*-alkylation under mild conditions (70 °C, 12 h) using **1e** was explored. Table 6 illustrates that both electron-rich and electron-deficient benzylic alcohols worked well, yielding alkylated aniline derivatives **2a**–**j** in 55%–94% isolated yield. Catalysis was compatible with several functional groups, including methoxy groups (**2c** and **2f**), halides (**2a** and **2d**), and trifluoromethyl groups (**2i**). Debromination was observed in the case of *para*-bromobenzyl alcohol, but the brominated product was extracted in a reasonable yield (Table 6, 55%). At 90 °C, the sterically hindered *ortho*-methyl benzylic alcohol and *ortho*-methoxy benzylic alcohol still allow monoalkylated amine products **2e** and **2f** in 90% and 87% yield, respectively. Products **2g** and **2h** were obtained in 65% and 71% yield when heterocyclic alcohols such as 2-furylmethanol and 2-thiophenemethanol were utilized as substrates. Using the aliphatic alcohol heptanol afforded aniline derivative **2j** in 75% isolated yield (Table 6). The *N*-alkylation of anilines with secondary alcohols like 1-phenethyl alcohol, cyclohexanol, and isopropyl alcohol, on the other hand, was ineffective, generating

Table 4. Selected geometric parameters for **1f** and **1g**.

Parameters	1f	1g	Parameters	1f	1g
Bond lengths (Å)			***Bond angles (°)***		
Ru1–Cg	1.7098(11)	1.7058(17)	Cl1–Ru1–Cl2	84.35(3)	84.05(4)
Ru1–Cl1	2.4122(7)	2.4193(11)	Cl1–Ru1–C1	95.53(7)	95.76(10)
Ru1–Cl2	2.4288(7)	2.4307(11)	Cl1–Ru1–Cg	124.38(4)	122.90(7)
Ru1–C1	2.074(2)	2.096(4)	Cl1–Ru1–C_{arene}	88.20(7)–158.11(7)	85.23(11)–159.05(10)
Ru1–C_{arene}	2.161(2)–2.249(2)	2.194(4)–2.240(4)	Cl2–Ru1–C1	90.89(7)	91.24(10)
N1–C1	1.361(3)	1.364(5)	Cl2–Ru1–Cg	127.60(4)	126.94(7)
N2–C1	1.370(3)	1.366(4)	Cl2–Ru1–C_{arene}	91.24(7)–156.33(6)	89.88(11)–157.66(11)
			C1–Ru1–Cg	123.23(7)	124.93(12)
			C1–Ru1–C_{arene}	86.78(9)–153.24(10)	87.70(14)–157.11(15)
			N1–C1–N2	105.29(18)	104.7(3)

Note: Cg represents the centroid of the arene ring.

Table 5. The use of benzyl alcohol to optimize the *N*-alkylation of 4-methoxyaniline.



Entry	Cat (mol %)	Base (75 mol %)	Temp (°C)	Time (h)	Conversion (%)	**A**/**B**
1	**1e** (1.0)	KO^{t}Bu	120	12	> 99	>99/0
2	**1e** (1.0)	KO^{t}Bu	70	12	98	92/8
3	**1e** (1.0)	KO^{t}Bu	50	12	96	88/12
4	**1e** (0.5)	KO^{t}Bu	70	12	96	65/35
5	**1e** (1.0)	KO^{t}Bu	70	5	98	87/13
6	**1f** (1.0)	KO^{t}Bu	70	12	94	85/15
7	**1g** (1.0)	KO^{t}Bu	70	12	92	78/22
8[a]	**1e** (1.0)	KO^{t}Bu	70	12	26	-[b]
9[c]	**1e** (1.0)	KO^{t}Bu	70	12	5	-[b]

Reaction conditions: All reactions were conducted in 2 mL of toluene and conversion is based on ^{1}H NMR spectroscopy. [a]An open-air environment. [b]Mixture of products. [c]Reaction was conducted in water.

only trace amounts of products. This observation is consistent with a mechanism that involves alcohol dehydrogenation to generate an aldehyde intermediate.

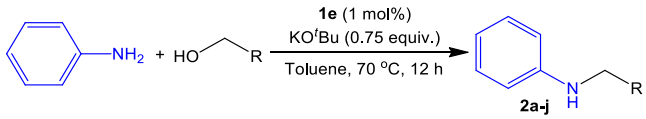
3.5. *N*-Alkylation of substituted anilines and heterocyclic amines with benzyl alcohol

The scope of amines that could undergo alkylation was then explored (Table 7). The *N*-alkylated products **3a**–**i** were obtained in good yield (81%–92%) from substrates containing either electron-donating or electron-withdrawing substituents. For example, 1,3-benzodioxan-5-amine was treated with benzyl alcohol to produce **3h** in high yield (Table 7, 87%). Heteroaromatic amines like 2-aminopyridine, 3-aminopyridine, and 2-aminopyrimidine were successfully converted into products **3d**–**f** in good yield (Table 7, 81%–86%). The secondary amine morpholine (**3i**), on the other hand, was not tolerated. The *N*-alkylation of *p*-nitroaniline with benzyl alcohol and the *N*-alkylation of aniline with 4-nitrobenzyl alcohol were also not successful, even with a greater catalyst loading (2 mol %) when conducted at 110 °C. These observations indicate that nitro groups are not tolerated by **1e**.

3.6. *N*-Methylation of anilines

N-Methylamines are commonly employed as intermediates and building blocks in the production of bulk and fine chemicals, as well as materials [64,65]. Due to the higher activation barrier (21 kcal mol^{-1}) of methanol dehydrogenation compared to that of higher alcohols, such as ethanol (16 kcal mol^{-1}), methanol can be a problematic substrate for the *N*-alkylation of amines [66]. Therefore, the *N*-methylation of amines with methanol was examined to further broaden the scope of **1e** promoted C–N bond formation. To our delight, we were able to successfully *N*-methylate anilines with methanol in the presence of 1.0 mol % of **1e** at 110 °C (Table 8). As indicated in Table 8, the majority of the catalytic reactions were efficient, yielding at least 81% of the desired product (Table 8, **4a**–**g** in 46%–97% yield). When 2-iodoaniline was used, the reaction produced **5g** in moderate isolated yields (46%) and was also dehalogenated. Biologically important motifs

Table 6. Aniline alkylation using a variety of primary alcohols.



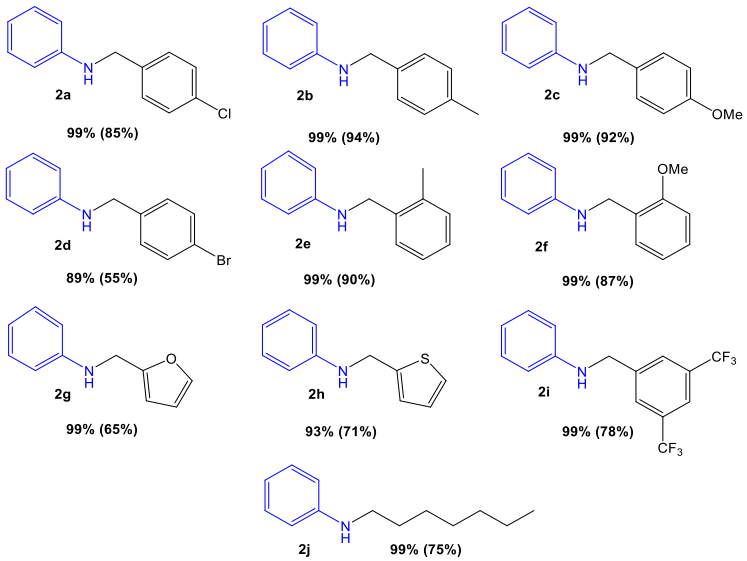
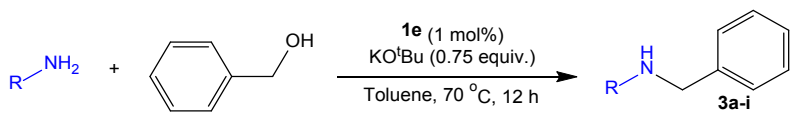


Table 7. The use of benzyl alcohol to alkylate a variety of primary amines.



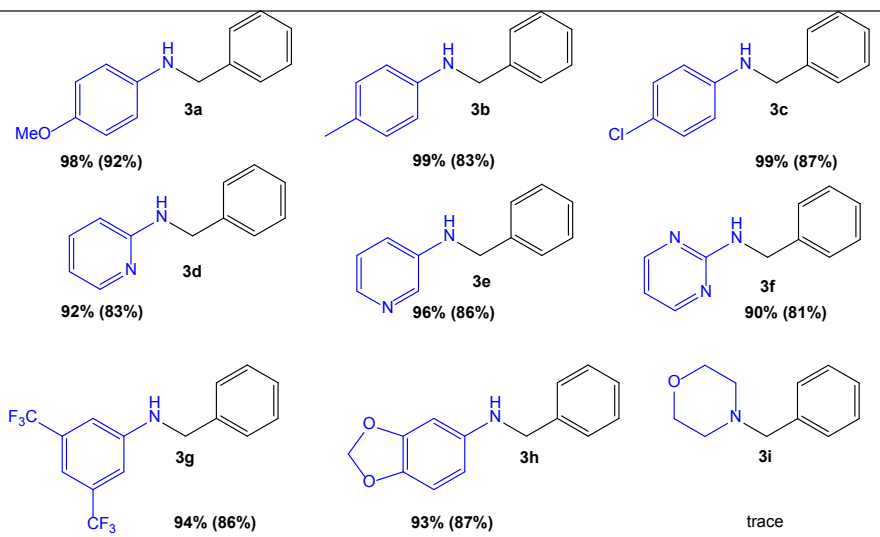
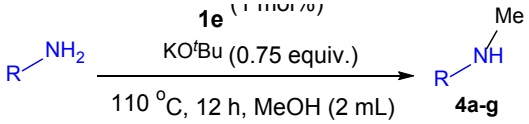


Table 8. Methylation of aromatic amines.



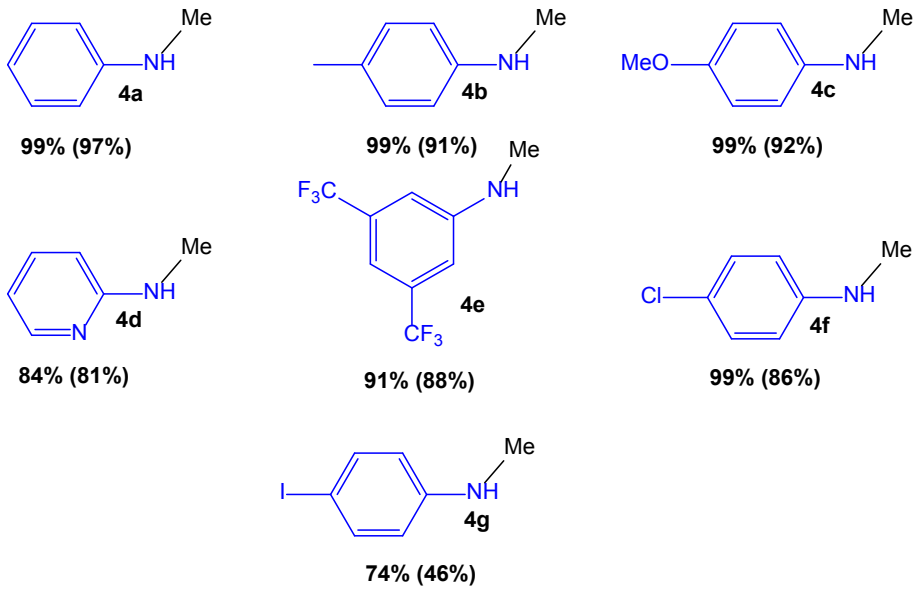


Table 9. Comparison of Ru–NHC catalyst (**1e**) with reported NHC systems.

S/NO	Cat (mol %)	Substrate 1 Alcohol	Substrate 2 Primary amine	Temp (°C)	Time (h)	Yield (%)	Reference
1	1	aniline	Substituted alcohol	70	12	92	This work
2	2.5	-	-	120	24	97	[38]
3[a]	1.0	Substituted aniline	MeOH	150	24	84	[67]
4	0.5	-	-	130	24	85	[68]
5	1.0	-	-	135	36	95	[69]

[a]For the same reaction we use **1e** (1 mol %) at 110 °C for 12 h and we get 97% selective yield.

like pyridine-2-amine and 3-trifluoromethylaniline were also successfully methylated (Table 8, **4d** and **4e**). Despite the use of copious MeOH and high temperatures, we did not observe dialkylation products in any case. Attempts to obtain *N*-methylate aliphatic amines like benzylamine and *n*-hexylamine, on the other hand, were ineffective, giving just traces of methylated product.

A comparison of the most active catalyst (**1e**) with other reported catalysts is shown in Table 9. It is the best Ru–NHC-based catalyst in terms of low catalyst loading (1 mol %) and low temperature (70 °C). Furthermore, most of the literature reports that the hydrogen transfer reaction is used to convert the alcohol into ketone or aldehyde using Ru–NHC complexes. Very few reports of such secondary amine products through the coupling of primary amine and alcohols have been reported using ruthenium–NHC complexes. These Ru–NHC complexes are also applicable for the conversion of highly complicated products like methanol and convert them into secondary amines.

3.7. Proposed mechanism

Given that catalysis requires the presence of KO^{t}Bu (75 mol % relative to 1.0 mol % of **1e**), it is reasonable to propose that a salt metathesis reaction occurs to form the corresponding bis(*tert*-butoxide) complex, which can undergo σ-bond metathesis with incoming benzyl alcohol to generate intermediate **A** (Scheme 2).

Alternatively, intermediate **A** may be generated directly from **1e** if any KOBn is generated in solution. This intermediate can undergo subsequent β-hydride elimination steps to generate **B** and ultimately dihydride complex **C**. As has been observed for other hydrogen borrowing C–N bond forming reactions, the in situ generation of aldehyde results in Schiff base condensation with any primary amine that is present to generate the corresponding aldimine (this is also the reason why secondary amines do not become alkylated again to yield tertiary amines). This aldimine can insert into dihydride **C** to generate intermediate **E**. At this point, the desired secondary amine product can be liberated in one of two ways. Reductive elimination from **E** can occur to generate intermediate **D** (as shown in Scheme 2) or **E** can undergo σ-bond metathesis with the next equivalent of benzyl alcohol to generate intermediate **B**. If Ru(0) intermediate **D** is formed during the reaction, it quickly reacts with any alcohol or hydrogen that is present to generate the corresponding hydride complex.

4. Conclusion

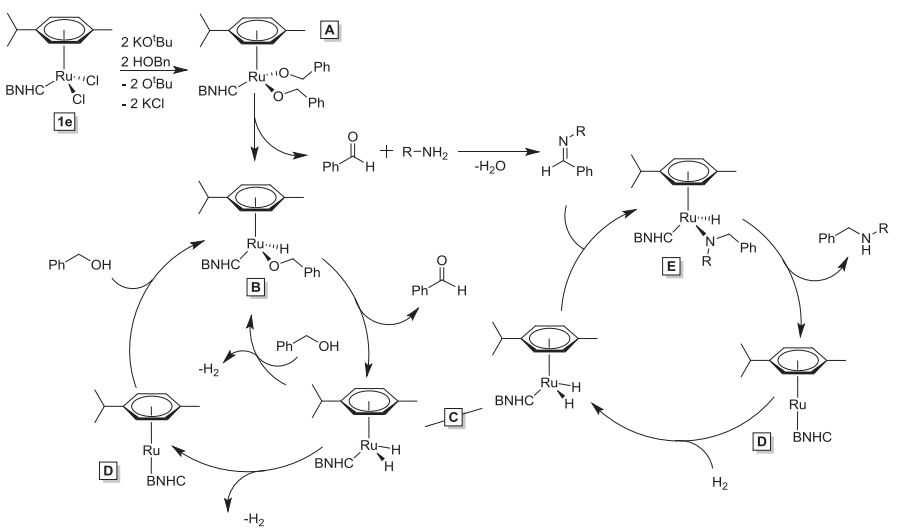
We have described the synthesis and characterization of a series of ruthenium complexes with BNHC proligands that feature a variety of benzyl group substitution patterns. Through a HB/HA mechanism, these compounds were discovered to be highly effective catalysts for the selective monoalkylation of aromatic primary amines. Complex **1e** was the most active of the catalysts tested, and it is one of the most active ruthenium catalysts ever reported for amine alkylation given that it operates efficiently at temperatures as low as 50 °C at low catalyst loadings (1.0 mol %). A wide range of (hetero) aromatic amines and primary alcohols were successfully converted into secondary amines in good to exceptional isolated yields, including physiologically relevant examples. The methylation of primary amines was also achieved using methanol, a transformation that is particularly difficult to demonstrate.

Acknowledgments

Z.N. gratefully acknowledges the Higher Education Commission of Pakistan (HEC) for research funding as an IRSIP fellow at Arizona State University (USA). The authors express their gratitude to TÜBİTAK for financing PhD research (2216 Research Fellowship Program) and BÇ thanks TÜBA for financial support. This study was supported by the Scientific Research Projects Unit of Ondokuz Mayıs University (Project No: PYO.FEN.1906.19.001).

Appendix A. Supplementary data

CCDC 2085163 and 2173756 contain the supplementary crystallographic data for the compounds reported in this article. These data can be obtained free of charge on application to CCDC, 12 Union Road, Cambridge CB2 1EZ, UK.



Scheme 2. A plausible mechanism for C–N bond formation catalyzed by **1e**.

References

[1] Brown BR. The Organic Chemistry of Aliphatic Nitrogen Compounds. Oxford, UK: Oxford University Press, 1994.

[2] Hu S, Tat D, Martinez CA, Yazbeck DR, Tao J. An efficient and practical chemoenzymatic preparation of optically active secondary amines. Organic Letters 2005; 7: 4329-4331. https://doi.org/10.1021/ol051392n

[3] Zhu A, Zhan W, Liang Z, Yoon Y, Yang H et al. Dipyrimidine amines: a novel class of chemokine receptor type 4 antagonists with high specificity. Journal of Medicinal Chemistry 2010; 53 (24): 8556-8568. https://doi.org/10.1021/jm100786g

[4] Chen J, Zhou H, Aguilar A, Liu L, Bai L et al. Structure-based discovery of BM-957 as a potent small-molecule inhibitor of Bcl-2 and Bcl-xL capable of achieving complete tumor regression. Journal of Medicinal Chemistry 2012; 55 (19): 8502-8514. https://doi.org/10.1021/jm3010306

[5] Salvatore RN, Yoon CH, Jung KW. Synthesis of secondary amines. Tetrahedron 2001; 57 (37): 7785-7812. https://doi.org/10.1016/S0040-4020(01)00722-0

[6] Boros EE, Thompson JB, Katamreddy SR, Carpenter AJ. Facile reductive amination of aldehydes with electron-deficient anilines by acyloxyborohydrides in TFA: application to a diazaindoline scale-up. The Journal of Organic Chemistry 2009; 74 (9): 3587-3590. https://doi.org/10.1021/jo900157z

[7] Alonso F, Riente P, Yus M. Nickel nanoparticles in hydrogen transfer reactions. Accounts of Chemical Research 2011; 44 (5): 379-391. https://doi.org/10.1021/ar1001582

[8] Yang BH, Buchwald SL. Palladium-catalyzed amination of aryl halides and sulfonates. Journal of Organometallic Chemistry 1999; 576 (1-2): 125-146. https://doi.org/10.1016/S0022-328X(98)01054-7

[9] Beller M, Seayad J, Tillack A, Jiao H. Catalytic Markovnikov and anti-Markovnikov functionalization of alkenes and alkynes: recent developments and trends. Angewandte Chemie International Edition 2004; 43 (26): 3368-3398. https://doi.org/10.1002/anie.200300616

[10] Hannedouche J, Schulz E. Asymmetric hydroamination: a survey of the most recent developments. Chemistry A European Journal 2013; 19 (16): 4972-4985. https://doi.org/10.1002/chem.201203956

[11] Ahmed M, Seayad AM, Jackstell R, Beller M. Amines made easily: a highly selective hydroaminomethylation of olefins. Journal of the American Chemical Society 2003; 125 (34): 10311-10318. https://doi.org/10.1021/ja030143w

[12] Guillena G, Ramon DJ, Yus M. Hydrogen autotransfer in the N-alkylation of amines and related compounds using alcohols and amines as electrophiles. Chemical Reviews 2010; 110 (3): 1611-1641. https://doi.org/10.1021/cr9002159

[13] Watson AJ, Williams JM. The give and take of alcohol activation. Science 2010; 329 (5992): 635-636. https://doi.org/10.1126/science.1191843

[14] Nandakumar A, Midya SP, Landge VG, Balaraman E. Transition-metal-catalyzed hydrogen-transfer annulations: access to heterocyclic scaffolds. Angewandte Chemie International Edition 2015; 54 (3): 11022-11034. https://doi.org/10.1002/anie.201503247

[15] Ma X, Su C, Xu Q. N-Alkylation by hydrogen autotransfer reactions. In: Guillena G, Ramón D (editors). Hydrogen Transfer Reactions. Topics in Current Chemistry Collections. Springer Cham. 2016, pp. 291-364.

[16] Grigg R, Mitchell T, Sutthivaiyakit S, Tongpenyai N. Transition metal-catalysed N-alkylation of amines by alcohols. Journal of the Chemical Society, Chemical Communications 1981; 611-612. https://doi.org/10.1039/C39810000611

[17] Watanabe Y, Tsuji Y, Ohsugi Y. The ruthenium catalyzed N-alkylation and N-heterocyclization of aniline using alcohols and aldehydes. Tetrahedron Letters 1981; 22 (28): 2667-2670. https://doi.org/10.1016/S0040-4039(01)92965-X

[18] Huang M, Li Y, Lan XB, Liu J, Zhao C et al. Ruthenium (II) complexes with N-heterocyclic carbene–phosphine ligands for the N-alkylation of amines with alcohols. Organic & Biomolecular Chemistry 2021; 19: 3451-3461. https://doi.org/10.1039/D1OB00362C

[19] Das K, Nandi PG, Islam K, Srivastava HK, Kumar A. N–alkylation of amines catalyzed by a ruthenium–pincer complex in the presence of in situ generated sodium alkoxide. European Journal of Organic Chemistry 2019; 2019 (40) 6855-6866. https://doi.org/10.1002/ejoc.201901310

[20] Celaje JJA, Zhang X, Zhang F, Kam L, Herron JR et al. A base and solvent-free ruthenium-catalyzed alkylation of amines. ACS Catalysis 2017; 7 (2): 1136-1142. https://doi.org/10.1021/acscatal.6b03088

[21] Imm S, Baehn S, Neubert L, Neumann H, Beller M. An efficient and general synthesis of primary amines by ruthenium-catalyzed amination of secondary alcohols with ammonia. Angewandte Chemie International Edition 2010; 49 (44): 8126-8129. https://doi.org/10.1002/anie.201002576

[22] Mamidala R, Mukundam V, Dhanunjayarao K, Venkatasubbaiah K. Cyclometalated palladium pre-catalyst for N-alkylation of amines using alcohols and regioselective alkylation of sulfanilamide using aryl alcohols. Tetrahedron 2017; 73 (16): 2225-223 https://doi.org/10.1016/j.tet.2017.03.001

[23] Dang TT, Ramalingam B, Shan SP, Seayad AM. An efficient palladium-catalyzed N-alkylation of amines using primary and secondary alcohols. ACS Catalysis 2013; 3 (11) 2536-2540. https://doi.org/10.1021/cs400799n

[24] Martinez-Asencio A, Yus M, Ramon DJ. Palladium (II) acetate as catalyst for the N-alkylation of aromatic amines, sulfonamides, and related nitrogenated compounds with alcohols by a hydrogen autotransfer process. Synthesis 2011; (22) 3730-3740. https://doi.org/10.1055/s-0030-1260238

[25] Guérin V, Legault CY. Synthesis of NHC-iridium (III) complexes based on N-iminoimidazolium ylides and their use for the amine alkylation by borrowing hydrogen catalysis. Organometallics 2021; 40 (3): 408-417. https://doi.org/10.1021/acs.organomet.0c00726

[26] Luo N, Zhong Y, Wen H, Luo R. Cyclometalated iridium complex-catalyzed *N*-alkylation of amines with alcohols via borrowing hydrogen in aqueous media. ACS Omega 2020; 5 (42): 27723-27732. https://doi.org/10.1021/acsomega.0c04192

[27] Fujita KI, Furukawa S, Morishima N, Shimizu M, Yamaguchi R. N-alkylation of aqueous ammonia with alcohols leading to primary amines catalyzed by water-soluble N-heterocyclic carbene complexes of iridium. ChemCatChem 2018; 10 (9): 1993-1997. https://doi.org/10.1002/cctc.201702037

[28] Tsuji Y, Takeuchi R, Ogawa H, Watanabe Y. Platinum complex catalyzed transformation of amine. N-alkylation and N-allylation using primary alcohols. Chemistry Letters 1986; 15 (3); 293-294. https://doi.org/10.1246/cl.1986.293

[29] Fertig R, Irrgang T, Freitag F, Zander J, Kempe R. Manganese-catalyzed and base-switchable synthesis of amines or imines via borrowing hydrogen or dehydrogenative condensation. ACS Catalysis 2018; 8 (9); 8525-8530. https://doi.org/10.1021/acscatal.8b02530

[30] Reed-Berendt BG, Polidano K, Morrill LC. Recent advances in homogeneous borrowing hydrogen catalysis using earth-abundant first row transition metals. Organic & Biomolecular Chemistry 2019; 17: 1595-1607. https://doi.org/10.1039/C8OB01895B

[31] Balamurugan G, Ramesh R, Malecki JG. Nickel (II)–N^N^O pincer type complex-catalyzed N-alkylation of amines with alcohols via the hydrogen autotransfer reaction. The Journal of Organic Chemistry 2020: 85 (11) 7125-7135. https://doi.org/10.1021/acs.joc.0c00530

[32] Polidano K, Allen BD, Williams JM, Morrill LC. Iron-catalyzed methylation using the borrowing hydrogen approach. ACS Catalysis 2018; 8 (7): 6440-6445. https://doi.org/10.1021/acscatal.8b02158

[33] Llabres-Campaner PJ, Ballesteros-Garrido R, Ballesteros R, Abarca B. β-Amino alcohols from anilines and ethylene glycol through heterogeneous Borrowing Hydrogen reaction. Tetrahedron 2017; 73 (37): 5552-5561. https://doi.org/10.1016/j.tet.2017.08.006

[34] Montgomery SL, Mangas-Sanchez J, Thompson MP, Aleku GA, Dominguez B et al. Direct alkylation of amines with primary and secondary alcohols through biocatalytic hydrogen borrowing. Angewandte Chemie International Edition 2017; 129 (35): 10627-10630. https://doi.org/10.1002/ange.201705848

[35] Thompson MP, Turner NJ. Two-enzyme hydrogen-borrowing amination of alcohols enabled by a cofactor-switched alcohol dehydrogenase. ChemCatChem 2017; 9 (20): 3833-3836. https://doi.org/10.1002/cctc.201701092

[36] Eka Putra A, Oe Y, Ohta T. Ruthenium-catalyzed enantioselective synthesis of β-amino alcohols from 1, 2-diols by "Borrowing Hydrogen." European Journal of Organic Chemistry 2013; 2013 (27): 6146-6151. https://doi.org/10.1002/ejoc.201300692

[37] Saidi O, Blacker AJ, Farah MM, Marsden SP, Williams JM. Selective amine cross-coupling using iridium-catalyzed "Borrowing Hydrogen" methodology. Angewandte Chemie International Edition 2009; 121 (40): 7511-7514. https://doi.org/10.1002/ange.200904028

[38] Kaloğlu M, Gürbüz N, Sémeril D, Özdemir İ. Ruthenium (II)-(p-cymene)-N-heterocyclic carbene complexes for the N-alkylation of amine using the green hydrogen borrowing methodology. European Journal of Organic Chemistry 2018; (10): 1236-1243. https://doi.org/10.1002/ejic.201701479

[39] Kaloğlu N, Achard M, Bruneau C, Özdemir İ. Ruthenium (II)-(arene)-N-heterocyclic carbene complexes: efficient and selective catalysts for the N-alkylation of aromatic amines with alcohols. European Journal of Organic Chemistry 2019; 2019 (21): 2598-2606. https://doi.org/10.1002/ejic.201900191

[40] Şahin N, Özdemir N, Gürbüz N, Özdemir İ. Novel N-alkylbenzimidazole-ruthenium (II) complexes: synthesis and catalytic activity of N-alkylating reaction under solvent-free medium. Applied Organometallic Chemistry 2019; 33 (2): e4704. https://doi.org/10.1002/aoc.4704

[41] Çicek M, Gürbüz N, Özdemir N, Özdemir İ, İspir E. Half-sandwich Ru (II) arene complexes bearing benzimidazole ligands for the N-alkylation reaction of aniline with alcohols in a solvent-free medium. New Journal of Chemistry 2021; 45: 11075-11085. https://doi.org/10.1039/D1NJ01539G

[42] Podyacheva E, Afanasyev OI, Vasilyev DV, Chusov D. Borrowing hydrogen amination reactions: a complex analysis of trends and correlations of the various reaction parameters. ACS Catalysis 2022; 12 (12): 7142-7198. https://doi.org/10.1021/acscatal.2c01133

[43] Banerjee D, Kabadwal LM, Bera S. Recent advances in sustainable organic transformations using methanol: expanding the scope of hydrogen borrowing catalysis, Organic Chemistry Frontiers 2021; 8: 7077-7096. https://doi.org/10.1039/D1QO01412A

[44] Moutaoukil Z, Serrano-Díez E, Collado IG, Jimenez-Tenorio M, Botubol-Ares JM. N-Alkylation of organonitrogen compounds catalyzed by methylene-linked bis-NHC; half-sandwich ruthenium complexes. Organic & Biomolecular Chemistry 2022; 20: 831-839. https://doi.org/10.1039/D1OB02214H

[45] Arduengo III AJ, Dias HR, Harlow RL, Kline M. Electronic stabilization of nucleophilic carbenes. Journal of the American Chemical Society 1992; 114 (14): 5530-5534. https://doi.org/10.1021/ja00040a007

[46] Sanford MS, Love JA, Grubbs RH. A versatile precursor for the synthesis of new ruthenium olefin metathesis catalysts. Organometallics 2021; 20 (25): 5314-5318. https://doi.org/10.1021/om010599r

[47] Herrmann WA, Köcher C. N-Heterocyclic carbenes. Angewandte Chemie International Edition 1997; 36 (20): 2162-2187. https://doi.org/10.1002/anie.199721621

[48] Meeniga I, Gokanapalli A, Peddiahgari VGR. Synthesis of environmentally benign new ionic liquids for the preparation of 2-aryl/heteroaryl benzimidazoles/benzoxazoles under ultrasonication. Sustainable Chemistry and Pharmacy 2022; 30: 100874-100879. https://doi.org/10.1016/j.scp.2022.100874

[49] Wang WQ, Wang ZQ, Sang W, Zhang R, Cheng H et al. Dehydrogenative amide synthesis from alcohols and amines utilizing N-heterocyclic carbene-based ruthenium complexes as efficient catalysts: the influence of catalyst loadings, ancillary and added ligands. Polyhedron 2021; 195: 114979-114981. https://doi.org/10.1016/j.poly.2020.114979

[50] Huang M, Li Y, Lan XB, Liu J, Zhao C et al. Ruthenium (II) complexes with N-heterocyclic carbene–phosphine ligands for the *N*-alkylation of amines with alcohols. Organic & Biomolecular Chemistry 2021; 19: 3451-3461. https://doi.org/10.1039/D1OB00362C

[51] Shan SP, Xiaoke X, Gnanaprakasam B, Dang TT, Ramalingam B et al. Benzimidazolin-2-ylidene N-heterocyclic carbene complexes of ruthenium as a simple catalyst for the N-alkylation of amines using alcohols and diols. RSC Advances 2015; 5: 4434-4442. https://doi.org/10.1039/C4RA15398G

[52] Şahin Z, Gürbüz N, Özdemir İ, Şahin O, Büyükgüngör O et al. N-Alkylation and N, C-dialkylation of amines with alcohols in the presence of ruthenium catalysts with chelating N-heterocyclic carbene ligands. Organometallics 2015; 34 (11): 2296-2304. https://doi.org/10.1021/om501066n

[53] Nawaz Z, Ullah H, Gürbüz N, Zafar MN, Verpoort F et al. Benzimidazole-based N-heterocyclic carbene silver complexes as catalysts for the formation of carbonates from carbon dioxide and epoxides. Molecular Catalysis 2022; 526 (60): 112369-112380. http://dx.doi.org/10.1016/j.mcat.2022.112369

[54] Burla MC, Caliandro R, Carrozzini B, Cascarano GL, Cuocci C et al. Crystal structure determination and refinement via SIR2014. Journal of Applied Crystallography 2015; 48: 306-309. https://doi.org/10.1107/S1600576715001132

[55] Sheldrick GM. A short history of SHELX. Acta Crystallographica Section A 2008; A64: 112-122. https://doi.org/10.1107/S0108767307043930

[56] Dolomanov OV, Bourhis LJ, Gildea RJ, Howard JA, Puschmann H. OLEX2: a complete structure solution, refinement and analysis program. Journal of Applied Crystallography 2009; 42: 339-341. https://doi.org/10.1107/S0021889808042726

[57] Nawaz Z, Gürbüz N, Zafar MN, Tahir MN, Ashfaq M et al. Direct arylation (hetero-coupling) of heteroarenes via unsymmetrical palladium-PEPPSI-NHC type complexes. Polyhedron 2021; 208: 115412-115410. https://doi.org/10.1016/j.poly.2021.115412

[58] Hackenberg F, Müller-Bunz H, Smith R, Streciwilk W, Zhu X et al. Novel ruthenium (II) and gold (I) NHC complexes: synthesis, characterization, and evaluation of their anticancer properties. Organometallics 2013; 32 (19): 5551-5560. https://doi.org/10.1021/om400819p

[59] Tay BY, Wang C, Phua PH, Stubbs LP, Huynh HV. Selective hydrogenation of levulinic acid to γ-valerolactone using *in situ* generated ruthenium nanoparticles derived from Ru–NHC complexes. Dalton Transactions 2016; 45: 3558-3563. https://doi.org/10.1039/C5DT03366G

[60] Lam NY, Truong D, Burmeister H, Babak MV, Holtkamp HU et al. From catalysis to cancer: toward structure–activity relationships for benzimidazol-2-ylidene-derived N-heterocyclic-carbene complexes as anticancer agents. Inorganic Chemistry 2018; 57 (22): 14427-14434. https://doi.org/10.1021/acs.inorgchem.8b02634

[61] Wang WQ, Yuan Y, Miao Y, Yu BY, Wang HJ et al. Well-defined N-heterocyclic carbene/ruthenium complexes for the alcohol amidation with amines: the dual role of cesium carbonate and improved activities applying an added ligand. Applied Organometallic Chemistry 2020; 34 (2): e5323-5333. https://doi.org/10.1002/aoc.5323

[62] Sarı Y, Gürses C, Celepci DB, Keleştemur Ü, Aktaş A et al. 4-Vinylbenzyl and 2-morpholinoethyl substituted ruthenium (II) complexes: design, synthesis, and biological evaluation. Journal of Molecular Structure 2020; 1202: 127355-127363. https://doi.org/10.1016/j.molstruc.2019.127355

[63] Kathuria L, Din Reshi NU, Samuelson AG. N-Heterocyclic carbene (NHC)-stabilized Ru^0 nanoparticles: in situ generation of an efficient transfer hydrogenation catalyst. Chemistry A European Journal 2020; 26 (34): 7622-7630. https://doi.org/10.1002/chem.202000142

[64] Dang TT, Ramalingam B, Seayad AM. Efficient ruthenium-catalyzed N-methylation of amines using methanol. ACS Catalysis 2015; 5 (7): 4082-4088. https://doi.org/10.1021/acscatal.5b00606

[65] Liu Z, Yang Z, Yu X, Zhang H, Yu B et al. Efficient cobalt-catalyzed methylation of amines using methanol. Advanced Synthesis & Catalysis 2017; 359 (24): 4278-4283. https://doi.org/10.1002/adsc.201701044

[66] Lin WH, Chang HF. A study of ethanol dehydrogenation reaction in a palladium membrane reactor. Catalysis Today 2004; 97 (2-3): 181-188. https://doi.org/10.1016/j.cattod.2004.03.068

[67] Illam PM, Rit A. Electronically tuneable orthometalated Ru^{II}–NHC complexes as efficient catalysts for C–C and C–N bond formations *via* borrowing hydrogen strategy. Catalysis Science & Technology 2022; 12: 67-74. https://doi.org/10.1039/D1CY01767E

[68] Donthireddy S, Mathoor Illam P, Rit A. Ruthenium (II) complexes of heteroditopic N-heterocyclic carbene ligands: efficient catalysts for C–N bond formation via a hydrogen-borrowing strategy under solvent-free conditions. Inorganic Chemistry 2020; 59 (3): 1835-1847. https://doi.org/10.1021/acs.inorgchem.9b03049

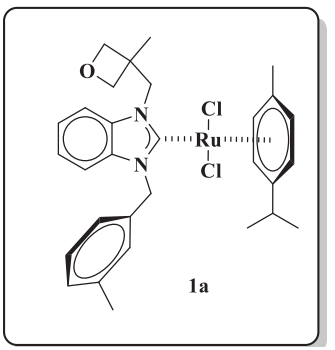
[69] Biswas N, Srimani D. Ru-catalyzed selective catalytic methylation and methylenation reaction employing methanol as the C1 source. The Journal of Organic Chemistry 2021; 86 (15): 10544-10554. https://doi.org/10.1021/acs.joc.1c01185

Supporting Information

Table of Contents

Characterizing data of ruthenium–BNHC complex **1a** S1-S2
Characterizing data of ruthenium–BNHC complex **1b** S3-S4
Characterizing data of ruthenium–BNHC complex **1c** S5-S6
Characterizing data of ruthenium–BNHC complex **1d** S7-S8
Characterizing data of ruthenium–BNHC complex **1e** S9-S10
Characterizing data of ruthenium–BNHC complex **1f** S11-S12
Characterizing data of ruthenium–BNHC complex **1g** S13-S14
Characterizing data of the tested (**2a**–**h**) substituted benzyl alcohol with aniline by the complex **1e** S15-S22
Characterizing data of the tested (**3a**–**h**) substituted aniline with benzyl alcohol by the complex **1e** S23-S30
Characterizing data of the tested (**4a**–**e**) substituted aniline with methanol by the complex **1e** S36-S36

Characterizing data of ruthenium–BNHC complex 1a
Dichloro-[1-((3-methyloxetan-3-yl)methyl)-3-(3-methylbenzyl)benzimidazole-2-ylidene](*p*-cymene) ruthenium(II) (1a)



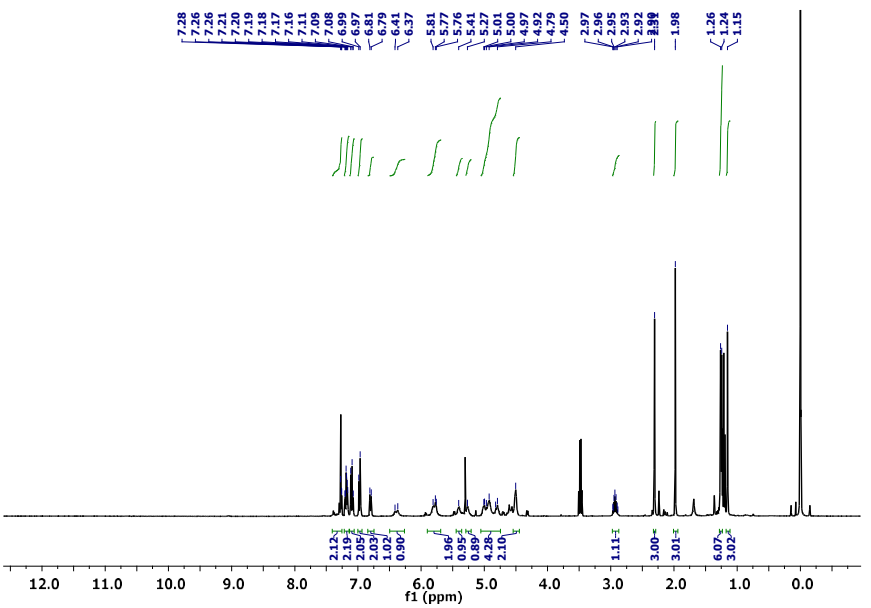


Figure S1. ^{1}H NMR spectrum of ruthenium–BNHC complex **1a** (in $CDCl_3$, 25 °C, TMS, 400 MHz).

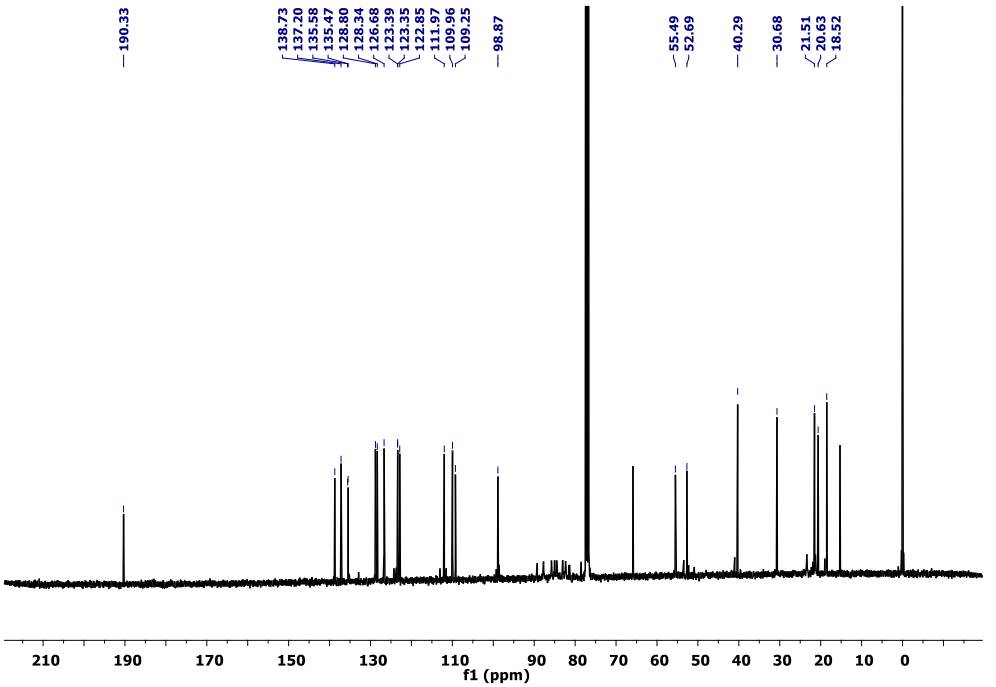


Figure S2. ^{13}C NMR spectrum of ruthenium–BNHC complex **1a** (in $CDCl_3$, 25 °C, TMS, 101 MHz).

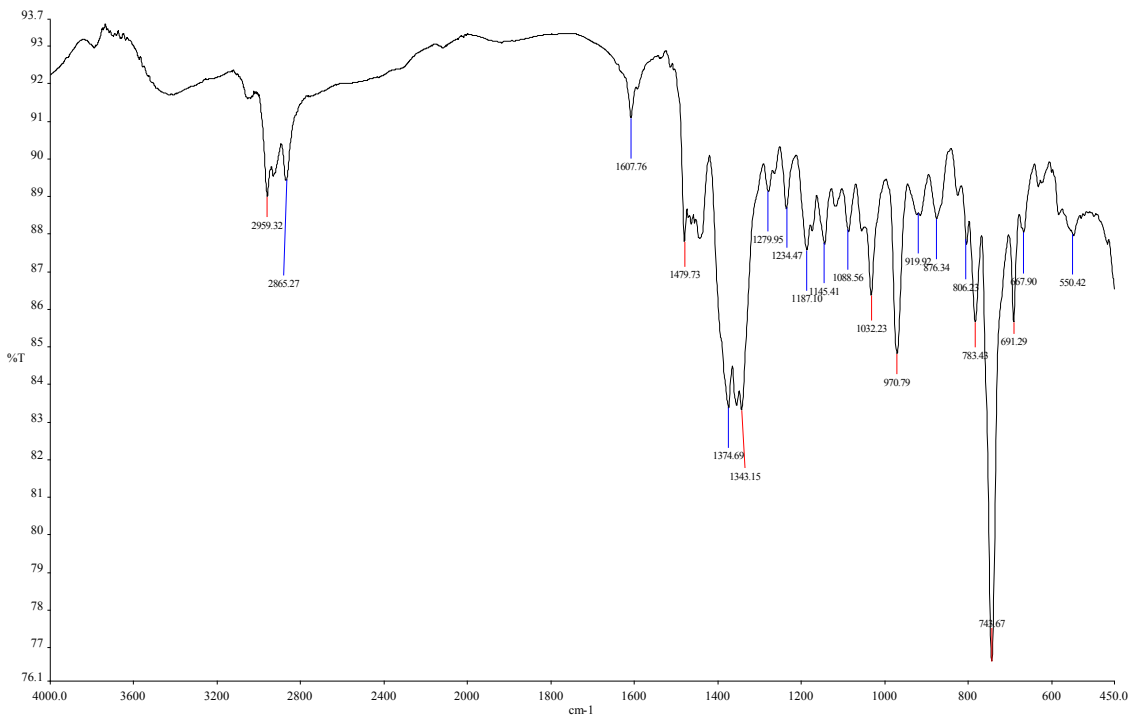
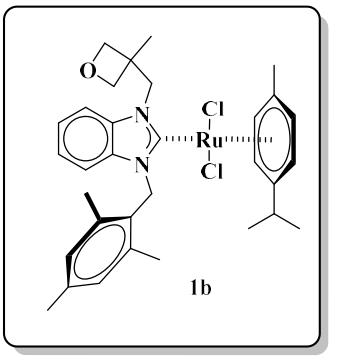


Figure S3. FT-IR spectrum of ruthenium–BNHC complex **1a**.

Characterizing data of ruthenium–BNHC complex 1b

Dichloro-[1-((3-methyloxetan-3-yl)methyl)-3-(2,4,6-trimethylbenzyl)benzimidazole-2-ylidene](*p*-cymene) ruthenium(II) (1b)



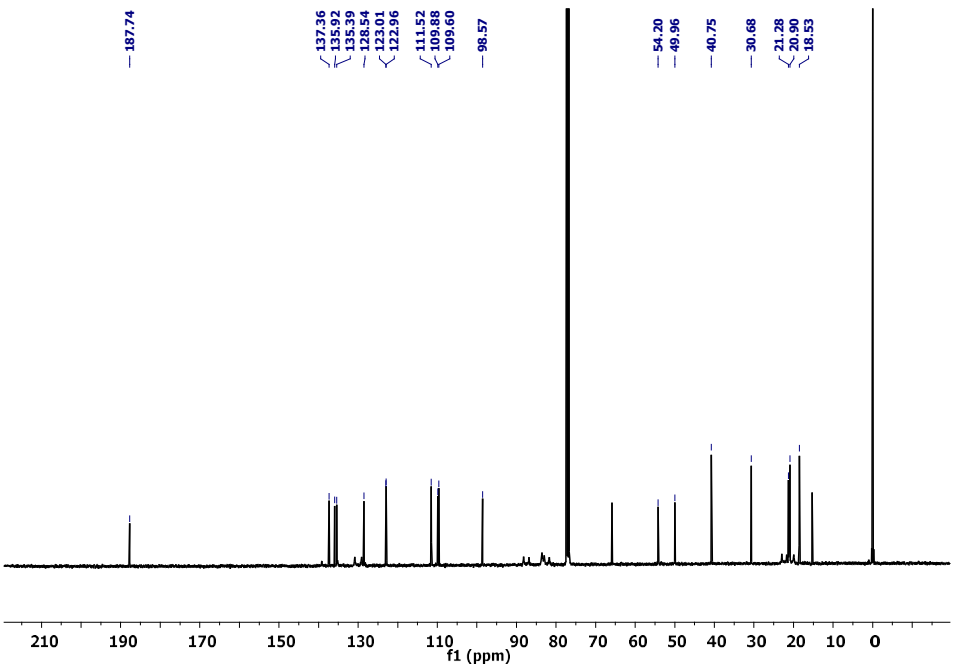


Figure S4. ^{1}H NMR spectrum of ruthenium–BNHC complex **1b** (in $CDCl_3$, 25 °C, TMS, 400 MHz).

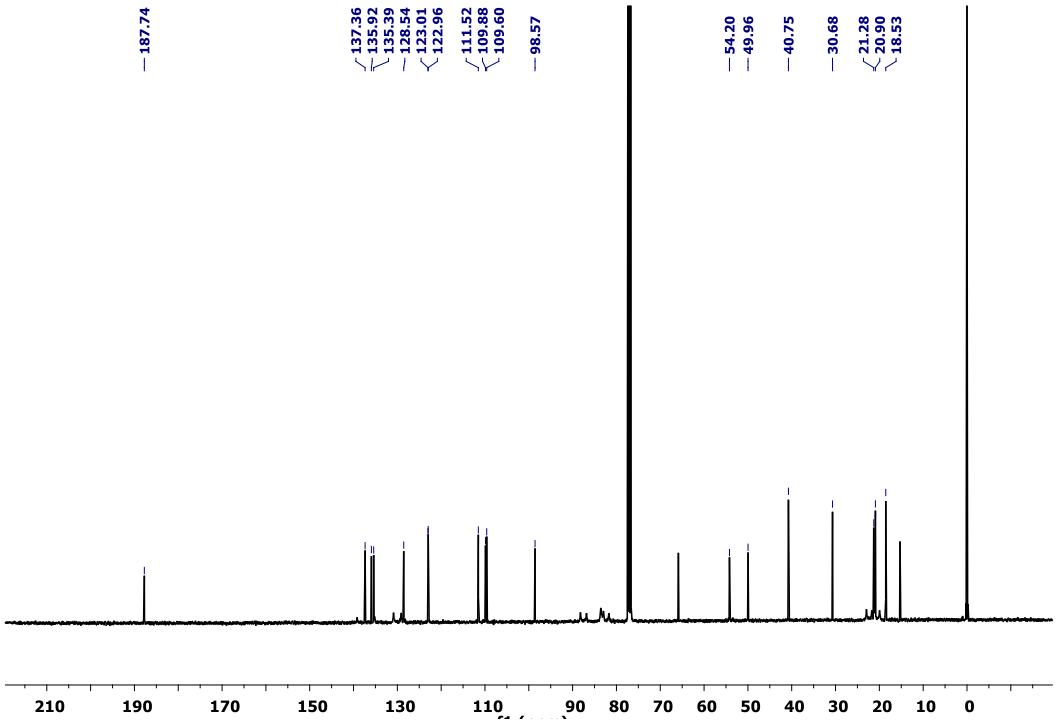


Figure S5. ^{13}C NMR spectrum of ruthenium–BNHC complex **1b** (in $CDCl_3$, 25 °C, TMS, 101 MHz).

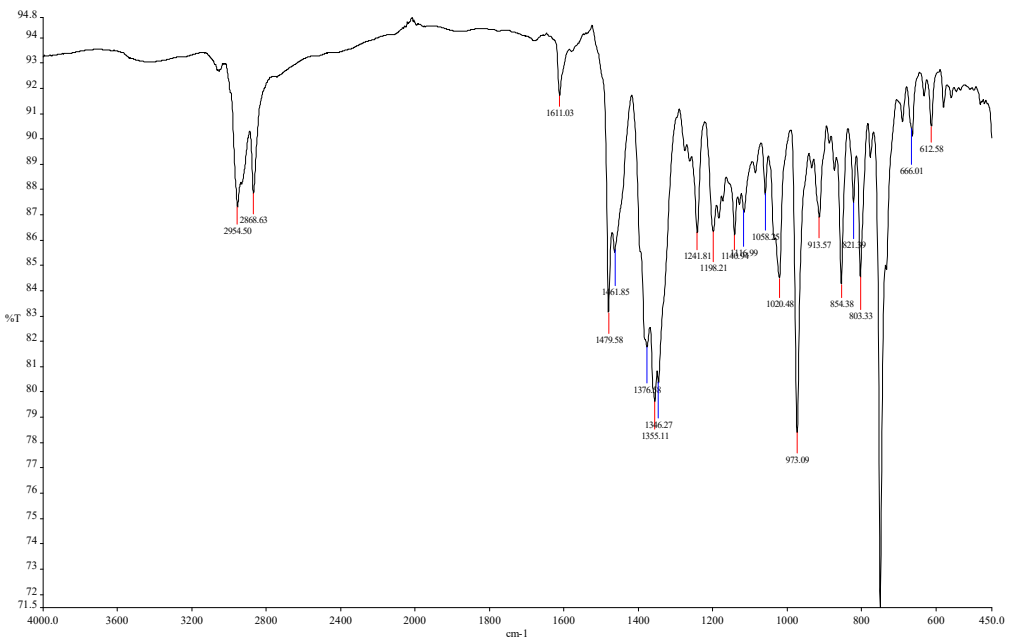
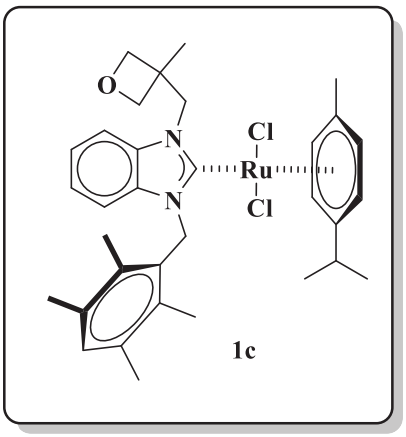


Figure S6. FT-IR spectrum of ruthenium–BNHC complex **1b**.

Characterizing data of ruthenium–BNHC complex 1c

Dichloro-[1-((3-methyloxetan-3-yl)methyl)-3-(2,3,5,6-tetramethylbenzyl)benzimidazole-2-ylidene](*p*-cymene) ruthenium(II) (1c)



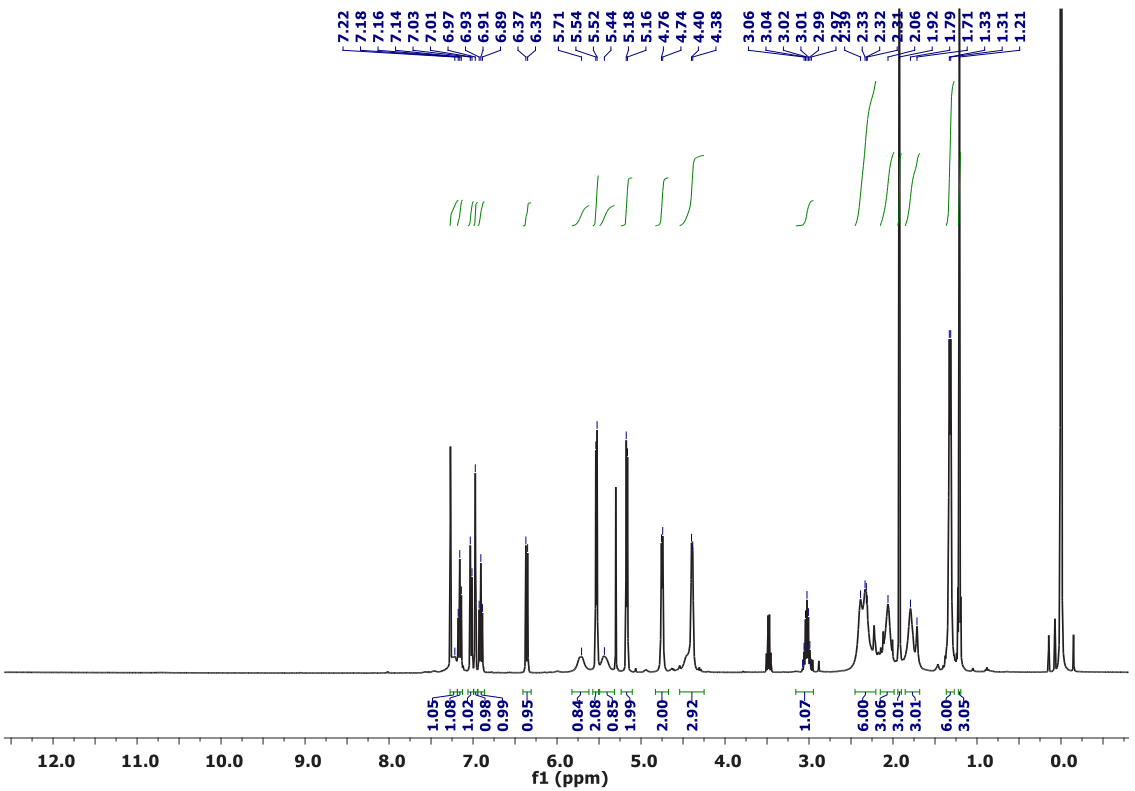


Figure S7. ^{1}H NMR spectrum of ruthenium–BNHC complex **1c** (in $CDCl_3$, 25 °C, TMS, 400 MHz).

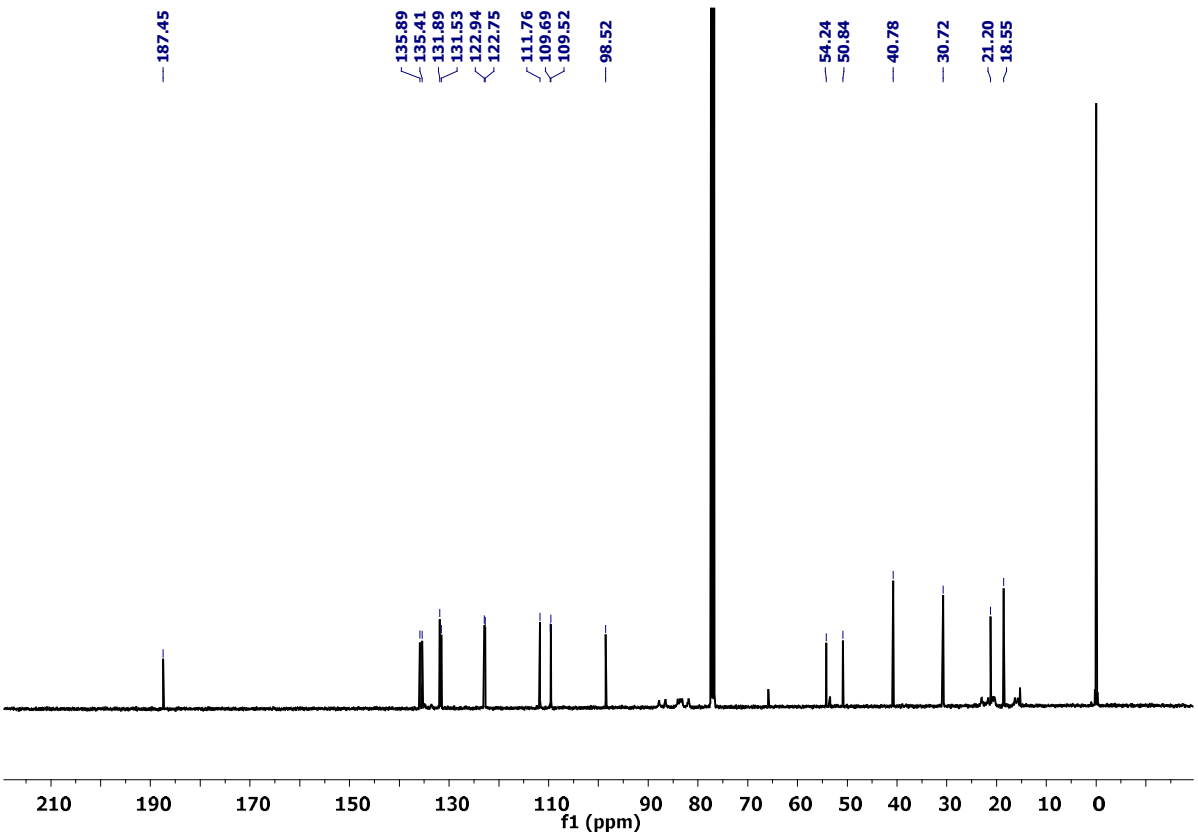


Figure S8. ^{13}C NMR spectrum of ruthenium–BNHC complex **1c** (in $CDCl_3$, 25 °C, TMS, 101 MHz).

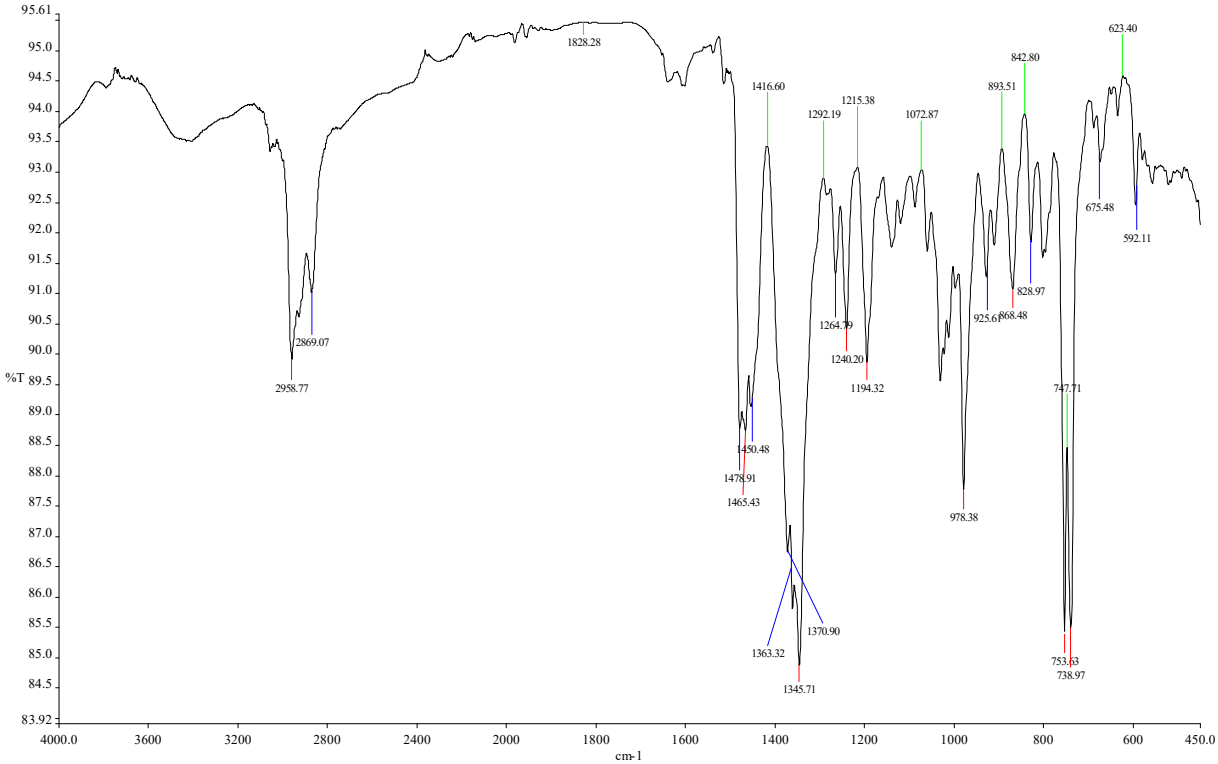
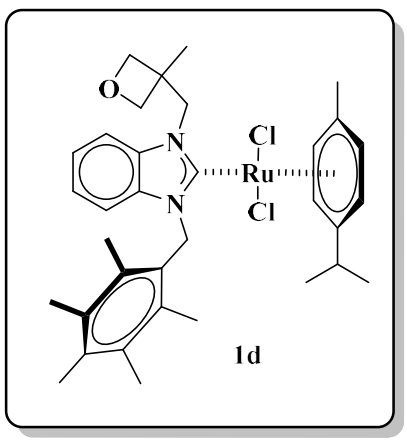


Figure S9. FT-IR spectrum of ruthenium–BNHC complex **1c**.

Characterizing data of ruthenium–BNHC complex 1d

Dichloro-[1-((3-methyloxetan-3-yl)methyl)-3-(2,3,4,5,6-pentamethylbenzyl)benzimidazole-2-ylidene](*p*-cymene) ruthenium(II) (1d)



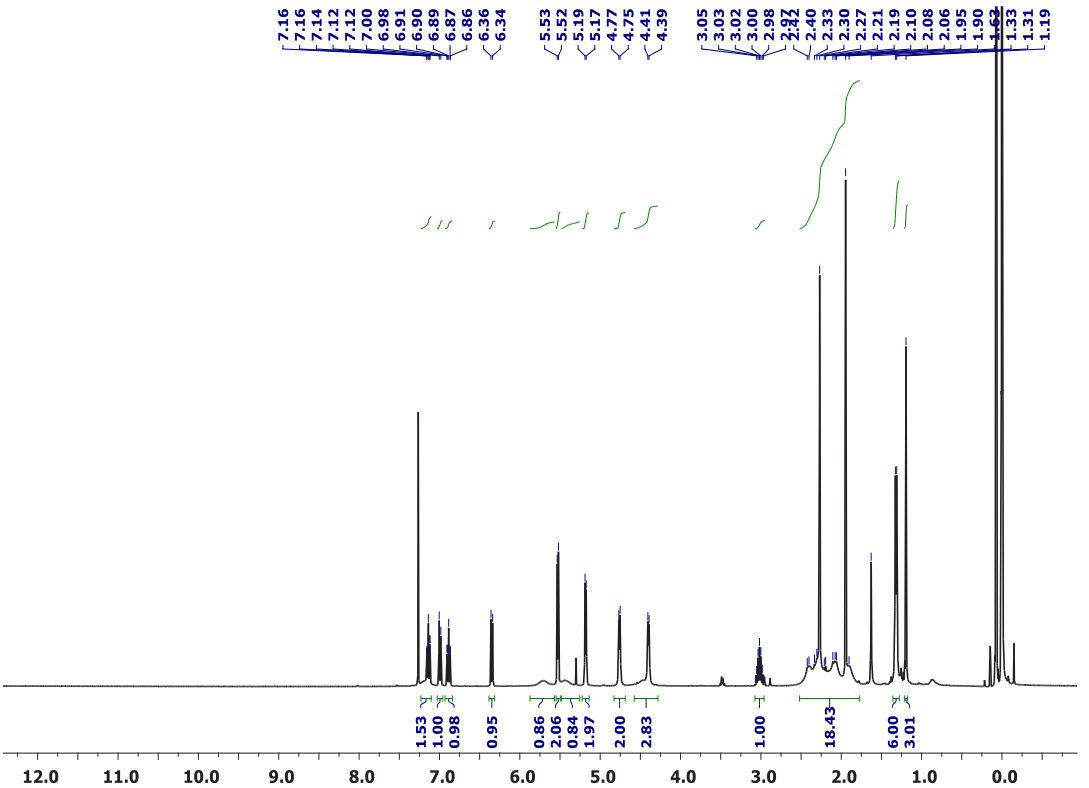


Figure S10. ^{1}H NMR spectrum of ruthenium–BNHC complex **1d** (in $CDCl_3$, 25 °C, TMS, 400 MHz).

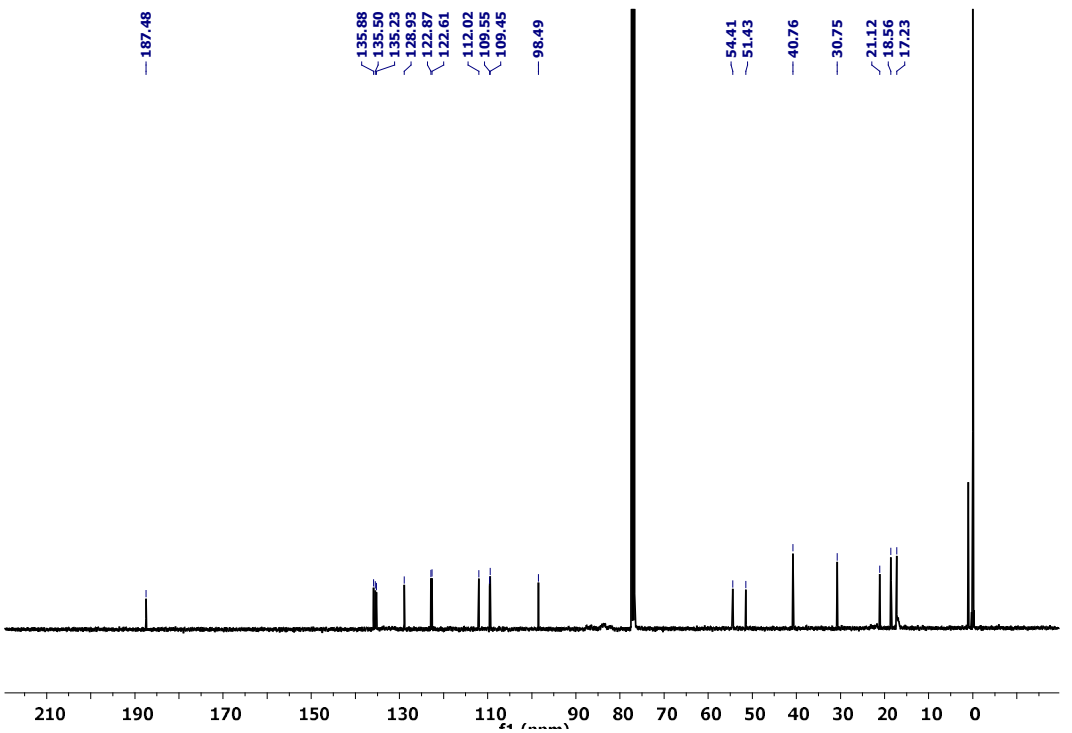


Figure S11. ^{13}C NMR spectrum of ruthenium–BNHC complex **1d** (in $CDCl_3$, 25 °C, TMS, 101 MHz).

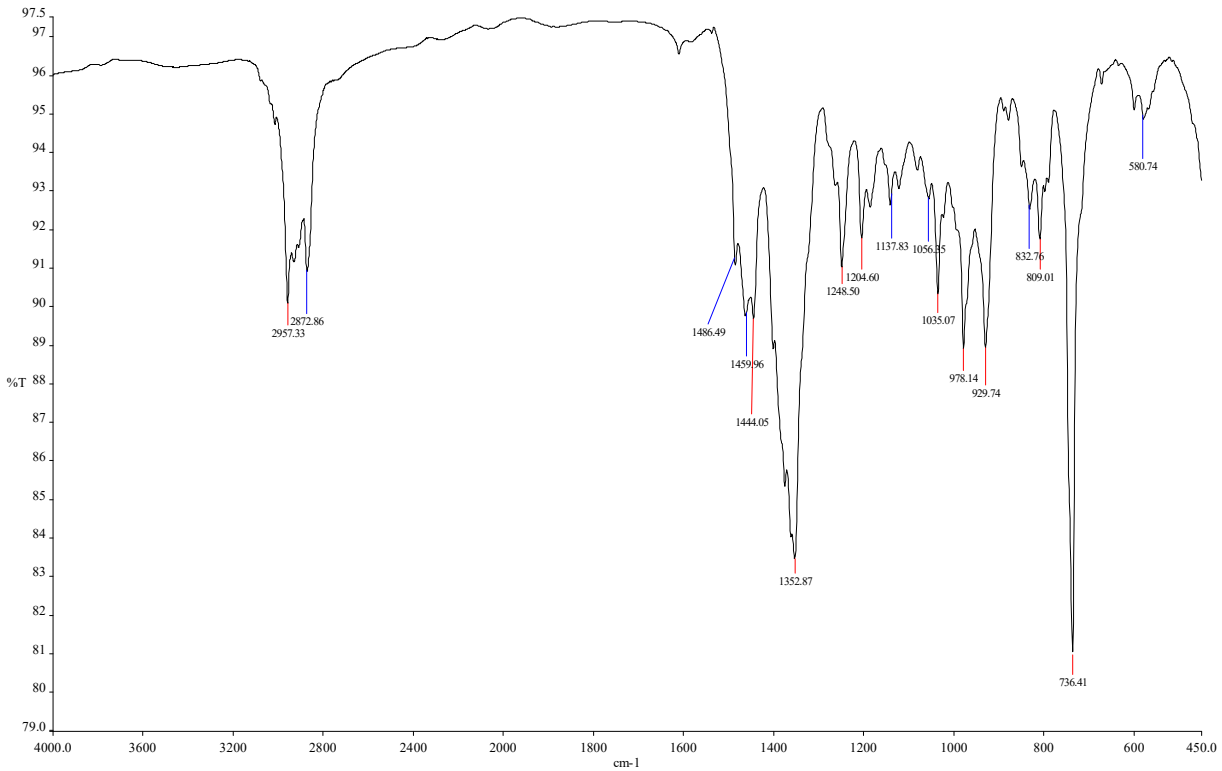
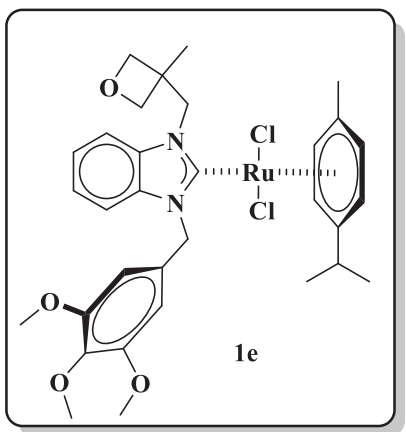


Figure S12. FT-IR spectrum of ruthenium–BNHC complex **1d**.

Characterizing data of ruthenium–BNHC complex 1e

Dichloro-[1-((3-methyloxetan-3-yl)methyl)-3-(3,4,5-trimethoxybenzyl)benzimidazole-2-ylidene](*p*-cymene) ruthenium(II) (1e)



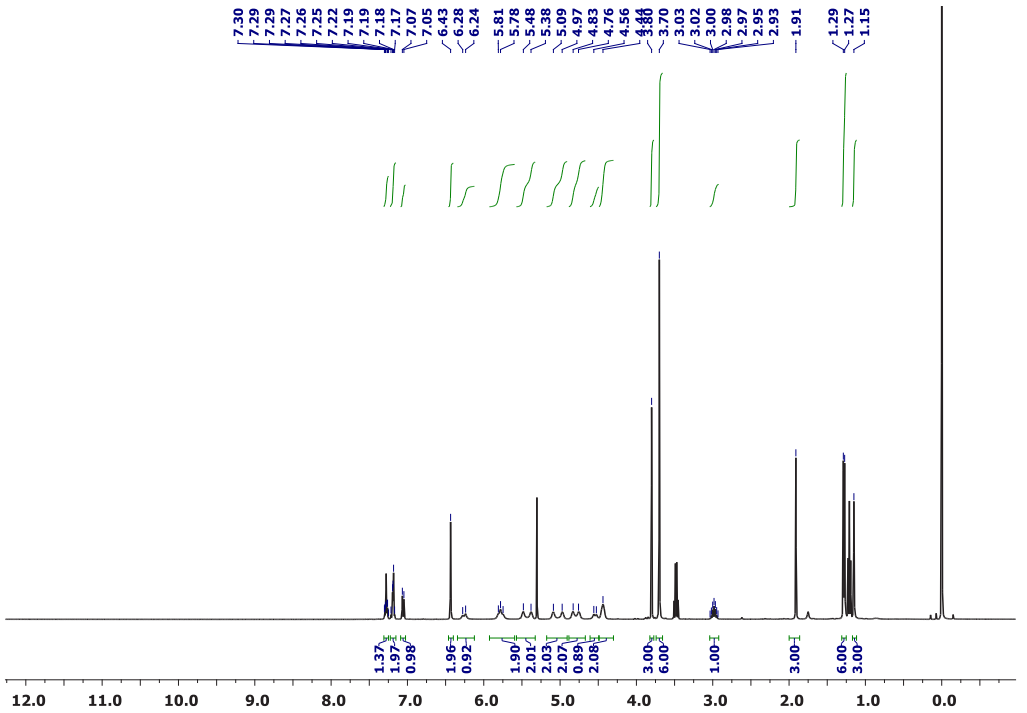


Figure S13. ^{1}H NMR spectrum of ruthenium–BNHC complex **1e** (in $CDCl_3$, 25 °C, TMS, 400 MHz).

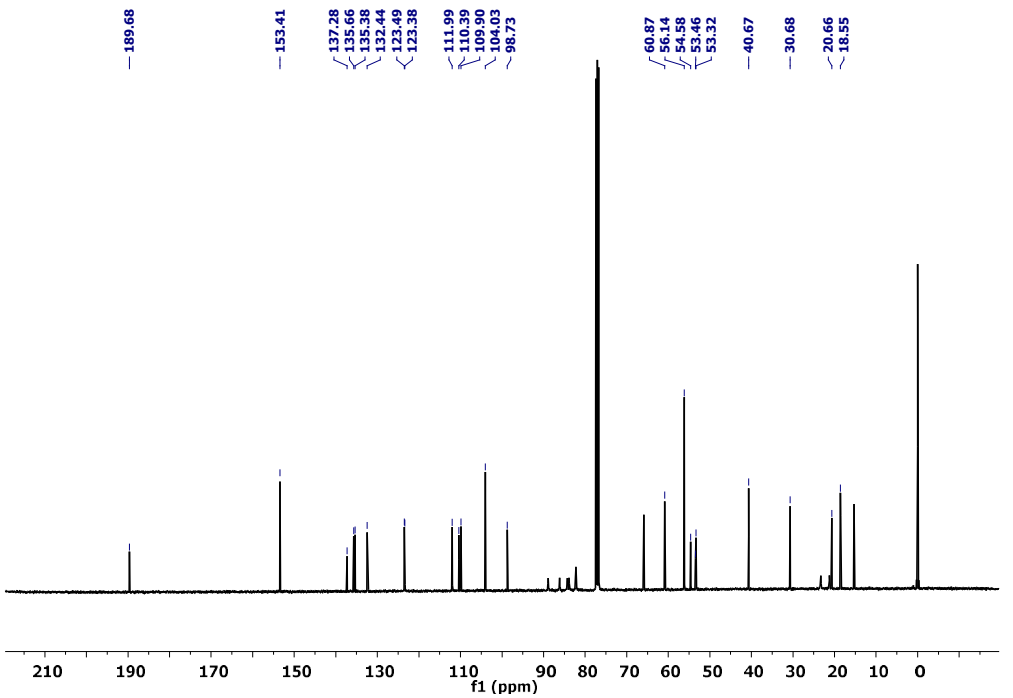


Figure S14. ^{13}C NMR spectrum of ruthenium–BNHC complex **1e** (in $CDCl_3$, 25 °C, TMS, 101 MHz).

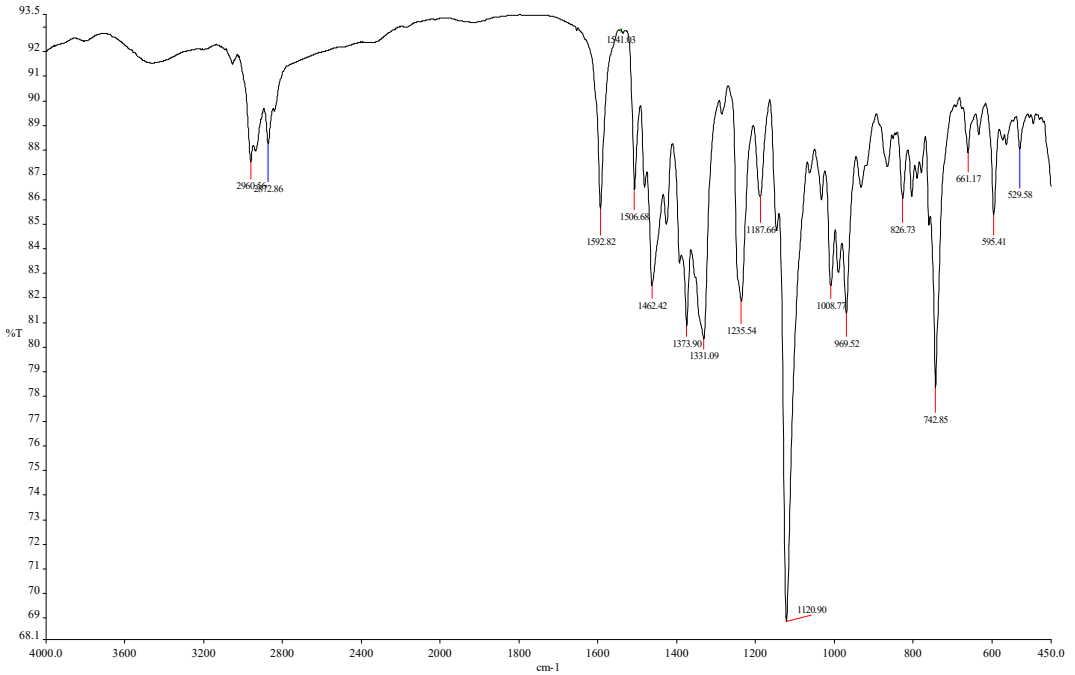
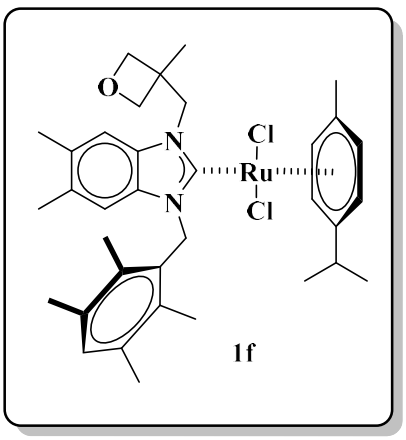


Figure S15. FT-IR spectrum of ruthenium–BNHC complex **1e**.

Characterizing data of ruthenium–BNHC complex 1f

Dichloro-[(5,6-dimethyl-1-((3-methyloxetan-3-yl)methyl)-3-(2,3,5,6-tetramethylbenzyl)benzimidazole-2-ylidene](*p*-cymene) ruthenium(II) (1f)



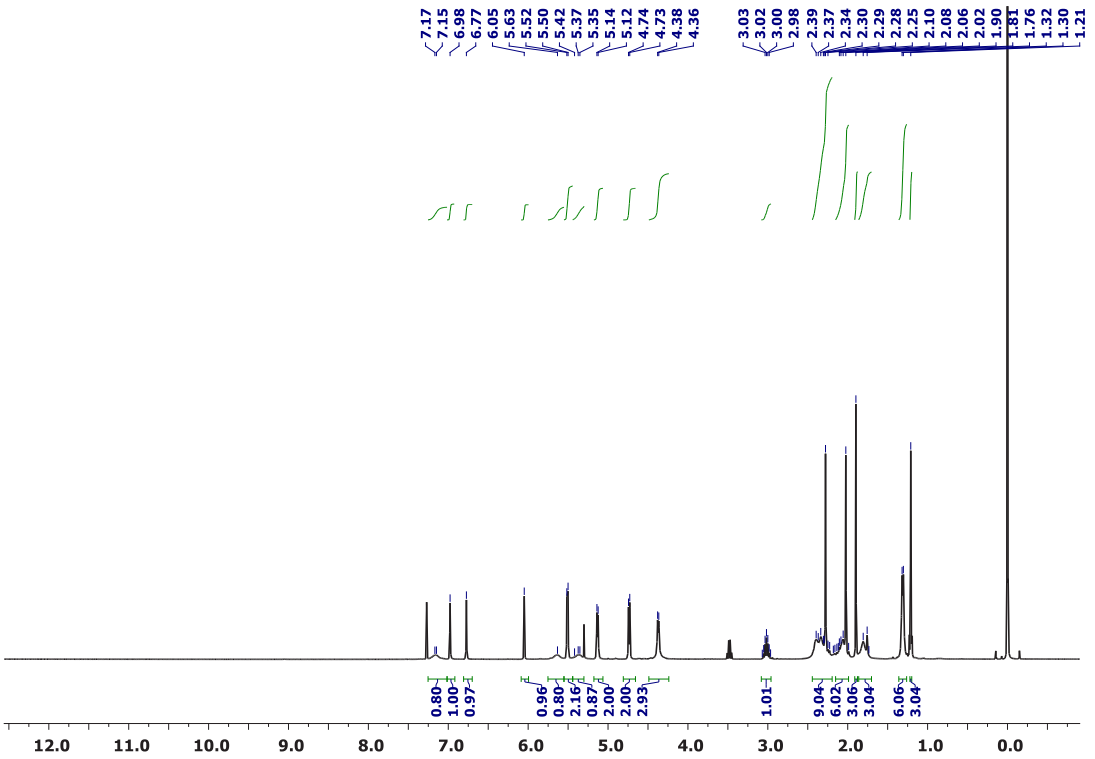


Figure S16. ^{1}H NMR spectrum of ruthenium–BNHC complex **1f** (in $CDCl_3$, 25 °C, TMS, 400 MHz).

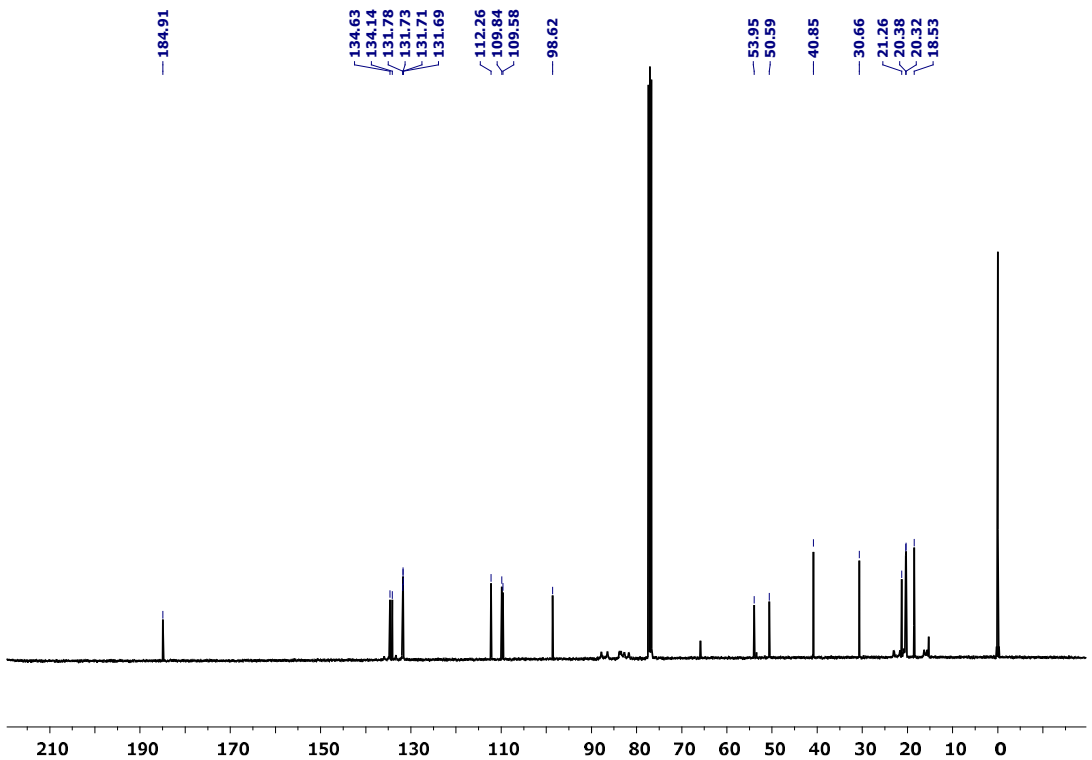


Figure S17. ^{13}C NMR spectrum of ruthenium–BNHC complex **1f** (in $CDCl_3$, 25 °C, TMS, 101 MHz).

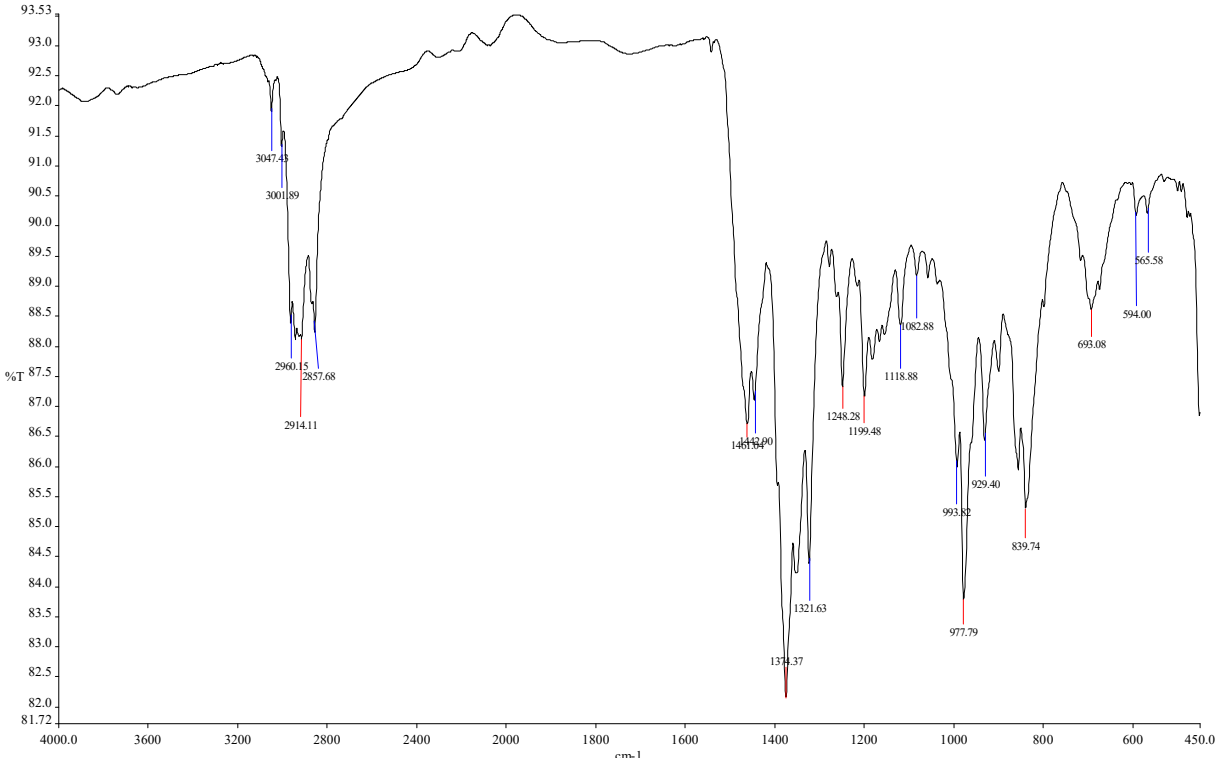
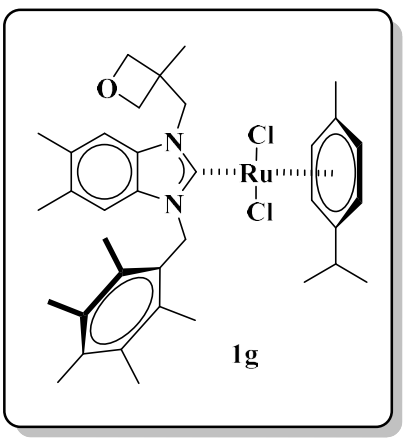


Figure S18. FT-IR spectrum of ruthenium–BNHC complex **1f**.

Characterizing data of ruthenium–BNHC complex 1g

Dichloro-[(5,6-dimethyl-1-((3-methyloxetan-3-yl)methyl)-3-(2,3,4,5,6-pentamethylbenzyl)benzimidazole-2-ylidene](*p*-cymene) ruthenium(II) (1g)



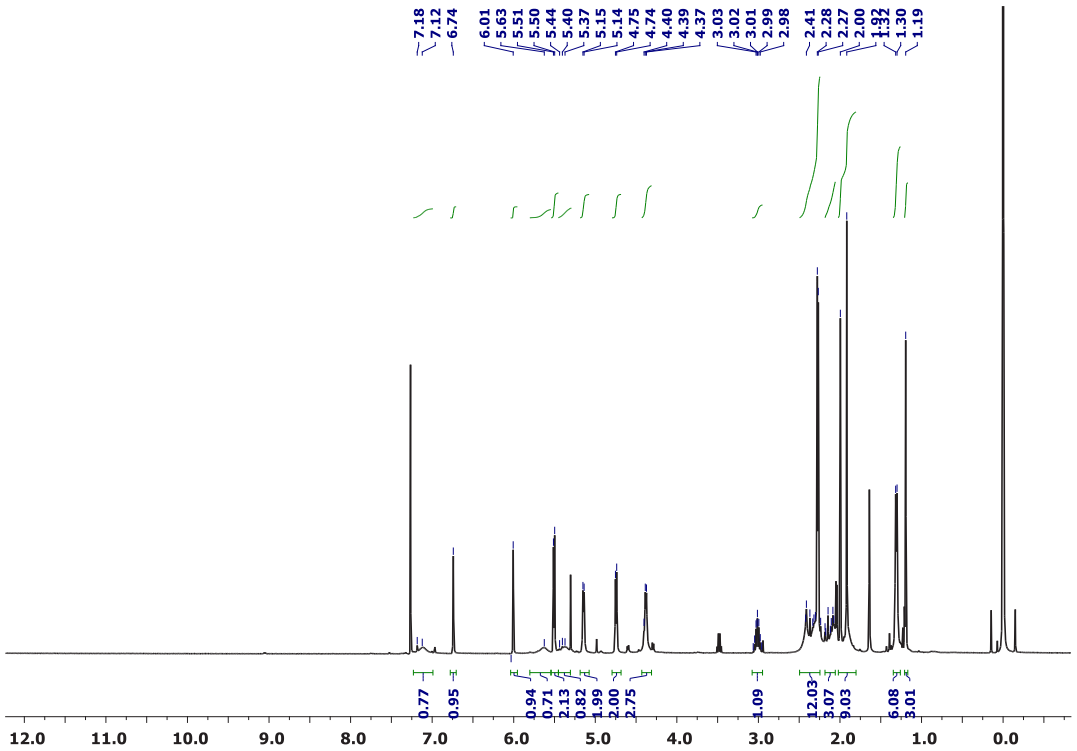


Figure S19. ^{1}H NMR spectrum of ruthenium–BNHC complex **1g** (in $CDCl_3$, 25 °C, TMS, 400 MHz).

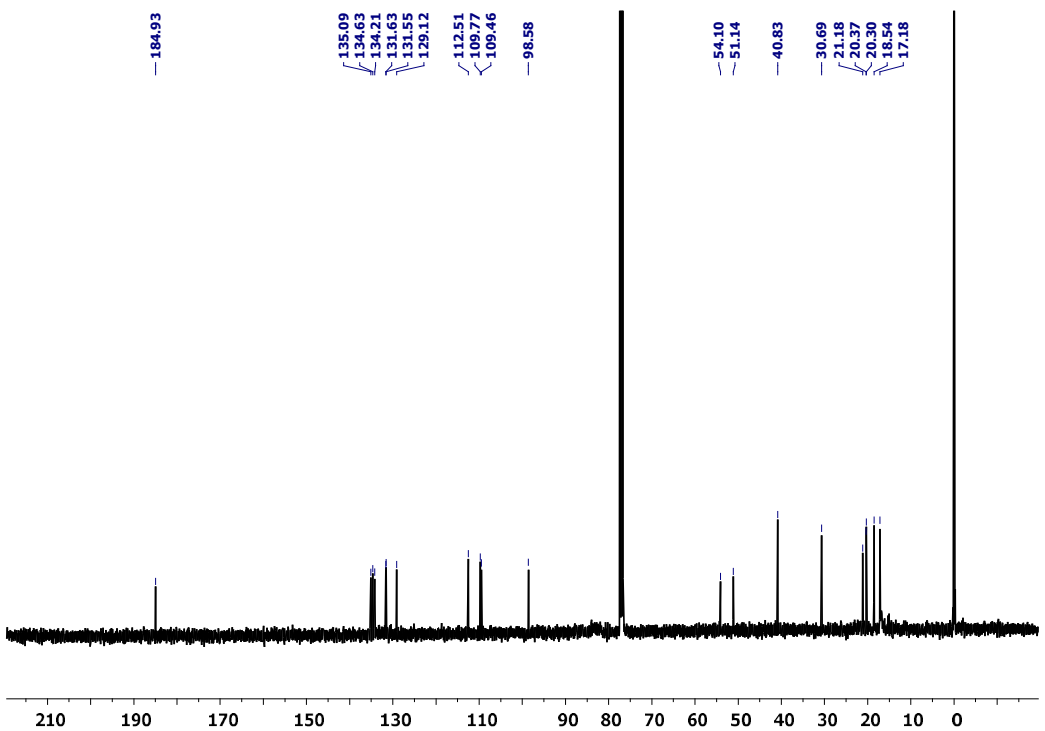


Figure S20. ^{13}C NMR spectrum of ruthenium–BNHC complex **1g** (in $CDCl_3$, 25 °C, TMS, 101 MHz).

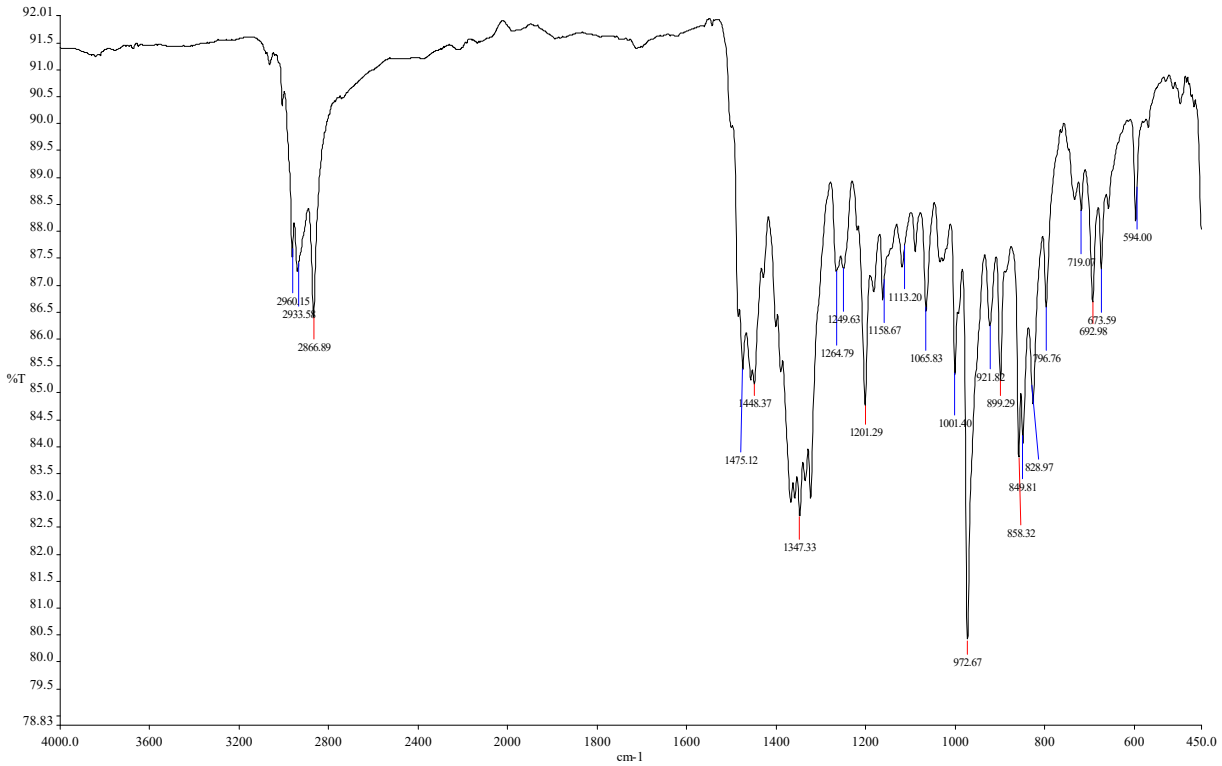


Figure S21. FT-IR spectrum of ruthenium–BNHC complex **1g**.

Characterizing data of the tested (2a–h) substituted benzyl alcohol with aniline by the complex 1e.
***N*-(4-chlorobenzyl)aniline (2a)**

^{1}H NMR (400 MHz, $CDCl_3$) δ 7.32 (s, 4H), 7.20 (dd, *J* = 8.4, 7.5 Hz, 2H), 6.76 (t, *J* = 7.3 Hz, 1H), 6.66–6.57 (m, 2H), 4.32 (s, 2H), 4.05 (s, 1H).
^{13}C NMR (101 MHz, $CDCl_3$) δ 147.9, 138.0, 132.9, 129.3, 128.7, 117.8, 112.9, 47.6.

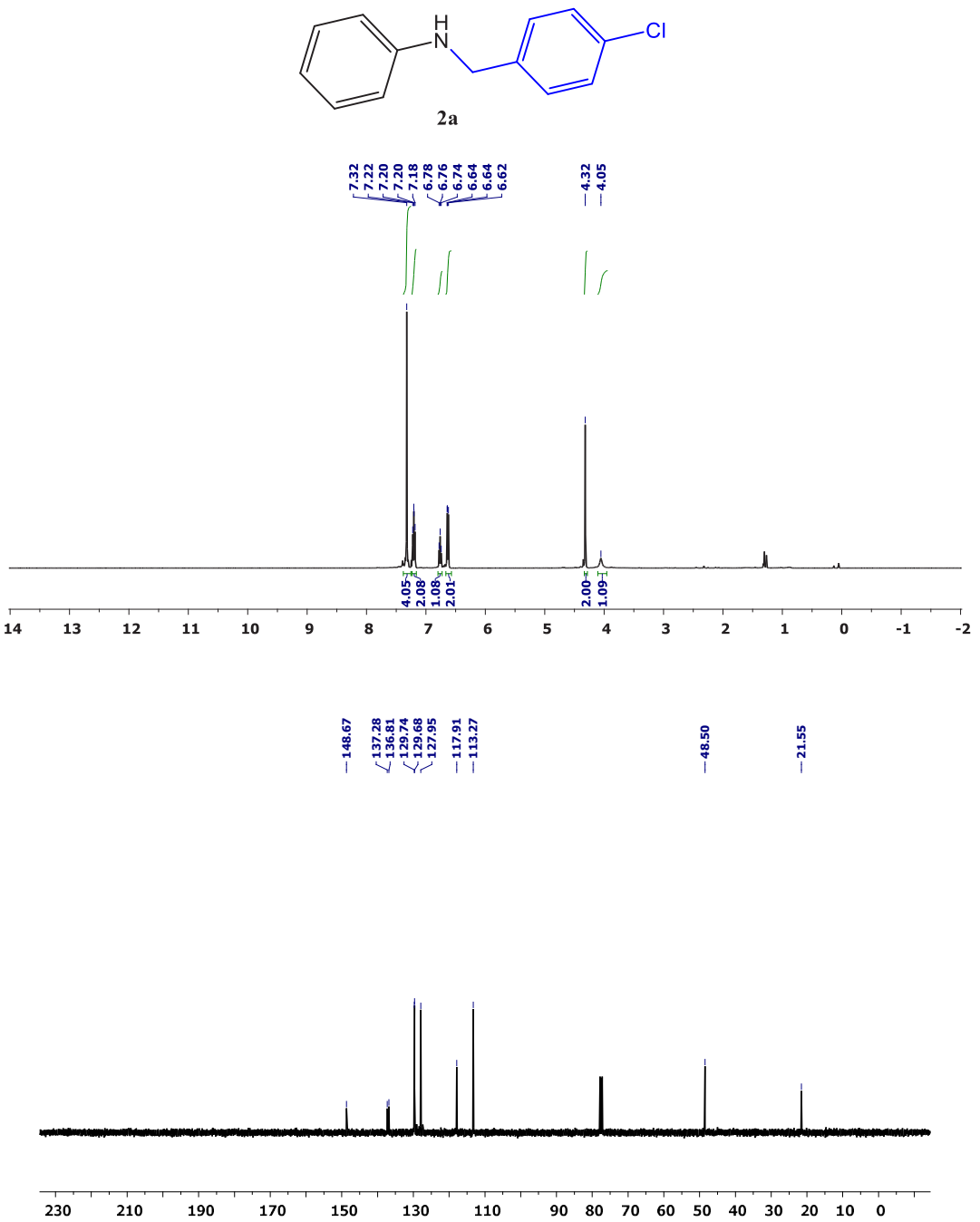
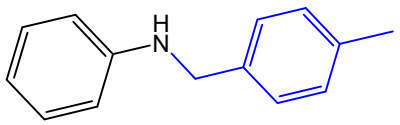


Figure S22. ^{1}H NMR and ^{13}C NMR spectrum of 2**a** (in $CDCl_3$, 25 °C, TMS, 400 MHz).

***N*-(4-methylbenzyl)aniline (2b)**

^{1}H NMR (400 MHz, $CDCl_3$) δ 7.76 (d, *J* = 7.4 Hz, 2H), 7.68 (d, *J* = 11.1 Hz, 4H), 7.21 (t, *J* = 7.2 Hz, 1H), 7.13 (d, *J* = 7.7 Hz, 2H), 4.77 (s, 2H), 4.31 (s, 1H), 2.85 (s, 3H). ^{13}C NMR (101 MHz, $CDCl_3$) δ 148.7, 137.3, 136.8, 129.7, 128.0, 117.9, 113.3, 48.5, 21.6.



2b

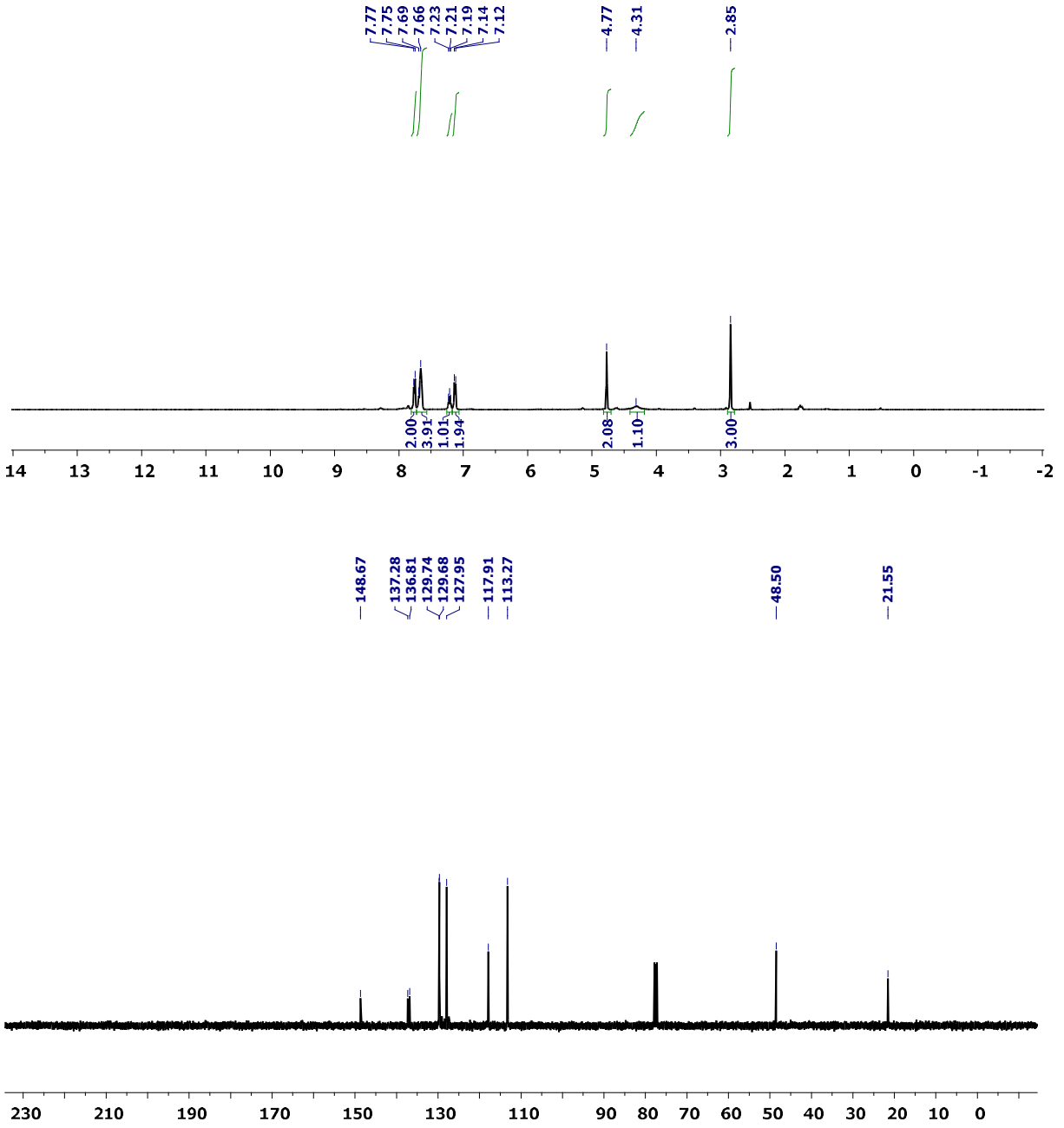


Figure S23. ^{1}H NMR and ^{13}C NMR spectrum of **2b** (in $CDCl_3$, 25 °C, TMS, 400 MHz).

***N*-(4-methoxybenzyl)aniline (2c)**

^{1}H NMR (400 MHz, $CDCl_3$) δ 7.33 (d, *J* = 8.6 Hz, 2H), 7.26–7.17 (m, 2H), 6.93 (dd, *J* = 9.2, 2.4 Hz, 2H), 6.76 (t, *J* = 7.3 Hz, 1H), 6.67 (d, *J* = 7.7 Hz, 2H), 4.28 (s, 2H), 3.98 (s, 1H), 3.83 (s, 3H). ^{13}C NMR (101 MHz, $CDCl_3$) δ 158.9, 148.3, 131.5, 129.3, 128.8, 117.5, 114.1, 112.9, 55.3, 47.8.

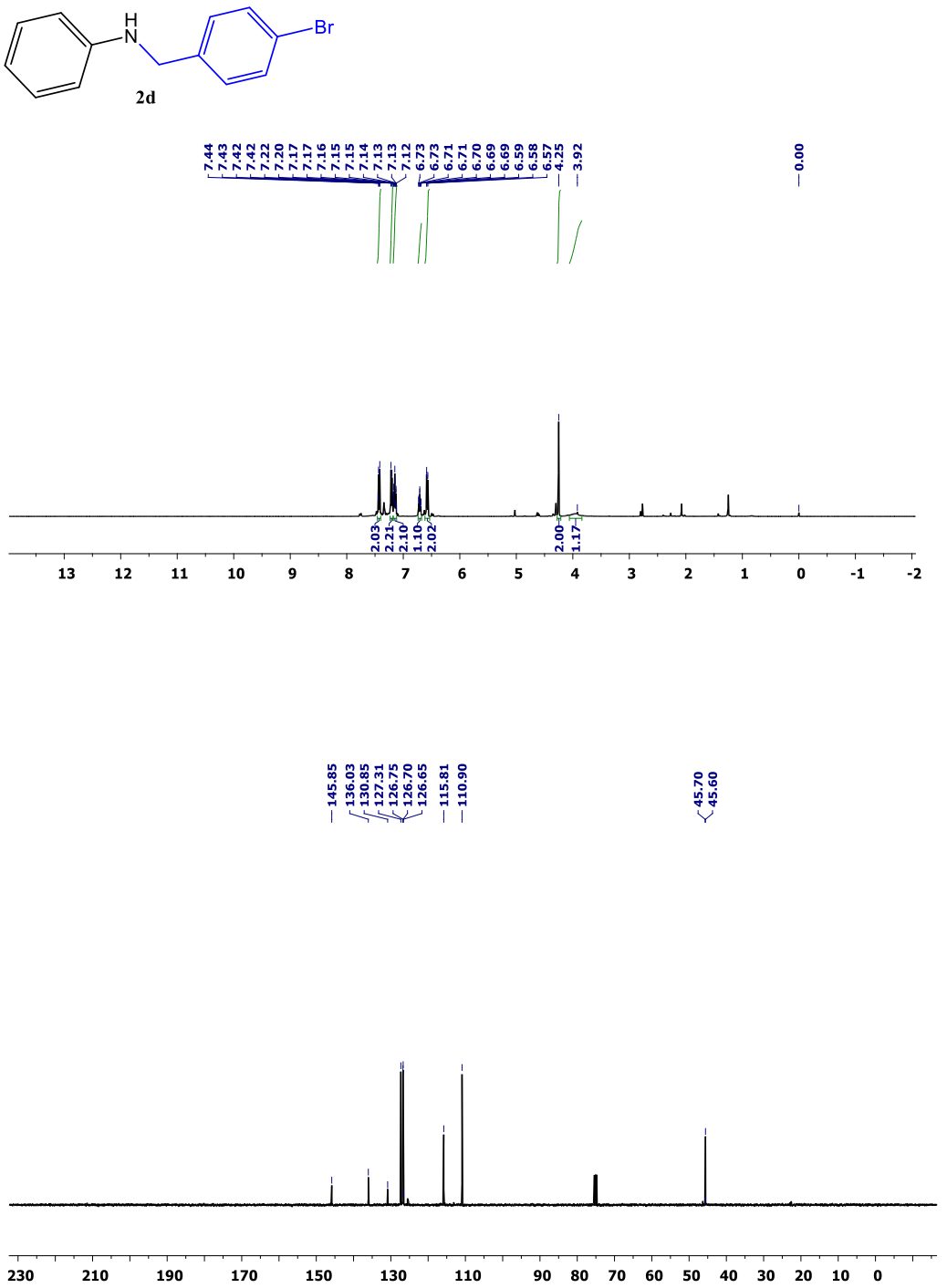


Figure S24. ^{1}H NMR and ^{13}C NMR spectrum of **2c** (in $CDCl_3$, 25 °C, TMS, 400 MHz).

***N*-(4-bromobenzyl)aniline (2d)**

^{1}H NMR (400 MHz, $CDCl_3$) δ 7.43 (dd, *J* = 6.8, 1.5 Hz, 2H), 7.21 (d, *J* = 7.3 Hz, 2H), 7.15 (tt, *J* = 7.2, 1.7 Hz, 2H), 6.74–6.68 (m, 1H), 6.62–6.53 (m, 2H), 4.25 (s, 2H), 3.92 (s, 1H). ^{13}C NMR (101 MHz, $CDCl_3$) δ 145.9, 136.0, 130.9, 127.3, 126.7, 115.8, 110.9, 45.6.

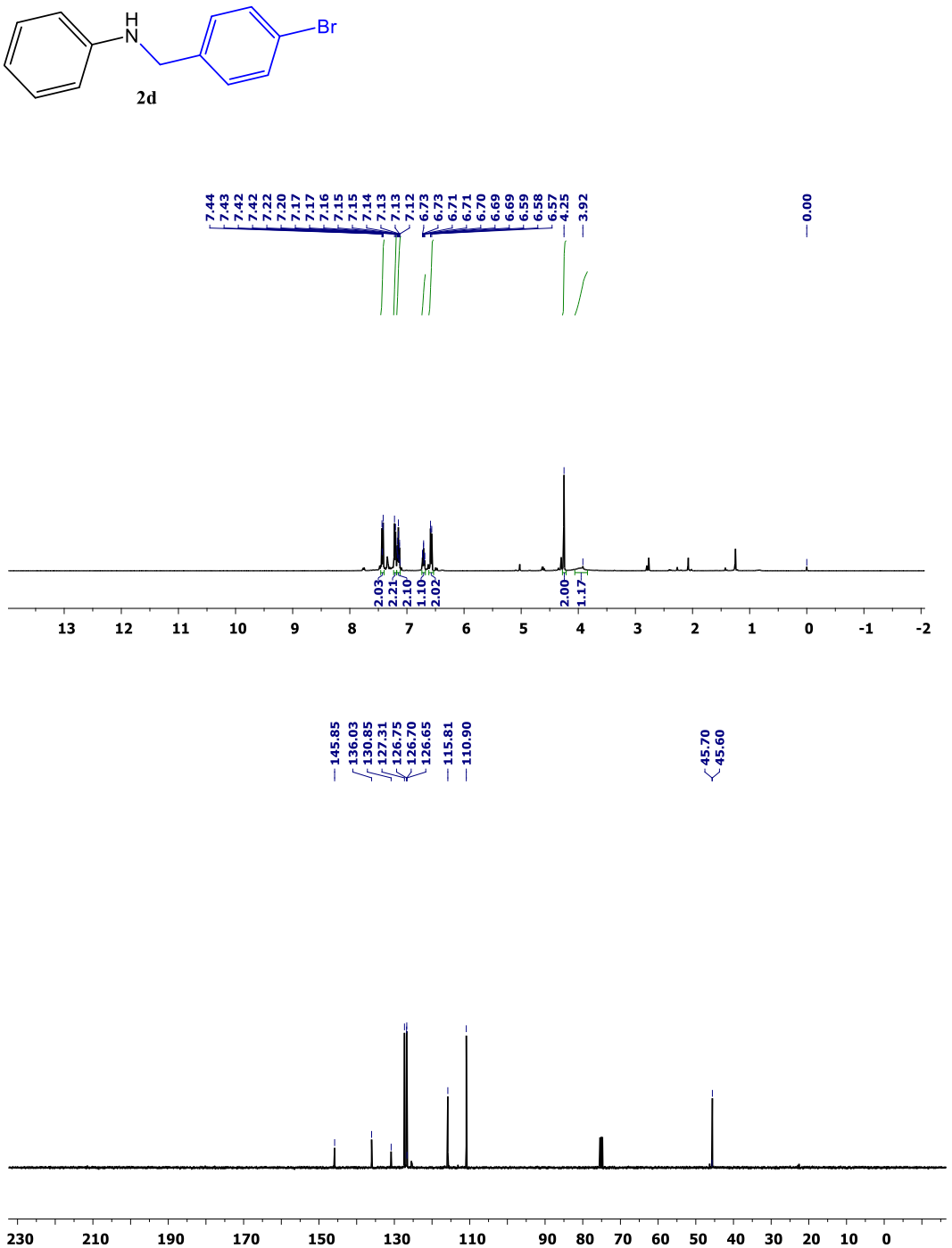


Figure S25. ^{1}H NMR and ^{13}C NMR spectrum of **2d** (in $CDCl_3$, 25 °C, TMS, 400 MHz).

***N*-(2-methylbenzyl)aniline (2e)**

^{1}H NMR (400 MHz, $CDCl_3$) δ 7.25 (dt, *J* = 14.9, 7.9 Hz, 5H), 7.13 (d, *J* = 7.3 Hz, 1H), 6.76 (t, *J* = 7.3 Hz, 1H), 6.68 (d, *J* = 7.8 Hz, 2H), 4.32 (s, 2H), 4.02 (s, 1H), 2.39 (s, 3H). ^{13}C NMR (101 MHz, $CDCl_3$) δ 148.3, 139.4, 138.3, 129.3, 128.6, 128.3, 128.0, 124.6, 117.5, 112.9, 48.4, 21.5.

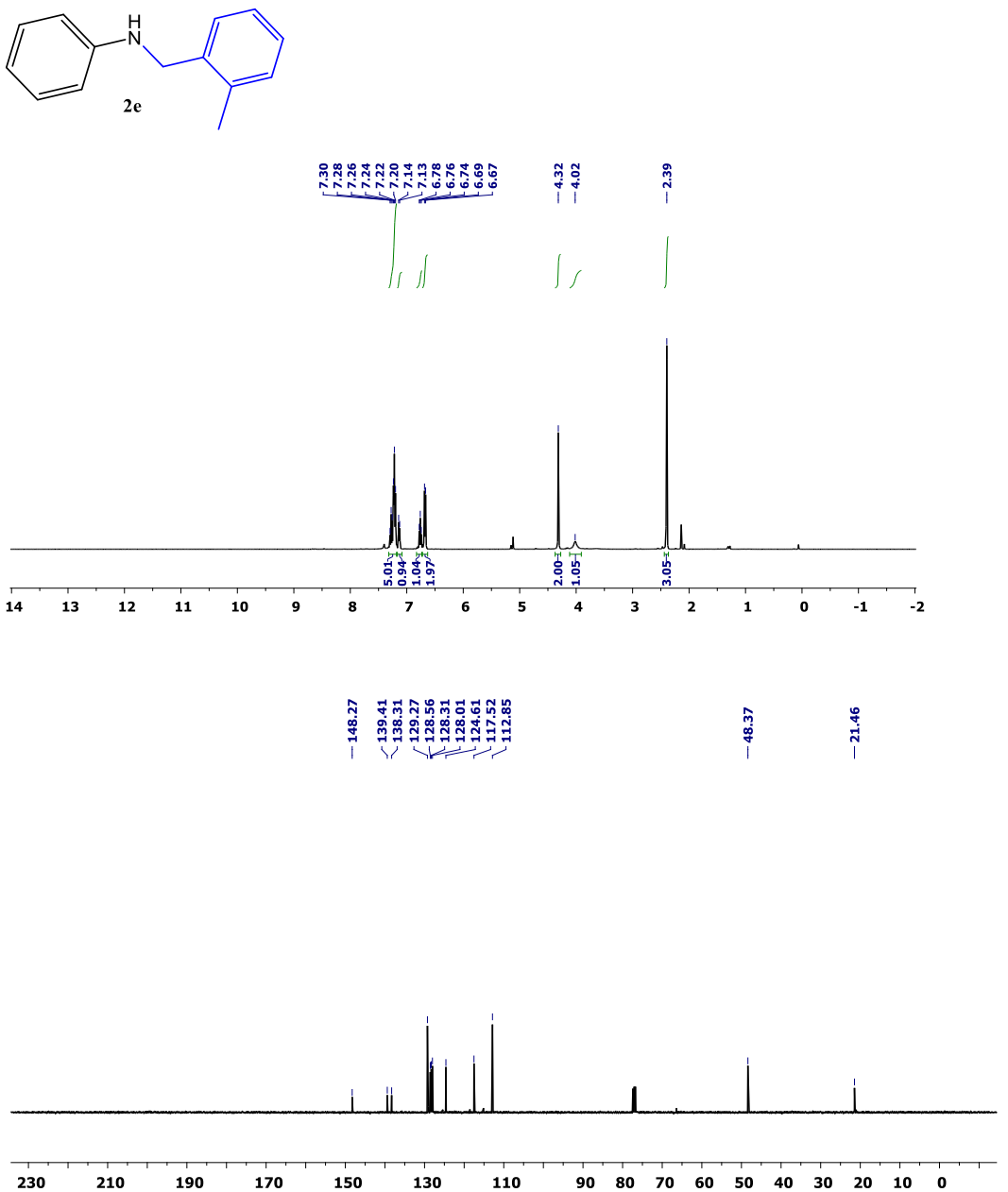


Figure S26. ^{1}H NMR and ^{13}C NMR spectrum of **2e** (in $CDCl_3$, 25 °C, TMS, 400 MHz).

***N*-(2-methoxybenzyl)aniline (2f)**

^{1}H NMR (400 MHz, $CDCl_3$) δ 7.26 (ddd, *J* = 14.8, 11.4, 4.3 Hz, 3H), 7.00 (d, *J* = 13.3 Hz, 2H), 6.87 (d, *J* = 8.1 Hz, 1H), 6.77 (dd, *J* = 10.4, 4.2 Hz, 1H), 6.68 (d, *J* = 7.5 Hz, 2H), 4.34 (s, 2H), 3.98 (s, 1H), 3.83 (s, 3H). ^{13}C NMR (101 MHz, $CDCl_3$) δ 160.0, 148.2, 141.3, 129.7, 129.3, 119.8, 117.6, 113.0, 112.7, 55.2, 48.3.

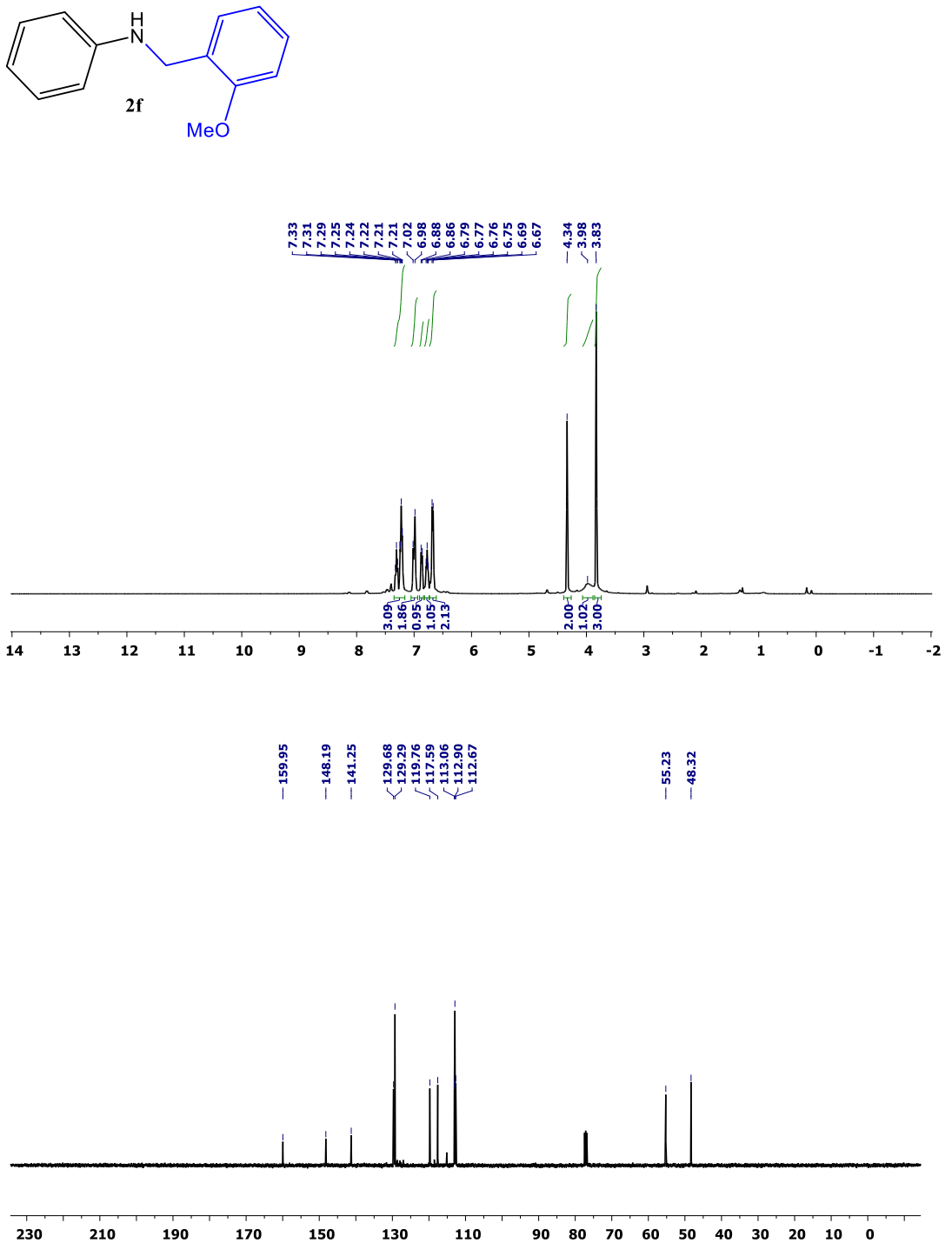


Figure S27. ^{1}H NMR and ^{13}C NMR spectrum of **2f** (in $CDCl_3$, 25 °C, TMS, 400 MHz).

***N*-(furan-2-ylmethyl)aniline (2g)**

^{1}H NMR (400 MHz, $CDCl_3$) δ 7.40–7.33 (m, 1H), 7.22–7.15 (m, 2H), 6.77–6.72 (m, 1H), 6.68 (ddd, *J* = 4.6, 2.1, 1.1 Hz, 2H), 6.36–6.29 (m, 1H), 6.23 (dd, *J* = 3.2, 0.8 Hz, 1H), 4.32 (s, 2H), 3.95 (s, 1H). ^{13}C NMR (101 MHz, CDC_3) δ 152.7, 147.6, 141.9, 129.2, 118.0, 113.1, 110.3, 106.9, 41.4.

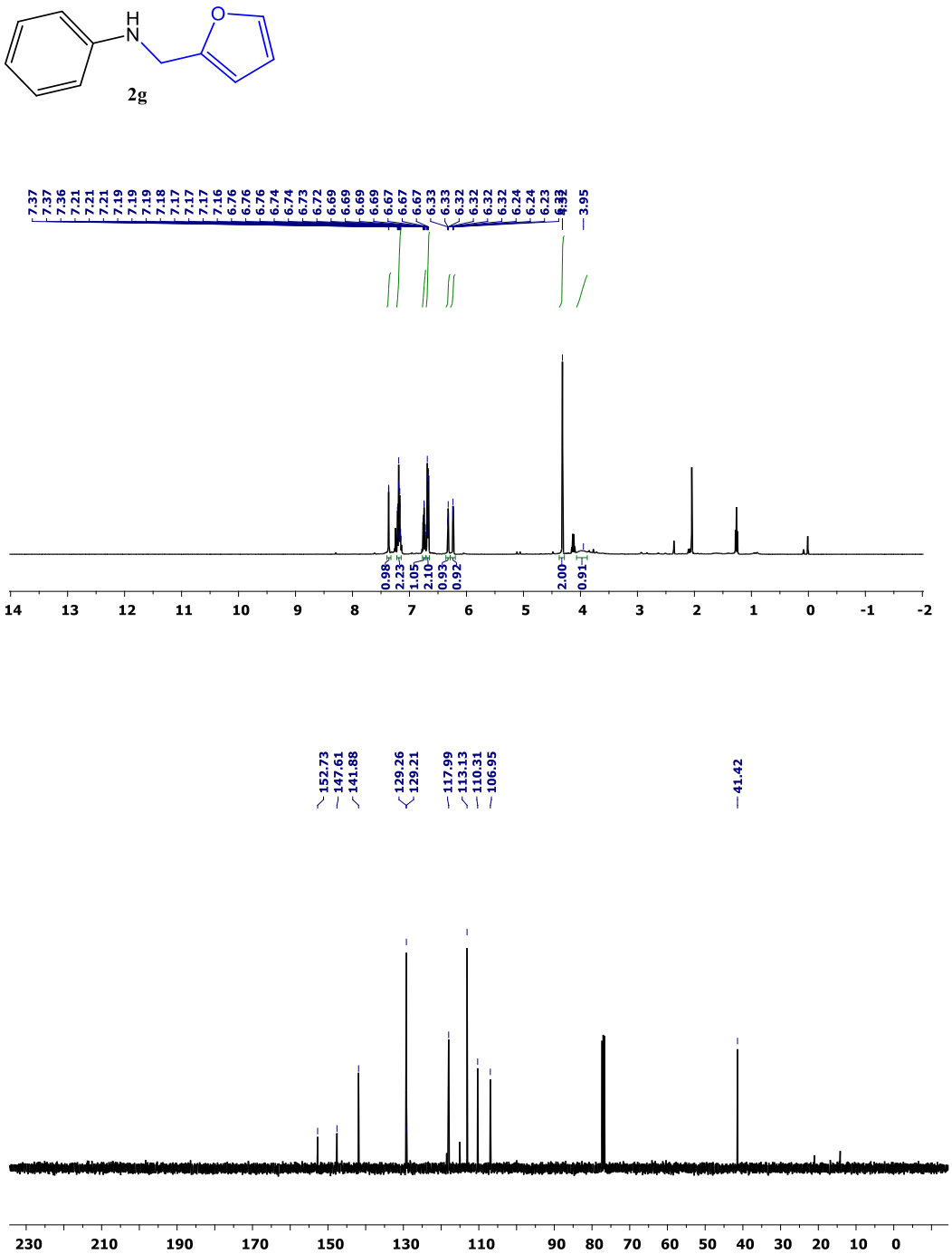


Figure S28. ^{1}H NMR and ^{13}C NMR spectrum of **2g** (in $CDCl_3$, 25 °C, TMS, 400 MHz).

***N*-(3,5-bis(trifluoromethyl)benzyl)aniline (2h)**

^{1}H NMR (400 MHz, $CDCl_3$) δ 7.84 (s, 2H), 7.79 (s, 1H), 7.18 (td, *J* = 7.8, 0.7 Hz, 2H), 6.77 (td, *J* = 7.4, 0.8 Hz, 1H), 6.60 (dd, *J* = 7.7, 0.8 Hz, 2H), 4.47 (s, 2H), 4.18 (s, 1H). ^{13}C NMR (101 MHz, $CDCl_3$) δ 147.2, 142.5, 129.4, 118.5, 113.0, 47.7.

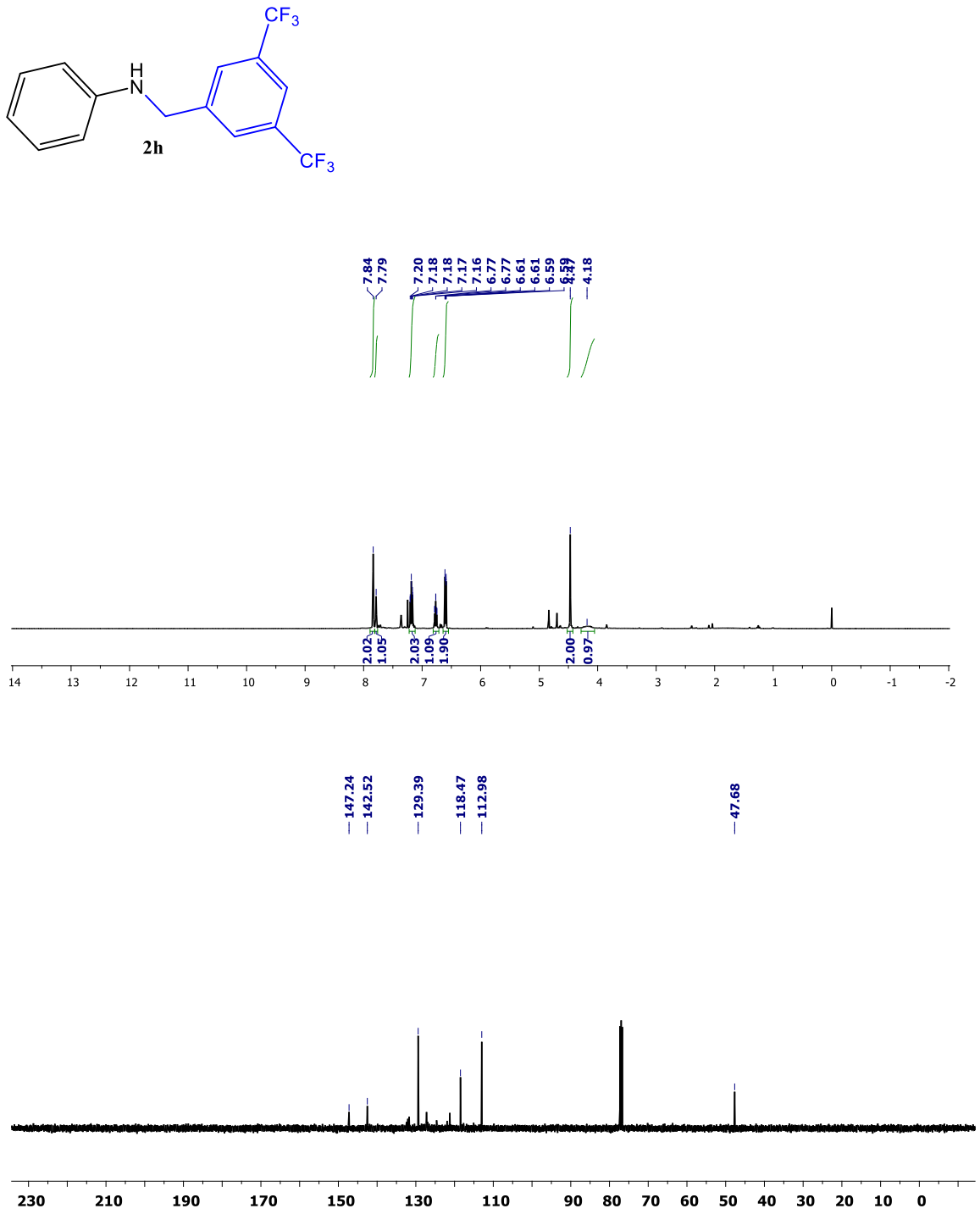


Figure S29. ^{1}H NMR and ^{13}C NMR spectrum of **2h** (in $CDCl_3$, 25 °C, TMS, 400 MHz).

Characterizing data of the tested (3a–h) substituted aniline with benzyl alcohol by the complex 1e.

***N*-benzyl-4-chloroaniline (3a)**

^{1}H NMR (400 MHz, $CDCl_3$) δ 7.34–7.30 (m, 4H), 7.26 (dd, *J* = 8.8, 4.6 Hz, 1H), 7.10–7.03 (m, 2H), 4.26 (d, *J* = 5.5 Hz, 2H), 4.02 (s, 1H).
^{13}C NMR (101 MHz, $CDCl_3$) δ 147.9, 138.0, 132.9, 129.3, 128.7, 117.8, 112.9, 47.6.

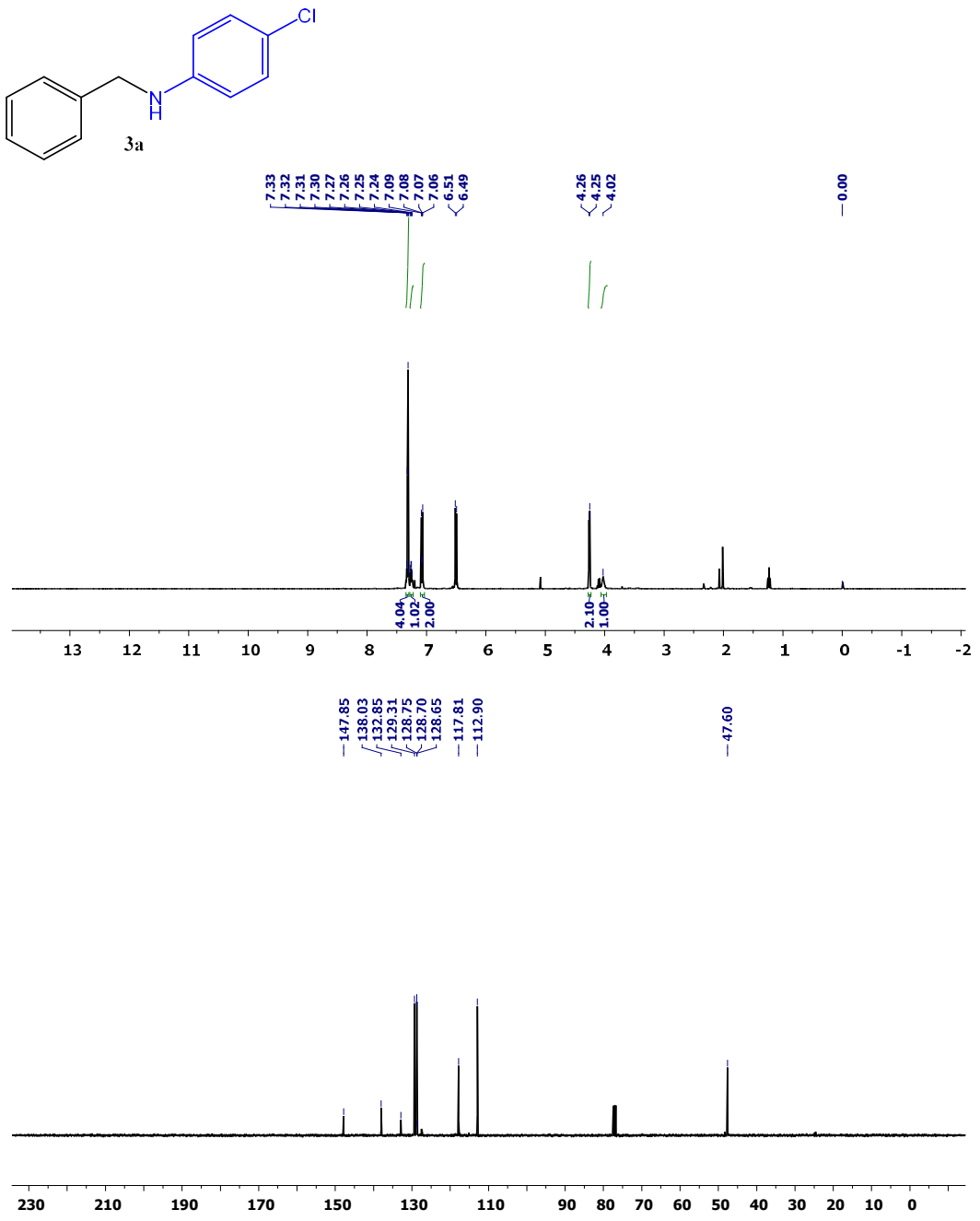


Figure S30. ^{1}H NMR and ^{13}C NMR spectrum of **3a** (in $CDCl_3$, 25 °C, TMS, 400 MHz).

***N*-benzyl-4-methylaniline (3b)**

^{1}H NMR (400 MHz, $CDCl_3$) δ 7.41–7.19 (m, 5H), 6.96 (d, *J* = 8.3 Hz, 2H), 6.53 (d, *J* = 8.4 Hz, 2H), 4.27 (s, 2H), 3.86 (s, 1H), 2.22 (s, 3H).
^{13}C NMR (101 MHz, $CDCl_3$) δ 146.0, 139.7, 129.8, 128.6, 127.5, 127.2, 113.0, 48.7, 20.4.

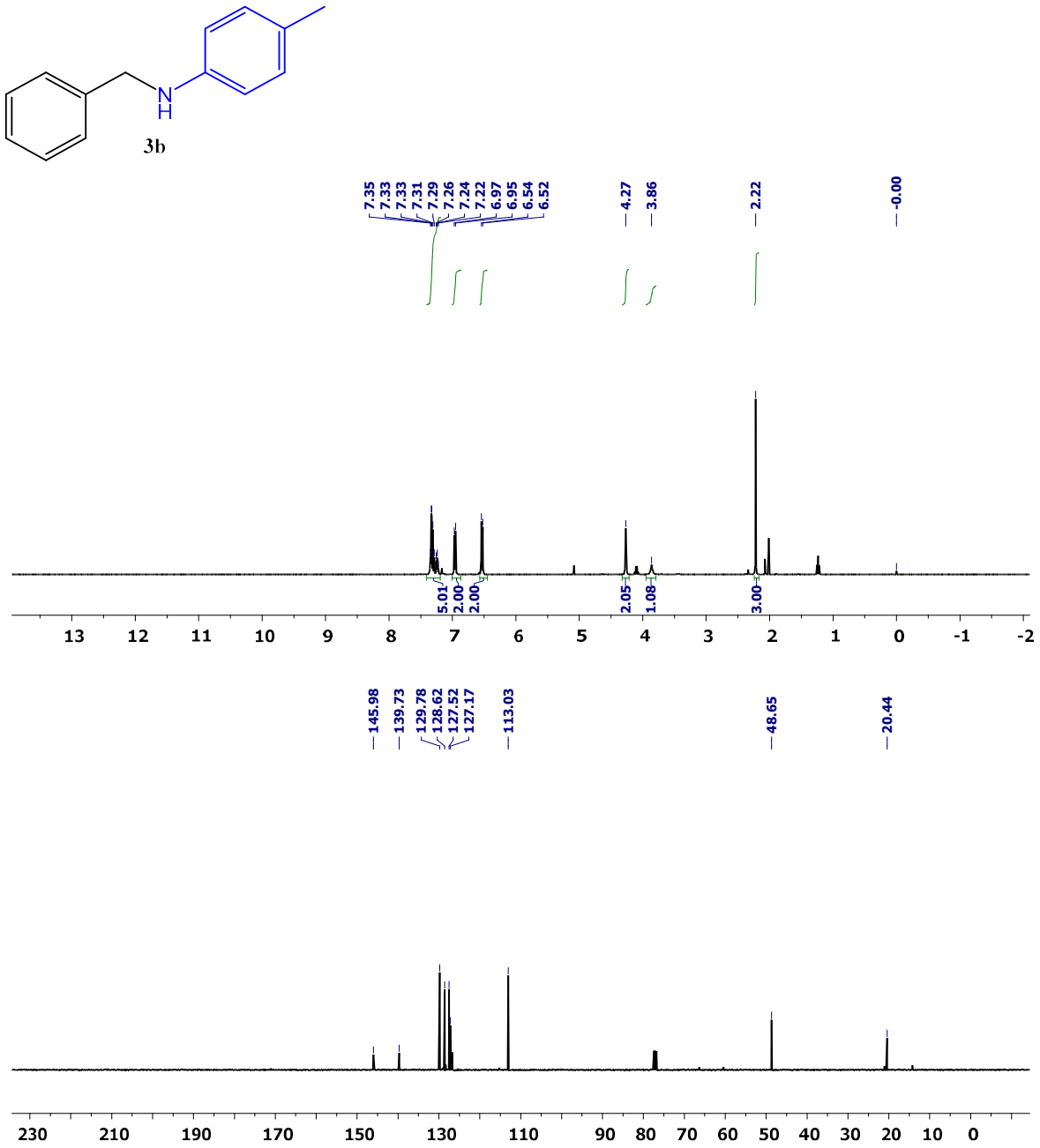


Figure S31. ^{1}H NMR and ^{13}C NMR spectrum of **3b** (in $CDCl_3$, 25 °C, TMS, 400 MHz).

***N*-benzyl-4-methoxyaniline (3c)**

^{1}H NMR (400 MHz, $CDCl_3$) δ 7.37 (dt, *J* = 20.8, 10.2 Hz, 4H), 7.31–7.24 (m, 1H), 6.81 (d, *J* = 8.8 Hz, 2H), 6.63 (d, *J* = 8.8 Hz, 2H), 4.30 (s, 2H), 3.76 (s, 4H). ^{13}C NMR (101 MHz, $CDCl_3$) δ 152.2, 142.4, 139.7, 128.6, 127.6, 114.9, 114.2, 55.8, 49.3.

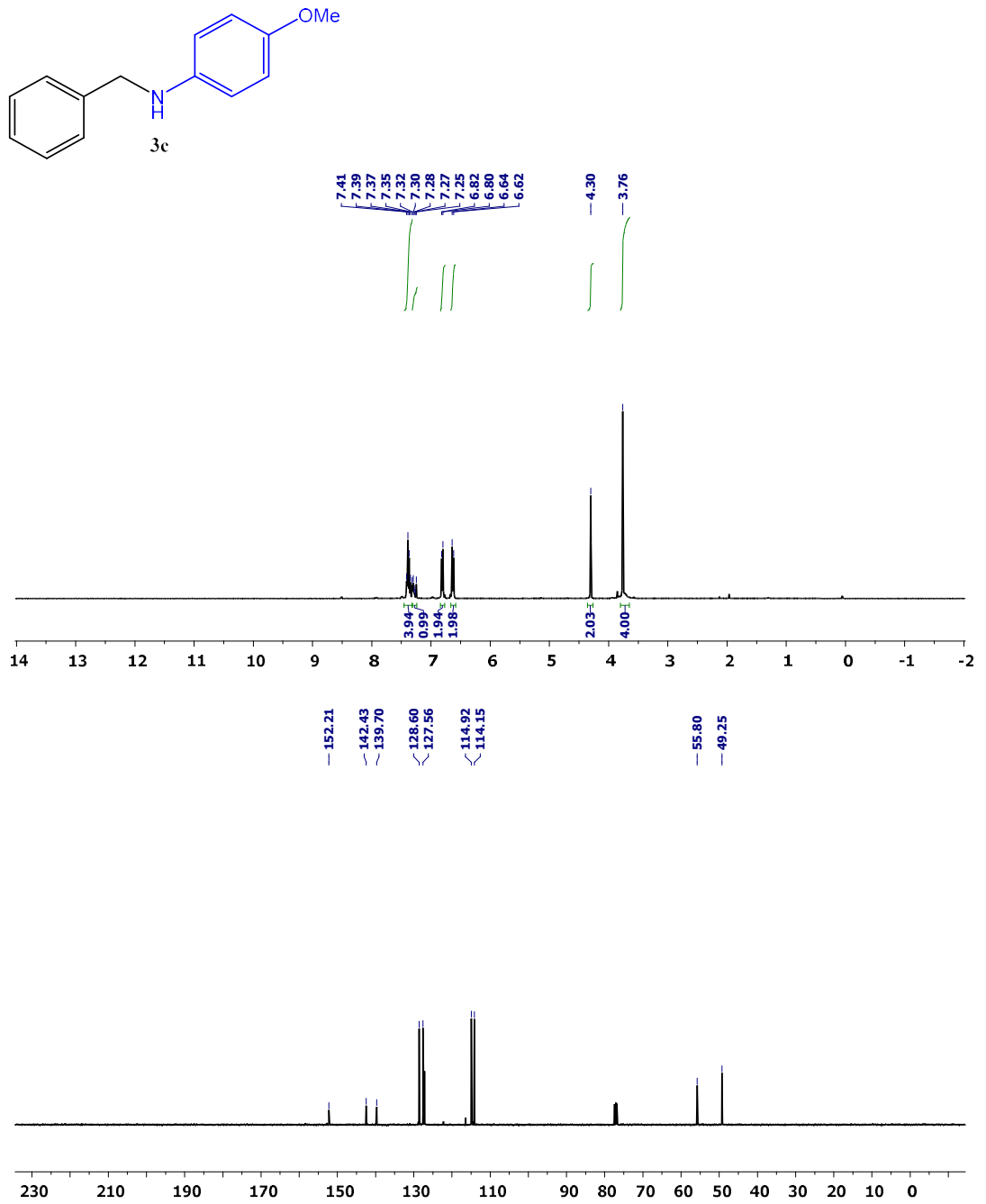


Figure S32. ^{1}H NMR and ^{13}C NMR spectrum of **3c** (in $CDCl_3$, 25 °C, TMS, 400 MHz).

***N*-benzylpyridin-2-amine (3d)**

^{1}H NMR (400 MHz, $CDCl_3$) δ 8.10–8.00 (m, 1H), 7.46–7.28 (m, 5H), 7.27–7.21 (m, 1H), 6.55 (ddd, *J* = 7.1, 5.0, 0.9 Hz, 1H), 6.33 (d, *J* = 8.4 Hz, 1H), 5.16 (s, 1H), 4.47 (d, *J* = 5.8 Hz, 2H). ^{13}C NMR (101 MHz, $CDCl_3$) δ 158.7, 148.2, 139.2, 128.6, 127.3, 113.1, 106.7, 46.3.

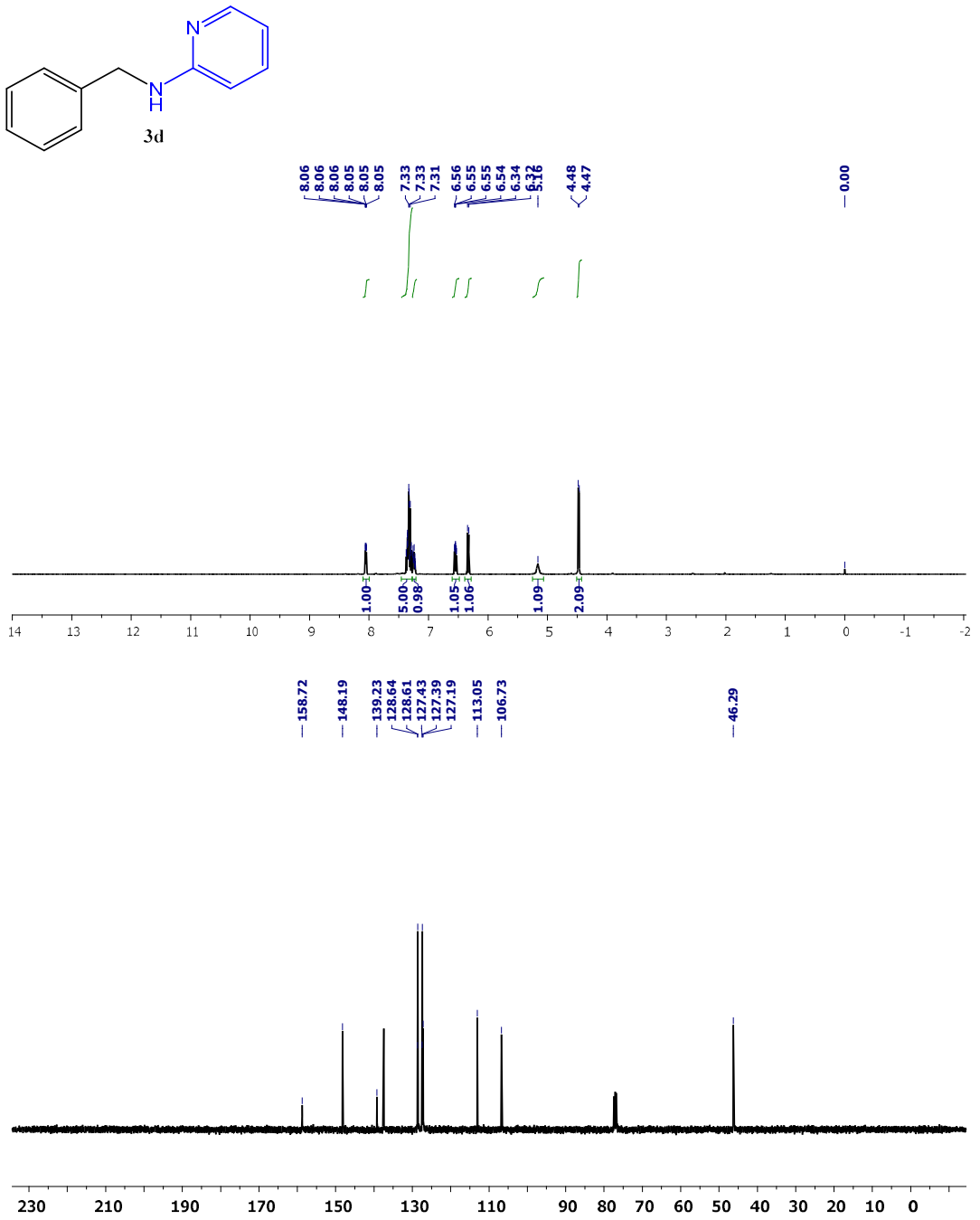


Figure S33. ^{1}H NMR and ^{13}C NMR spectrum of **3d** (in $CDCl_3$, 25 °C, TMS, 400 MHz).

***N*-benzylpyridin-3-amine (3e)**

^{1}H NMR (400 MHz, $CDCl_3$) δ 8.04 (d, *J* = 2.9 Hz, 1H), 7.94 (dd, *J* = 4.7, 1.2 Hz, 1H), 7.34 (d, *J* = 4.4 Hz, 4H), 7.30–7.24 (m, 1H), 7.04 (dd, *J* = 8.3, 4.7 Hz, 1H), 6.85 (ddd, *J* = 8.3, 2.8, 1.2 Hz, 1H), 4.32 (s, 2H), 4.25 (s, 1H). ^{13}C NMR (101 MHz, $CDCl_3$) δ 144.0, 138.8, 138.5, 136.1, 128.7, 127.4, 123.7, 118.5, 47.8.

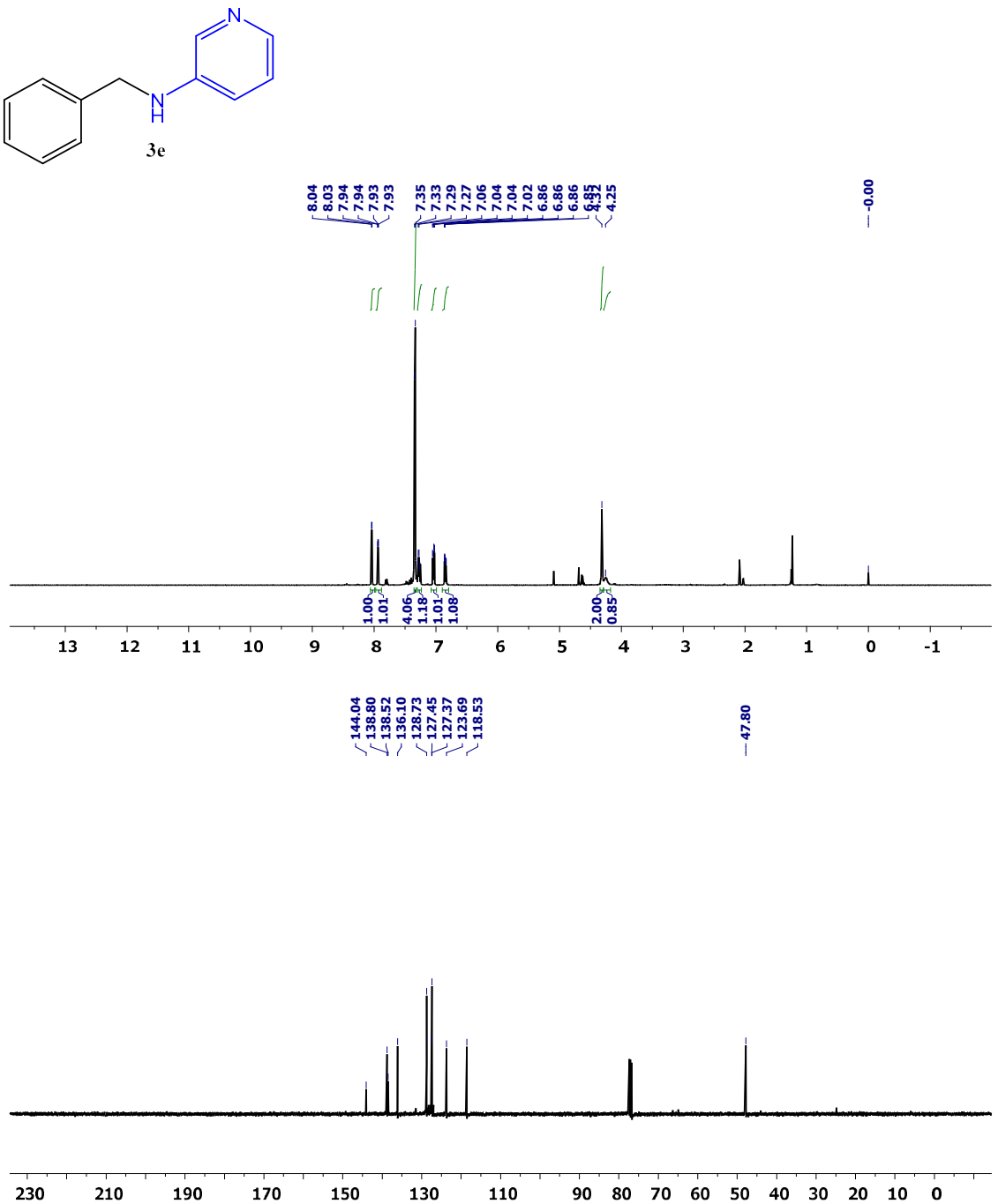


Figure S34. ^{1}H NMR and ^{13}C NMR spectrum of **3e** (in $CDCl_3$, 25 °C, TMS, 400 MHz).

***N*-benzylpyrimidin-2-amine (3f)**

^{1}H NMR (400 MHz, $CDCl_3$) δ 8.19 (d, *J* = 3.3 Hz, 2H), 7.33 (q, *J* = 7.9 Hz, 4H), 7.28–7.23 (m, 1H), 6.50 (t, *J* = 4.8 Hz, 1H), 5.96 (s, 1H), 4.62 (d, *J* = 5.9 Hz, 2H). ^{13}C NMR (101 MHz, $CDCl_3$) δ 158.0, 139.1, 128.6, 127.5, 127.2, 110.7, 45.4.

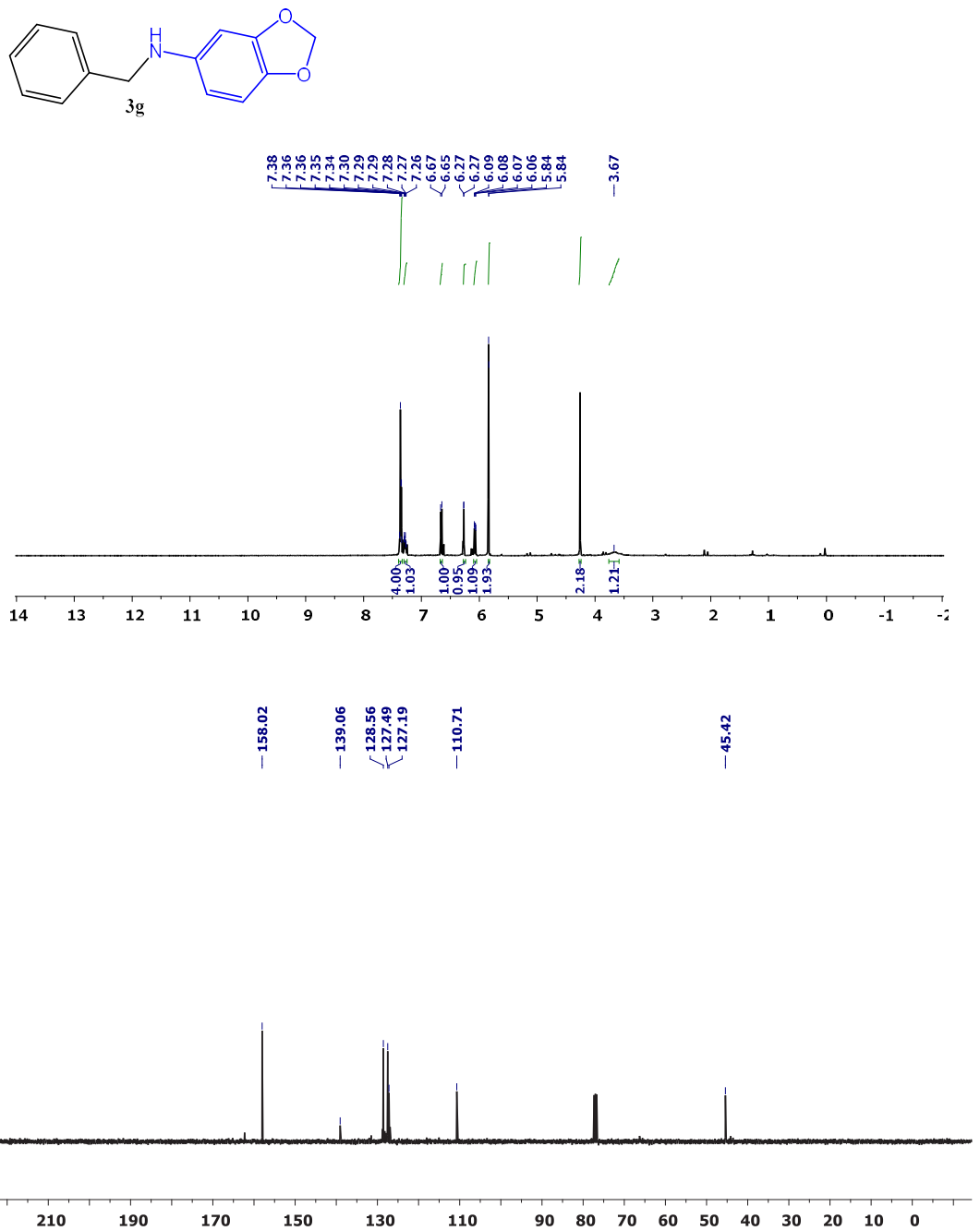


Figure S35. ^{1}H NMR and ^{13}C NMR spectrum of **3f** (in $CDCl_3$, 25 °C, TMS, 400 MHz).

***N*-benzylbenzo[1,3]dioxol-5-amine (3g)**

^{1}H NMR (400 MHz, $CDCl_3$) δ 7.40–7.33 (m, 4H), 7.30–7.25 (m, 1H), 6.66 (d, *J* = 8.2 Hz, 1H), 6.27 (d, *J* = 2.3 Hz, 1H), 6.07 (dd, *J* = 8.3, 2.3 Hz, 1H), 5.84 (d, *J* = 0.5 Hz, 2H), 4.26 (s, 2H), 3.67 (s, 1H). ^{13}C NMR (101 MHz, $CDCl_3$) δ 148.3, 143.9, 139.7, 139.4, 128.6, 127.5, 127.2, 108.6, 104.4, 100.6, 96.0, 49.2.

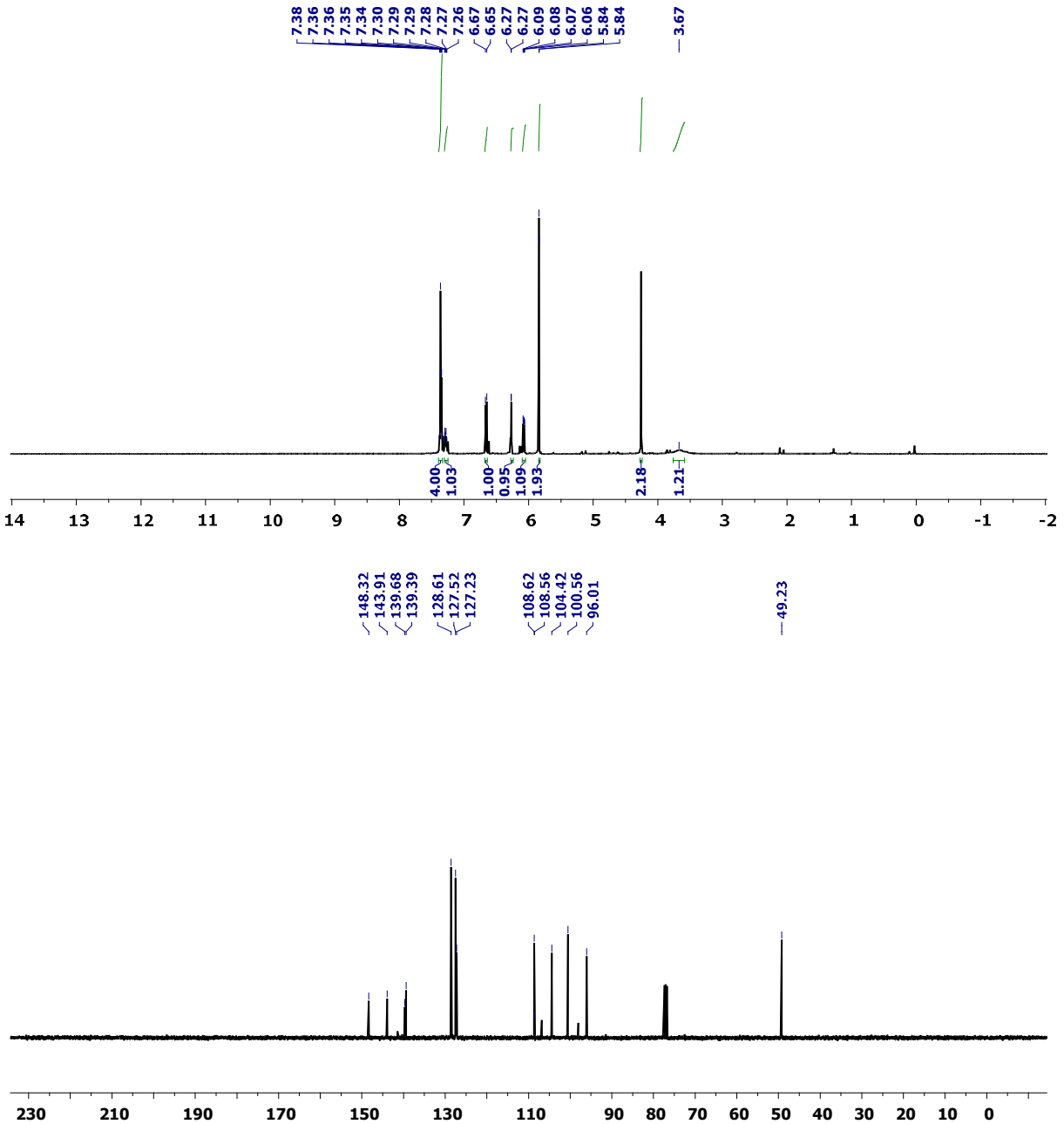


Figure S36. ^{1}H NMR and ^{13}C NMR spectrum of **3g** (in $CDCl_3$, 25 °C, TMS, 400 MHz).

***N*-benzyl-3,5-bis(trifluoromethyl)aniline (3h)**

^{1}H NMR (400 MHz, $CDCl_3$) δ 7.43–7.31 (m, 5H), 7.17 (s, 1H), 6.97 (s, 2H), 4.45 (s, 1H), 4.36 (d, *J* = 5.4 Hz, 2H). ^{13}C NMR (101 MHz, $CDCl_3$) δ 148.6, 137.6, 128.9, 127.8, 127.5, 111.9, 111.0, 48.0.

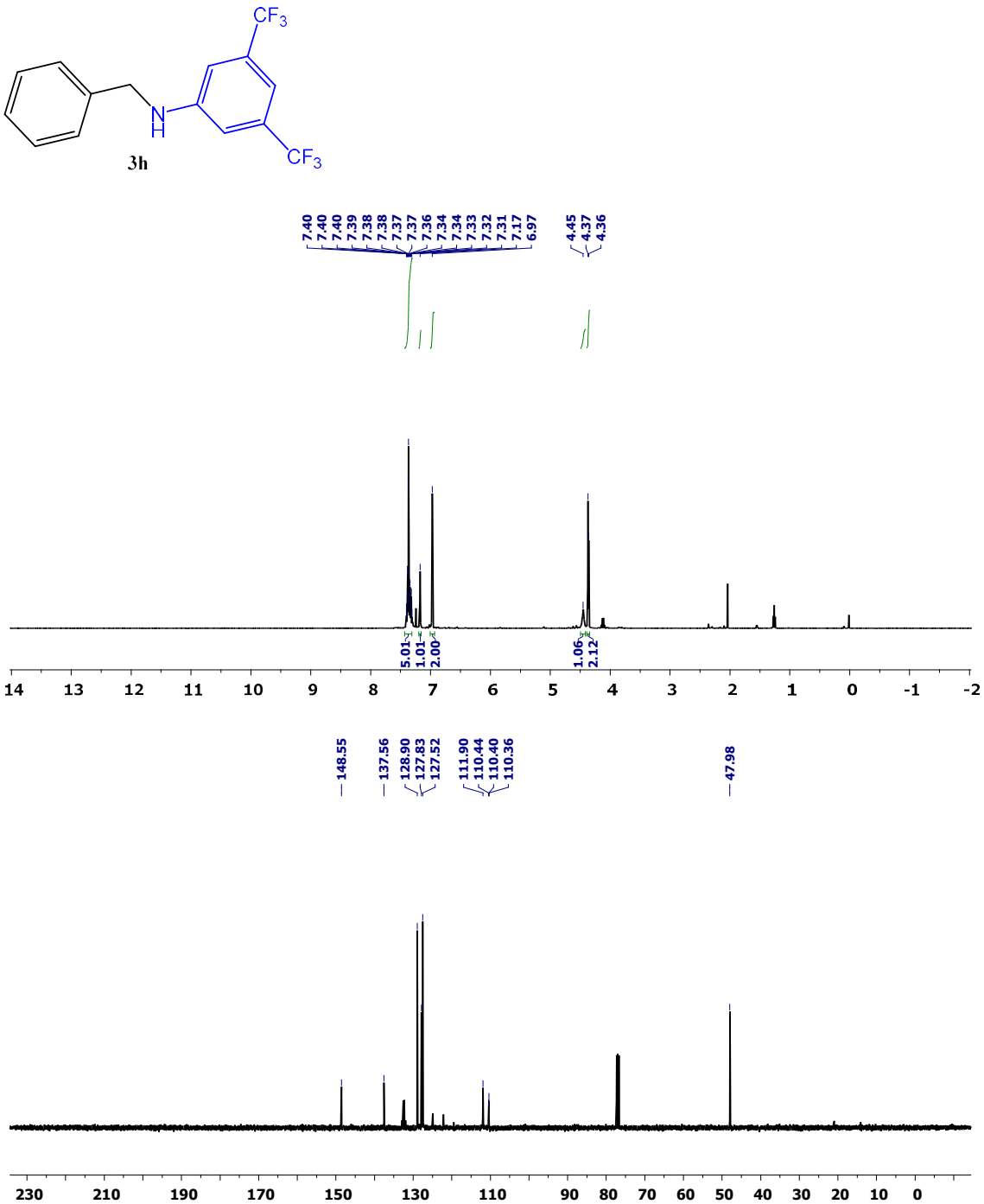


Figure S37. ^{1}H NMR and ^{13}C NMR spectrum of **3h** (in $CDCl_3$, 25 °C, TMS, 400 MHz).

Characterizing data of the tested (4a–e) substituted aniline with methanol by the complex 1e.

***N*-methylaniline (4a)**

^{1}H NMR (400 MHz, $CDCl_3$) δ 6.72 (t, *J* = 7.8 Hz, 2H), 6.24 (t, *J* = 7.3 Hz, 1H), 6.15 (d, *J* = 7.8 Hz, 2H), 3.21 (s, 1H), 2.36 (s, 3H).

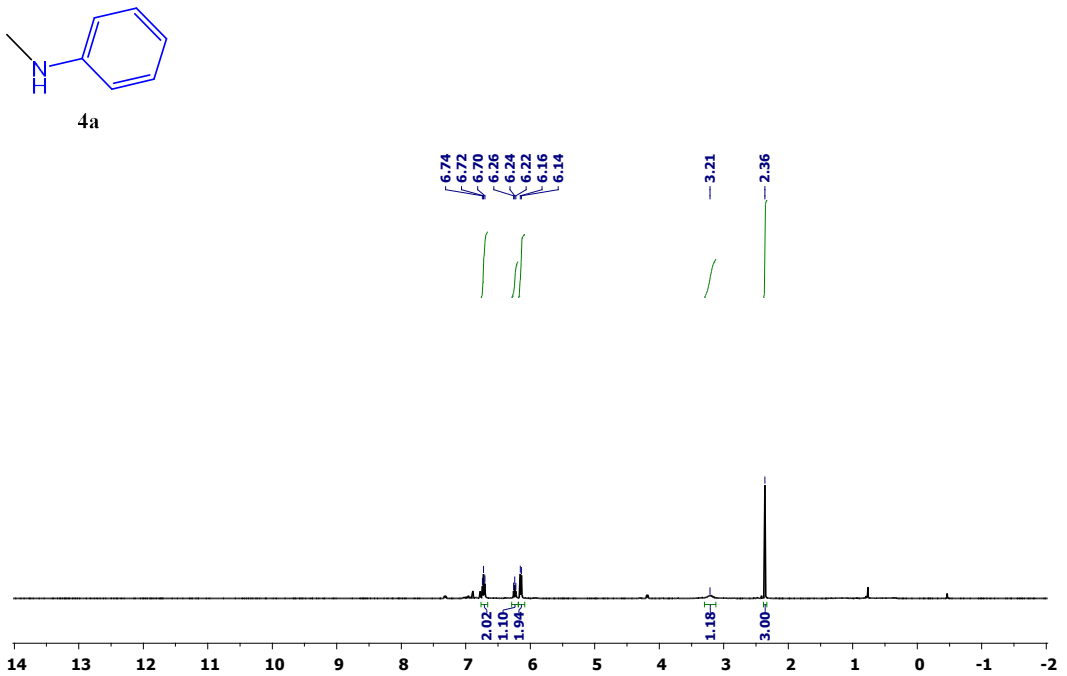


Figure S38. ^{1}H NMR and ^{13}C NMR spectrum of **4a** (in $CDCl_3$, 25 °C, TMS, 400 MHz).

***N*,4-dimethylaniline (4b)**

^{1}H NMR (400 MHz, $CDCl_3$) δ 7.02 (d, *J* = 8.5 Hz, 2H), 6.56 (d, *J* = 8.3 Hz, 2H), 3.44 (s, 1H), 2.82 (s, 3H), 2.26 (s, 3H).

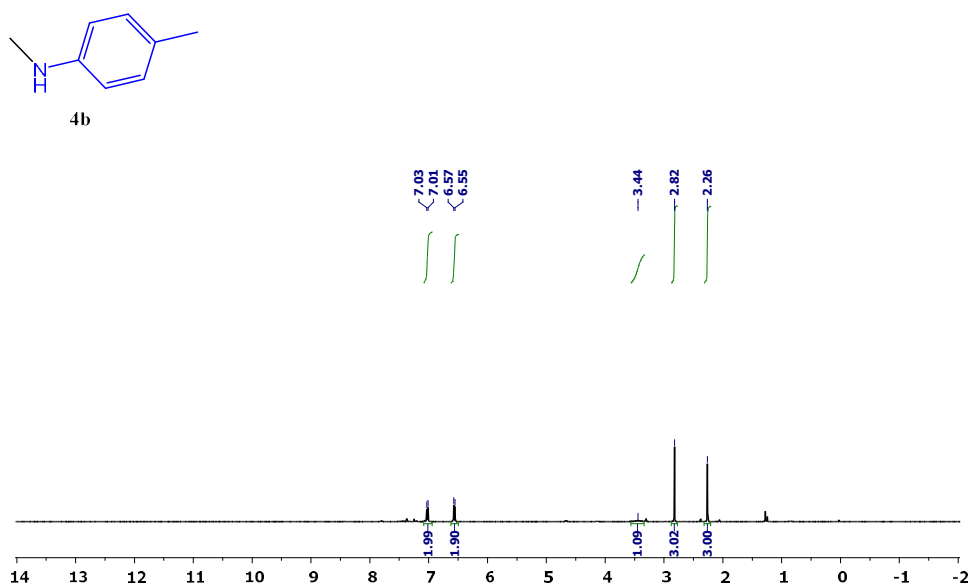


Figure S39. ^{1}H NMR spectrum of **4b** (in $CDCl_3$, 25 °C, TMS, 400 MHz).

4-Methoxy-*N*-methylaniline (4c)

^{1}H NMR (400 MHz, $CDCl_3$) δ 6.82–6.74 (m, 2H), 6.63–6.55 (m, 2H), 3.74 (s, 3H), 2.79 (s, 3H), 0.82 (s, 1H).

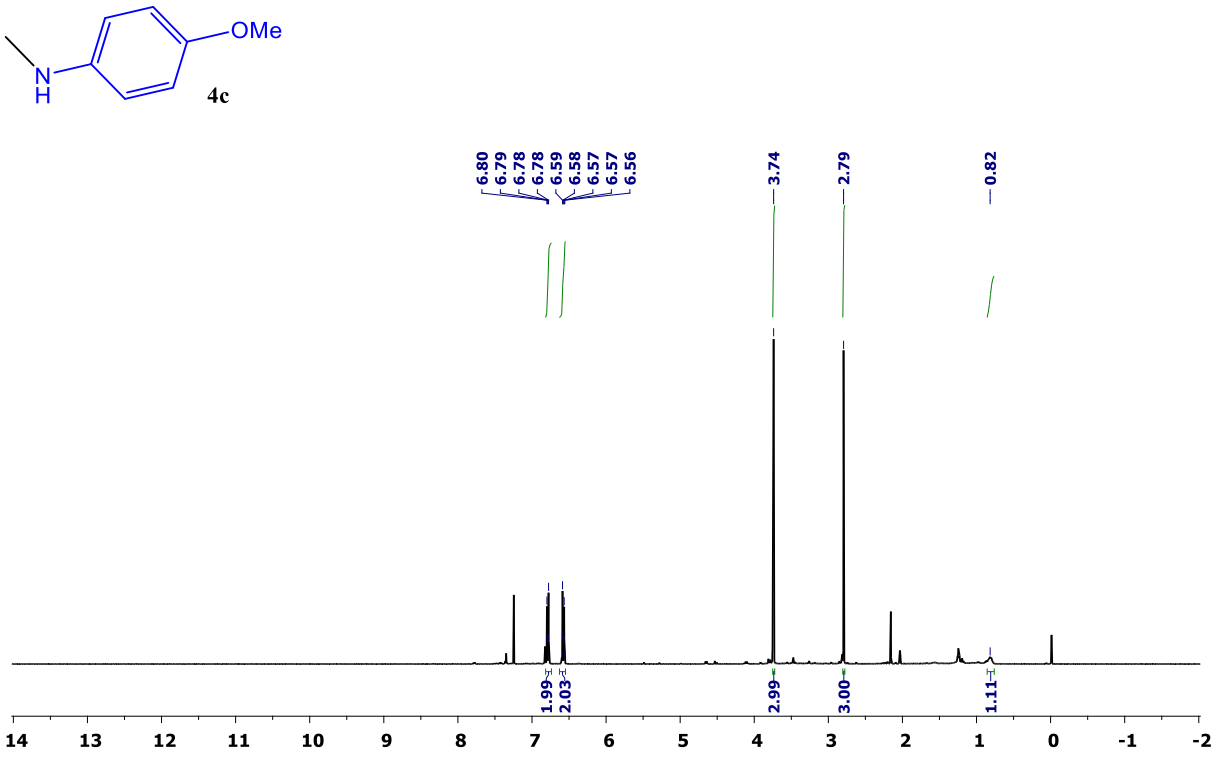


Figure S40. ^{1}H NMR spectrum of **4c** (in $CDCl_3$, 25 °C, TMS, 400 MHz).

Chloro-*N*-methylaniline (4d)

^{1}H NMR (400 MHz, $CDCl_3$) δ 6.11 (dd, *J* = 4.5, 3.8 Hz, 2H), 5.50 (d, *J* = 8.1 Hz, 2H), 2.62 (s, 1H), 1.78 (s, 3H).

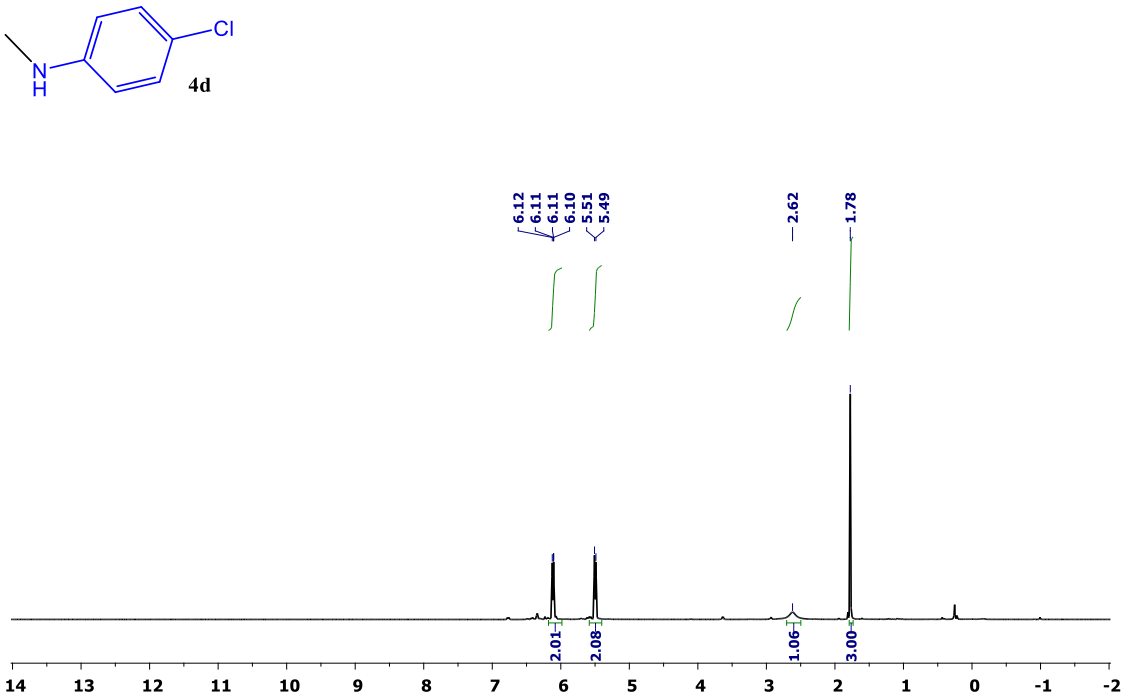


Figure S41. ^{1}H NMR spectrum of **4d** (in $CDCl_3$, 25 °C, TMS, 400 MHz).

***N*-methylpyridin-2-amine (4e)**

^{1}H NMR (400 MHz, $CDCl_3$) δ 7.98 (d, *J* = 2.8 Hz, 1H), 7.91 (dd, *J* = 4.7, 1.1 Hz, 1H), 7.05 (dd, *J* = 8.3, 4.7 Hz, 1H), 6.82 (ddd, *J* = 8.3, 2.8, 1.3 Hz, 1H), 3.80 (dd, *J* = 14.9, 10.1 Hz, 1H), 2.80 (s, 3H).



4e

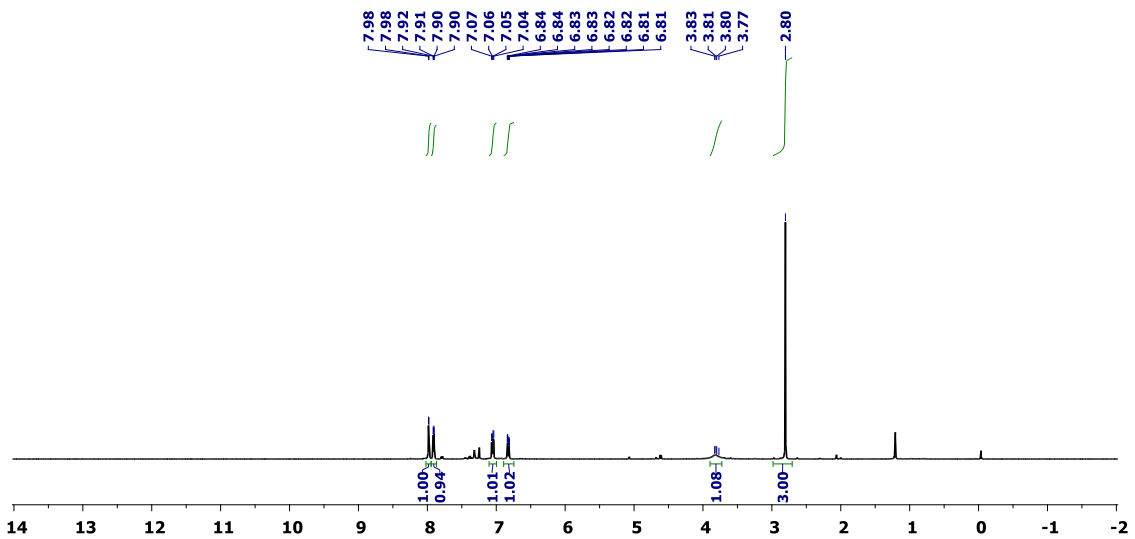
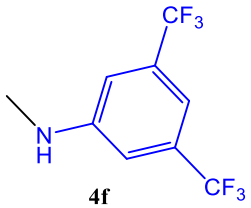


Figure S42. ^{1}H NMR spectrum of **4e** (in $CDCl_3$, 25 °C, TMS, 400 MHz).

***N*-methyl-3,5-bis(trifluoromethyl)aniline (4f)**

^{1}H NMR (400 MHz, $CDCl_3$) δ 7.13 (s, 1H), 6.91 (s, 2H), 4.16 (s, 1H), 2.89 (d, *J* = 5.0 Hz, 3H).



4f

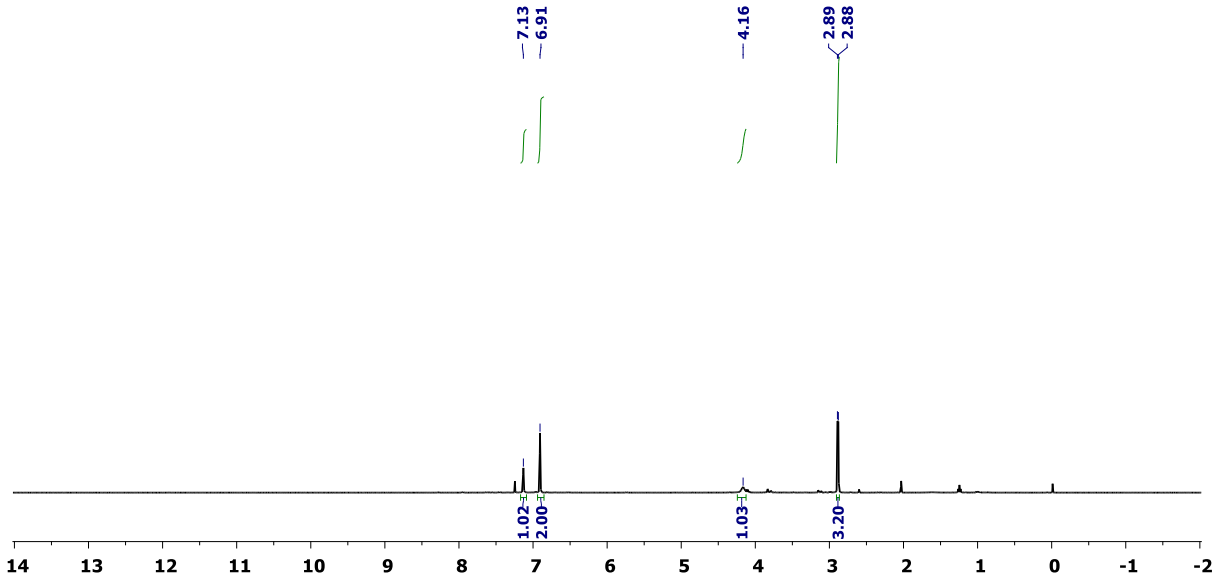


Figure S43. ^{1}H NMR spectrum of **4f** (in $CDCl_3$, 25 °C, TMS, 400 MHz).